SULFATE AND ALKALI SILICA RESISTANCE

OF CLASS C & F FLY ASH REPLACED BLENDED CEMENTS

by

Sudheen Anantharaman

A Thesis Presented in Partial Fulfillment
of the Requirements for the Degree
Master of Science

ARIZONA STATE UNIVERSITY

May 2008

SULFATE RESISTANCE AND ALKALI SILICA RESISTANCE

OF CLASS C & F REPLACED BLENDED CEMENTS

by

Sudheen Anantharaman

has been approved

December 2007

Graduate Supervisory Committee:

Barzin Mobasher, Chair
Apostolos Fafitis
Claudia Zapata

APPROVED BY THE GRADUATE COLLEGE

ABSTRACT

Methodologies to reduce the dependence on Portland cement in concrete production are desirable from a sustainability perspective since Portland cement production is a major contributor to the greenhouse gas emission. The use of fly ash as a cement replacement makes the concrete less permeable to harmful ions due to its finer particle size distribution and pozzolanic reactions. This results in an enhanced high performance and more durable concrete.

The concrete industry faces questions involving the characteristics of fly ash that can be tolerated for the performance-based specification. The current trends are limited to the production of Type IP cements containing 20% Class F fly ash. Two main degradation mechanisms of sulfate attack (SA) and alkali silica reaction (ASR) are addressed in this study. The effect of fly ash in changing the sulfate attack and Alkali-Silica resistance of concrete for a range of replacement (10-40 %) of Class F and Class C fly ashes was determined using both experimental and theoretical modeling.

A series of durability tests on the proposed mixes were conducted and guidelines were developed for concrete containing high doses of Class C and F fly ash. The model used for the prediction of sulfate resistance of blended cement samples was developed by Tixier and Mobasher. A simplified version of this model based on diffusion reaction assumption with a series solution was used. Diffusivity measures were obtained by applying the model to the expansion time-history data. Results show that both Class C and F fly ash replacements enhanced the resistance of mortars and pastes specimen to both sulfate attack and alkali silica reaction. It was also observed that Class C fly ash needs to be used in higher replacement levels to achieve satisfactory results.

The study of different specimen sizes showed that smaller specimens could be used to understand the mechanism of degradation in a much shorter duration of time, while modeling techniques helped in understanding the diffusion and elastic modulus behavior with the addition of fly ash.

TABLE OF CONTENTS

Page

CHAPTER Page

CHAPTER Page

APPENDIX Page

LIST OF TABLES

Table Page

LIST OF FIGURES

Figure Page

NOMENCLATURE

C	CaO (Lime)
S	SiO_2 (Silica)
$\bar{S}$	SO_3 (Sulfur trioxide)
F	Fe_2O_3 (Iron Oxide)
A	Al_2O_3 (Aluminum Oxide)
H	H_2O (Water)
NH	Sodium Hydroxide
$N\bar{S}$	Sodium Sulfate Attack
C_3A	3CaO. Al_2O_3 (Tri Calcium Aluminate)
C_3S	3CaO. SiO_2 (Tri Calcium Silicate)
C_2S	2CaO. SiO_2 (Di Calcium Silicate)
CH	$Ca(OH)_2$ (Calcium hydroxide)
C_4AF	Tetra Calcium Alumino Ferrite
C_4A_3S	Calcium Aluminate Silicate
CSH	xCaO. SiO_2. $y H_2O$ (Calcium silicate hydrate)
CAH	xCaO. Al_2O_3. $y H_2O$ (Calcium Aluminate Hydrate)
$C\bar{S}H_2$	$CaSO_4$. $2H_2O$ (Gypsum)
$C_3A.C\bar{S}.H_{12}$	Mono-sulfate Hydrate
$C_3A.CH.H_{12}$	Hydro Garnet
$C_3A.3C\bar{S}.H_{32}$	Ettringite
$CS.C\bar{S}.C\bar{C}.H_{15}$	Thaumasite

DEDICATION

I would like to dedicate this thesis

from the deepest place in my heart to my parents

H.S.Anantharaman and S.Nagapadmini,

who put the happiness and well being of their four children

ahead of their own interests for the greater part of their lives.

It is to them that I owe my good fortune in life.

ACKNOWLEDGMENTS

I would like to express my deep and sincere gratitude to my adviser, mentor and chair of the committee, Dr. Barzin Mobasher, for providing me the opportunity to work under him at Arizona State University. He has been actively interested in my work and has always been available to advise me. I am very grateful for his support, patience, motivation, and immense knowledge in cement chemistry and modeling techniques that made my thesis work possible.

I would also like to thank my committee members Dr. Apostolos Fafitis and Dr. Claudia Zapata for taking time to serve on my committee and give their valuable advice for the completion of this thesis.

I would like to thank Salt River Project (SRP) for their financial support and the fly ash samples without which this thesis would not be possible. I would also like to thank Mr. Jeff Hearne of Salt River Materials Group (SRMG) for the supply of cement and his help in chemical analysis of the raw flyash and cement samples.

I am very thankful to Peter Goguen, Jeffrey Long and Danny Clevenger for the perpetual energy and enthusiasm they showed in teaching me to conduct experiments. I would also like to thank my family and friends for their constant support and motivation. I would like to extend my special thanks to Amir Bonakdar and Juan Alfredo Erni, as they were my source of inspiration throughout my graduate studies and research work. I would also like to thank my roommates for their great company during my graduate studies here at ASU. Last but not the least, I would like to thank my sister Divya who never let me miss my family and encouraged me in every step during my graduate studies here at ASU.

1. INTRODUCTION

1.1. Overview

Most people do not realize that durability and strength are not synonymous when talking about concrete. Durability is the ability to maintain integrity and strength over time. Strength is only a measure of the ability to sustain loads at a given point in time. Two concrete mixes with equal cylinder breaks of 4,000 psi at 28 days can vary widely in their permeability, resistance to chemical attack, resistance to cracking and general deterioration over time, all of which are important to durability.

Fly ash is a pozzolanic material. A Pozzolan is defined by the American Society for Testing and Materials (ASTM) as "a siliceous or siliceous and aluminous material which in itself possesses little or no cementitious value but which will, in finely divided form and in the presence of moisture, chemically react with calcium hydroxide at ordinary temperature to form compounds possessing cementitious properties."[1]. Fly ash has been successfully used in Portland cement concrete (PCC) as a mineral admixture for nearly 60 years, and more recently as a component of blended cement. The principal benefits ascribed to the use of fly ash in concrete include enhanced workability due to the spherical shape of the fly ash particle, reduced bleeding and less water demand, increased ultimate strength, reduced permeability, lower heat of hydration, greater resistance to sulfate attack, greater resistance to alkali-silica reaction, and reduced shrinkage. [5]

1.2. Problem Statement

Today, there is a general trend to replace higher levels of Portland cement with fly ash in concrete. The increased pressure to use higher levels of fly ash in concrete systems is due to three main reasons.

- The first reason being the economical aspect. As the replacement level of fly ash increases, the cost to produce concrete decreases.
- The second reason and arguably the most important is the environment aspect. Fly ash is an industrial by-product, much of which is deposited in landfills if not used in concrete. Also from an environmental perspective, the more fly ash being utilized in concrete, the less the demand for Portland cement, the less Portland cement production and therefore the lower CO2 emissions.
- The third and final aspect influencing the use of higher replacement levels is the technical benefits of high volume fly ash concrete (HVFAC > 30%). HVFAC has improved performance over ordinary Portland cement concrete, especially in terms of durability when appropriately used.

Although there are clearly economic and environmental benefits associated with the use of high levels of fly ash in concrete, there is relatively little information on the behavior of such concrete and almost no guidance on its production or use.

1.3. Objective of the Study

The objective of this research was to inspect the performance of class C and F fly ash concrete material with replacement level from 10-40 %. The overall research included studies on the effects of sulfate attack and alkali silica reaction on time dependent

properties such as compressive strength and durability issues by means of Micro-structural studies using Scanning Electron Microscope (SEM) and Energy dispersive X-ray spectroscopy (EDS or EDX). Theoretical modeling was used to analyze the service life and degradation (expansion) of specimen exposed to External Sulfate Attack (ESA). The studies included different levels of fly ash replacements, different levels of water to cementitious material ratio (W/Cm), mortar and paste specimens and different size of the specimens.

1.4. Scope of the Study

The analysis of sulfate attack expansions was obtained from the experimental results obtained from the average of 4 samples in each batch. 9 batches of mortar specimens and 14 paste specimens were used for this analysis.

The 9 batches of standard size (1”x1”x11”) mortar specimens were prepared with water to cementitous material ratio of 0.6 and the 9 batches of mortar specimens consisted of 1 batch for the control specimen, 4 batches for class C and 4 batches for class F fly ash, the replacement levels of fly ash were considered at 10, 20, 30 and 40 %.

The 14 batches of paste specimens were prepared with water to cementitous material ratio of 0.4 and the 14 batches of paste specimens consisted of 7 batches of the standard size (1”x1”x11”) and 7 batches of the modified size (0.4”x0.4”x4”) paste specimens. One batch for control specimen was used in both cases, 3 batches for class C and 3 batches for class F fly ash. The replacement levels of fly ash were considered at 10, 20 and 30 %.

The analysis of change in compressive strength due to the degradation of sulfate attack was obtained from the experimental result of the average of 2 samples in each

batch and 27 batches of mortar specimens were used for this analysis. The water to cementitious material ratio was 0.6 for all the batches. Furthermore the compressive strength for 2" x 6" cylinder specimens were tested at 1, 28 and 126 days.

The analysis of alkali silica reaction expansions was obtained from the experimental results obtained from the average of 4 samples in each batch. The 9 batches of standard size (1"x1"x11") mortar specimens were prepared with water to cementitous material ratio of 0.47 and the 9 batches of mortar specimens consisted of 1 batch for the control specimen, 4 batches for class C and 4 batches for class F fly ash. The replacement levels of fly ash was considered at 20, 25, 30 and 40 %.

The micro-structural analysis performed for sulfate attack was on the control, 20 % class C and F paste specimens after a exposure period of 80 weeks and the micro-structural analysis performed for the alkali silica reaction consisted of control, 20 % class C and F mortar specimens with a exposure time of 1, 2 and 4 weeks.

1.5. Organization of Report

Chapter 1 provides the introduction, overview, problem statement, objectives, and scope of work.

Chapter 2 presents a brief literature review, including fly ash and its engineering properties, chemical reaction involving fly ash (pozzolanic reaction) and a brief introduction of SEM and EDS.

Chapter 3 describes the material used (Class C and F fly ash, different sand particles for sulfate attack and alkali silica reaction). It also provides the chemical and microstructural properties of the materials used.

Chapter 4 describes the procedure adopted for the experimental work. It provides the procedures involving sample and solution preparation, curing and exposure conditions and the method used for calculating the length change measurements.

Chapter 5 provides a brief introduction on the theory of sulfate attack, types of sulfate attack, the mechanism of degradation involving sulfate attack, factors effecting sulfate attack. It also discusses in detail the results, experimental observations for both expansion calculations and compression strength at different time intervals and the micro-structural studies obtained for both mortar and paste specimens.

Chapter 6 provides a brief introduction on the different theories proposed for alkali silica reaction, factors affecting alkali silica reactions such as composition of cement, fly ash, pessimum effect and aggregate size effect. It also discusses in detail, the results of the experimental observations for both experimental and micro-structural studies.

Chapter 7 provides a detailed explanation of the model used for the predictions of expansion. It also provides the detailed modeling observations made during the course period of time.

Finally, Chapter 8 provides the concluding remarks of the summarized work presented in this thesis.

2. LITERATURE REVIEW

2.1. Fly Ash and its Engineering Properties

Fly ash is the finely divided residue that results from the combustion of pulverized coal. The pulverized coal, when blown with air into the boiler's combustion chamber immediately ignites generating heat and producing a molten mineral residue. Boiler tubes extract the heat from the boiler, cooling the flue gas and causing the molten mineral residue to harden and form ash. The coarse ash particles, referred to as bottom ash or slag, fall to the bottom of the combustion chamber, while the lighter fine residue particles, termed fly ash, remain suspended in the flue gas. Prior to exhausting the flue gas, fly ash is captured by particulate emission control devices, such as electrostatic precipitators (ESP) or filter fabric collectors, commonly referred to as bag houses. [5]

According to Kruger report [7] US congress has classified fly ash as the sixth most abundant resource in The United States of America. Out of the 62 million metric tons of fly ash produced in 2001, only 32 % (20 million metric tons) of the total produced was used in various non-landfill applications of which only two thirds was used in the cement/concrete industry.

Fly ash is used in concrete where cementitous or pozzolanic action, or both, is desired. The use of fly ash in cement/concrete makes it more cost effective, environment friendly and also improves its performance in both fresh and hardened state. [5, 6]. The principal benefits ascribed to the use of fly ash in fresh concrete includes enhanced workability due to the spherical fly ash particles, called cenospheres; reduction in bleeding and water demand; and lowering the heat of hydration. The hardened concrete enhances the

ultimate strength, reduces permeability, reduces shrinkage and increases durability by increasing its resistance to sulfate attack and alkali silica reaction with its pozzolanic action. The principal precautions that need to be taken while using fly ash in concrete are its potential to decrease the air entraining ability with high carbon content fly ashes, thereby reducing its durability; the extended initial setting time; the reduced heat of hydration in colder climates which set seasonal limitations and the slow initial rate of hydration which reduces the early strength.

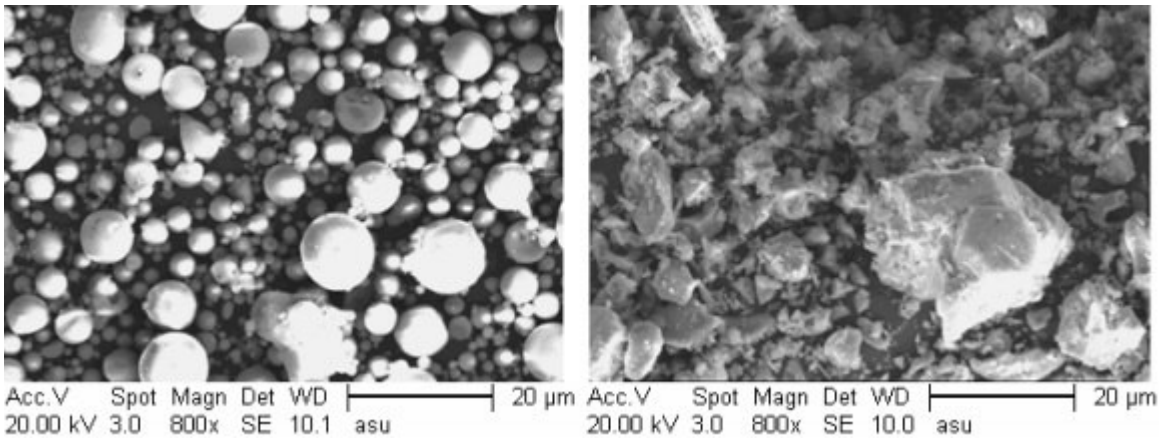

Figure.2.1.1 SEM for Fly ash and Cement

Fly ashes are typically finer than Portland cement and lime. As observed in Figure2.1.1, the SEM images with the same magnifications (800x), the fly ash particles are much smaller than the cement particles. Usually fly ash particles are silt-sized ranging from 10-100 microns and are generally spherical in shape. Sub bituminous fly ashes (Class C) are generally slightly coarser than bituminous fly ash (Class F).

The spherical hollow particles (As observed in Figure.2.1.1) called the cenospheres are believed to be formed by the expansion of CO_2 and H_2O gases evolved from the minerals within the coal being burnt. The predominant forces helping the formation are, however,

the pressure and surface tension on the melts, as well as gravity. The predominantly spherical microscopic structure of the fly ash is related to the equilibrium of the forces on the molten inorganic particle as it is forced up the furnace or smoke stack against gravity. The molten particles cool down rapidly, maintaining their equilibrium shape. A similar situation is found in spherical drops of water falling from a faucet [6]

The engineering properties of fly ash that are of a particular interest when fly ash is used in concrete or cement as an Supplementary Cementing Material are as following [5, 8]

1. Fineness: Fineness is the primary physical characteristic of fly ash that relates to pozzolanic activity. As the fineness increases, the pozzolanic activity can be expected to increase.
2. Pozzolanic activity: Pozzolanic activity refers to the ability of the silica and alumina components of fly ash to react with available calcium and/or sodium from the hydration products of the Portland cement.
3. Workability: At a given water-cement ratio, the spherical shape of most fly ash particles permits greater workability than that acquired with conventional concrete mixes. When fly ash is used, the absolute volume of cement plus fly ash usually exceeds that of cement in conventional concrete mixes. The increased ratio of solids volume to water volume produces a paste with improved plasticity and more cohesiveness.
4. Time of setting: When replacing up to 25 percent of the Portland cement in concrete, all Class F fly ashes and most Class C fly ashes increase the time of setting. However,

some Class C fly ashes may have little effect on, or possibly even decrease, the time of setting.

5. Bleeding: Bleeding is usually reduced because of the greater volume of fines and lower required water content for a given degree of workability.
6. Strength Development: Both Class C and Class F fly ashes when used as SCM are believed to be beneficial in the development of ultimate strength than that developed by the conventional PCC concrete. It is believed that Class F fly ash has a slow rate of strength gain in the initial time period, whereas the Class C fly ash has almost equal or greater rate of strength gain than the conventional PCC.
7. Mix Design: American concrete institute (ACI) recommends that Class F fly ash replacements from 15 to 25 percent of the Portland cement and Class C fly ash replacements from 20 to 35 percent needs to be used in the mix design to get a durable and better performing concrete.
8. Heat of Hydration : As the fly ash reacts slowly than the conventional PCC it tends to generate less heat per unit of time Thus, the temperature rise in large masses of concrete (such as dams) can be significantly reduced if fly ash is substituted for cement. Class F fly ashes are generally more effective than Class C fly ashes in reducing the heat of hydration.
9. Permeability: As the size of fly ash is much smaller than the cement the mix is much denser there by reducing the permeability and the reduced water content also plays an important factor. The pozzolanic reaction produced by fly ash generates additional cementitous compounds that act to block bleed channels, filling pore space and

reducing the permeability of the hardened concrete. The pozzolanic reaction consumes calcium hydroxide (Ca OH $_2$), which is leach able, replacing it with insoluble calcium silicate hydrates (CSH).

10. Sulfate Attack resistance: The hydration products such as calcium hydroxide or portlandite and alumina-bearing phases react with the cat ions such as (Sodium and magnesium) in the presence of water to form gypsum which in turn form expansive material called ettringite which causes the damage of concrete. When Fly ash is used as a replacement of cement the fly ash entailing a reduction in the C3A content (i.e., dilution effect) and the silica present in the fly ash react with calcium hydroxide or portlandite to form CSH thereby reducing the formation of ettringite and mitigating sulfate attack.
11. Alkali-Silica Reaction resistance: The alkalis present in cement reacts with the silica present in aggregates causing expansive reactions, which can in turn cause failure. When fly ash is used as a replacement of cement the total alkalis in the mix reduces there by mitigates ASR. The silica present in the fly ash reacts with the alkalis present in cement to form a no expansive calcium-alkali-silica gel there by reducing free alkalis to react with the aggregates.

Fly ashes are classified based on their chemical composition and the source from which they have been derived. The chemical and mineral compositions vary the color of the fly ash from brown to tan and gray to black, depending on the amount of unburnt carbon in the fly ash. The lighter the color, lower is the carbon content. ASTMC618 specifies two classes of fly ash for the use in concrete 1) Class C fly ash,

and 2) Class F fly ash. These fly ashes should satisfy some ASTMC618 specifications as specified in Table 2.1.1 for their use in concrete.

Figure.2.1.2 Class C and F Fly ash

Table 2.1.1

Specifications for fly ash in PCC. (ASTM C 618) - Class F and C

ASTMC618 Chemical Requirement	Min/Max	Class F	Class C
SiO2 + Al2O3 + Fe2O3	min %	70	50
SO3	max %	5	5
Moisture Content	max %	3	3
LOI	max %	5	5
Optional Chemical Requirement			
Available Alkalies	max %	1.5	1.5
Physical Requirement			
Fineness (+325)	max %	34	34
Pozzolanic Activity / Cement (7 Days)	min %	75	75
Pozzolanic Activity / Cement (28 Days)	min %	75	75
Water Requirement	max %	105	105
Autoclave Expansion	max %	0.8	0.8
Uniformity Requirement: Density	max %	5	5
Uniformity Requirement: Fineness	max %	5	5
Optional Physical Requirement			
Multiple Factor (LOI x Fineness)		255	--
Increase in Drying Shrinkage	max %	0.03	0.03
Uniformity Requirement: Air Entraining Agent	max %	20	20
Cement / Alkali Reaction: Mortar Expansion (14	max %	0.01	0.01

2.2. Pozzolanic Reaction

The main benefit of fly ash as SCM in concrete is that it not only reduces the amount of non-durable calcium hydroxide (lime or portlandite), but in the process converts it into calcium silicate hydrate (CSH), which is the strongest and most durable portion of the paste in concrete. The paste is the key to durable and strong concrete, at full hydration; concrete made with typical cements produces approximately 1/4 pound of non-durable lime per pound of cement in the mix. [A]

Both Class C and Class F fly ashes react in concrete in similar ways they undergo a "pozzolanic reaction" with the lime (calcium hydroxide) created by the hydration of cement and water, to create the same binder (calcium silicate hydrate) as cement. The chemical reactions involved in the pozzolanic reactions are shown in equations 2.2.1 and 2.2.2 In addition, some Class C fly ashes may possess enough lime to be self-cementing, in addition to the pozzolanic reaction with lime from cement hydration.

Tricalcium silicate + water = Calcium silicate hydrate + Calcium hydroxide

$$2C_3S + 6H_2O \longrightarrow CSH + 3Ca(OH)_2 \quad \text{(2.2.1)}$$

Calcium hydroxide + silica = Tricalcium silicate + water

$$2CH_2 + S \longrightarrow 2C_3S + 2H \quad \text{(2.2.2)}$$

Pozzolanic Reaction in ESA

Fly ash reduces calcium hydroxide, which combines with sulfates to produce gypsum. Gypsum is a material that has greater volume than the calcium hydroxide and sulfates that combine to form it, causing damaging expansion.

Typical Sulfate Attack Reaction [10]

Sodium Sulfate + Calcium hydroxide + water = Gypsum

$$Na_2SO_4 + Ca(OH)_2 + 2H_2O \longrightarrow C\bar{S}H_2 + 2Na(OH) \quad \text{(2.2.3)}$$

Tricalcium Aluminate + Gypsum + water = Ettringite

$$C_3A + 3C\bar{S}H_2 + 26H_2O \longrightarrow C_3A.3C\bar{S}.H_{32} \quad \text{(2.2.4)}$$

Pozzolanic Reaction Mitigating Sulfate Attack

$$3Ca(OH)_2 + SiO_2 \longrightarrow 2C_3S + 2H_2O \quad \text{(2.2.5)}$$

Pozzolanic Reaction in ASR

The glass in Fly ash is itself a very high reactive fine form of silica and has the ability to react with alkalies (Sodium or potassium) hydroxides in Portland cement paste, making them unavailable for expansive reaction with reactive silica in certain aggregates.

Typical Alkali Silica Reaction [11]

Calcium hydroxide + silica + Sodium hydroxide + Water = Alkali silica gel

$$Ca(OH)_2 + SiO_2 + Na(OH) + H_2O \longrightarrow wNa_2O.xCao.ySiO_2.zH_2O \quad \text{(2.2.6)}$$

Here the gels formed are more or less expansive depending on the CaO content. However, the presence of calcium appears to be essential for the ASR gel to expand, the role of which in the reaction mechanism continues to be a matter of controversy. [11]

Pozzolanic Reaction Mitigating ASR [C]

$$3Ca(OH)_2 + SiO_2 \longrightarrow 2C_3S + 2H_2O \quad \text{(2.2.7)}$$

Sodium hydroxide + silica = Non expansive silica gel

$$yNa(OH) + xSiO_2 \longrightarrow Na_ySi_xO_z(\text{Aqueous}) \quad \text{(2.2.8)}$$

2.3. SEM and EDS

SEM: Scanning Electron Microscope

SEM is a type of electron microscope capable of producing high-resolution images of a sample surfaces. SEM does not contain objective, intermediate and projector lenses to magnify the image as in the optical microscope. Instead magnification results from the ratio of the area scanned on the specimen to the area of the television screen. (http://acept.asu.edu/PiN/rdg/elmicr/elmicr.shtml)

SEM images have a characteristic three-dimensional appearance and are useful for judging the surface structure of the sample, which makes it perfect to analyze different elements in cement-based materials. The resolution of the SEM can approach a few nm and it can operate at magnifications that are easily adjusted from about 10 times - 300,000 times. [12]

In the SEM, the image is formed and presented by a very fine electron beam, which is focused on the surface of the specimen. The beam is scanned over the specimen in a series of lines and frames called a raster, just like the (much weaker) electron beam in an ordinary television. At any given moment, the specimen is bombarded with electrons over a very small area. Several things may happen to these electrons, usually they may be absorbed by the specimen and give rise to secondary electrons of very low energy, together with X- rays.

The secondary electrons are attracted to a grid held at a low (50 volt) positive potential with respect to the specimen. Behind the grid is a disc held at about 10 kilovolts positive with respect to the specimen. The disc consists of a layer of scintillant coated

with a thin layer of aluminum. The secondary electrons pass through the grid and strike the disc, causing the emission of light from the scintillant. The light is led down a light pipe to a photomultiplier tube, which converts the photons of light into a voltage. Thus the secondary electrons produced from a small area of the specimen give rise to a voltage signal of a particular strength. The voltage is led out of the microscope column to an electronic console, where it is processed and amplified to generate a point of brightness on a cathode ray tube (or television) screen forming an image. In most currently available SEM's, the energy of the primary electron beam can range from a few hundred eV up to 30 keV. (SEM/EDS devise at the School of Materials Science, ASU was 20 keV)

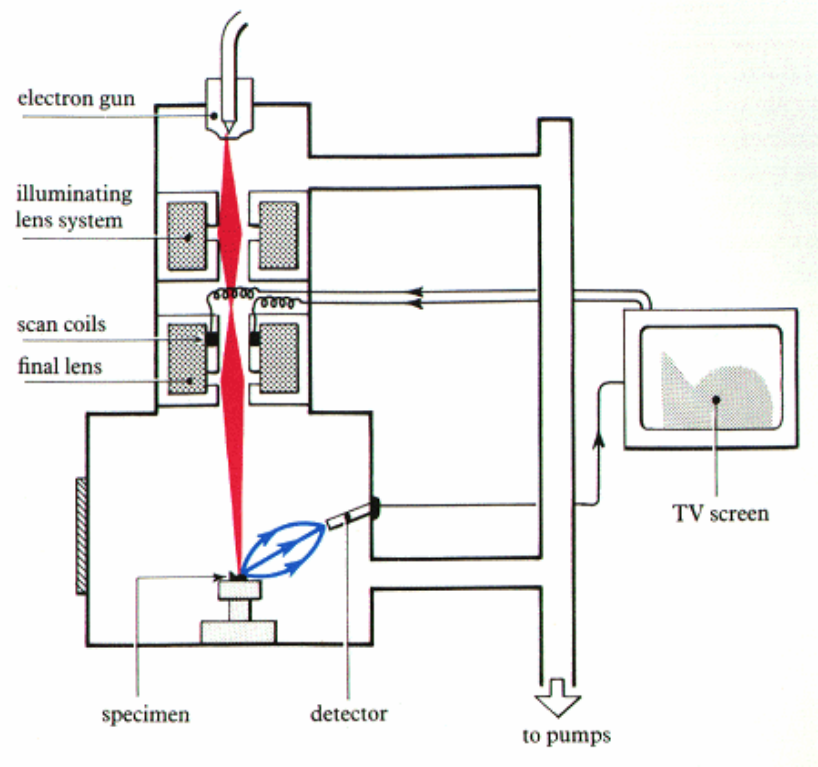

Figure.2.3.1 Schematic drawing of a scanning electron microscope

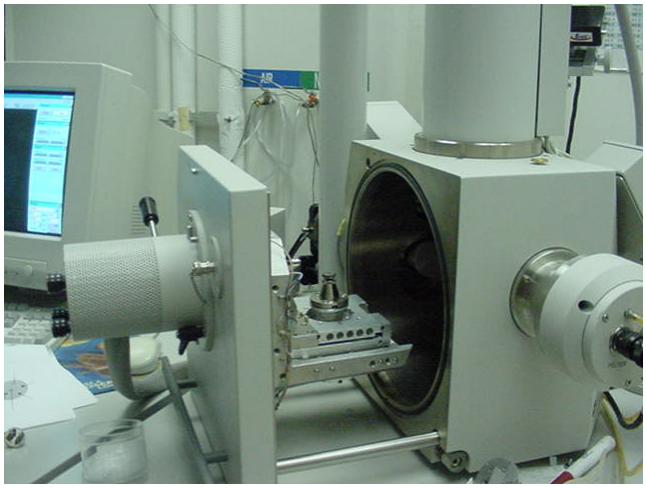

Figure.2.3.2 SEM Chamber where the samples are loaded (http://wikipedia.org)

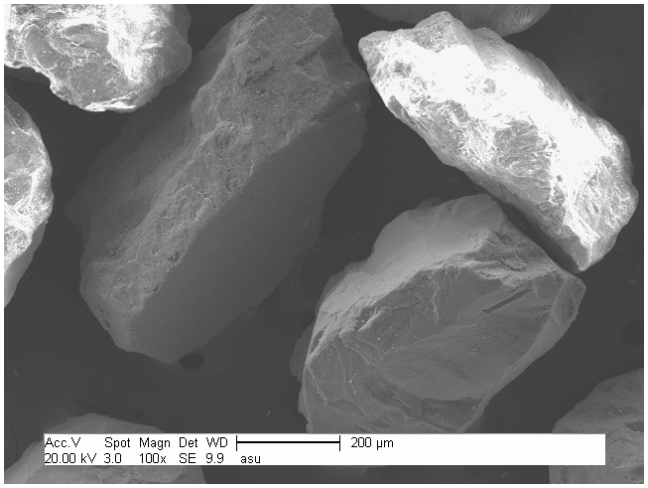

Figure.2.3.3 Sample SEM image taken at ASU

EDS: Energy-Dispersive X-Ray Spectroscopy

EDS also called EDX/EDAX is an analytical tool for analyzing qualitatively and quantitatively the chemical compositional of materials. The electron beams used are either that of the SEM or electron beam columns specially constructed for themselves. The EDS system can detect X-rays (emitted along with the secondary electrons) only from elements in the periodic table above beryllium, Z-4.

When the specimen's atoms electrons are bombarded with electrons, they knock some of them off in the process. A position vacated by an ejected inner shell electron is eventually occupied by a higher-energy electron from an outer shell. To be able to do so, however, the transferring outer electron must give up some of its energy by emitting an X-ray.

The amount of energy released by the transferring electron depends on which shell it is transferring from, as well as which shell it is transferring to. Furthermore, the atom of every element releases X-rays with unique amounts of energy during the transferring process. Thus, EDS measures the amounts of energy present in the X-rays being released by a specimen during electron beam bombardment, Hence the identification of the atom from which the X-ray was emitted is established.

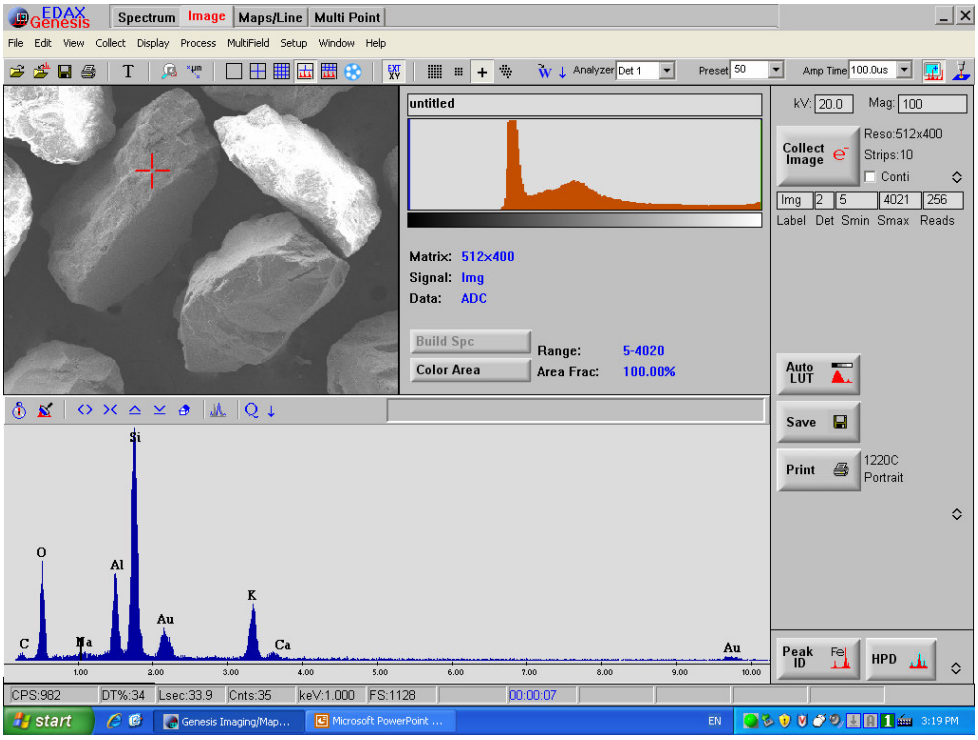

Figure.2.3.4 Sample EDS image taken at ASU

3. MATERIALS USED

3.1. Cement

Commercially available Portland cement type I/II was used for the entire research. This kind of cement is used for general use, more especially when moderate sulfate resistance or moderate heat of hydration is desired. The chemical analysis of the cement used is as given in the table below and it satisfies all the requirements of ASTM C150 (i.e. Total (S+A+F), Total Alkali content = (Na2O + 0.658K2O), Compressive strength for 1, 3,7,28 days, loss of ignition, etc).

Table 3.1.1

Chemical analyses of cement used

	Cement Used		Cement Used
SiO2	21.62	Free Lime	0.98
Al2O3	4.06	C3S	55.41
Fe2O3	3.54	C2S	20.27
CaO	**63.9**	C3S/ C2S	**2.73**
MgO	1.4	C3A	**4.78**
SO3	2.81	C4AF	10.76
L.O.I.	1.42	Blaine	4260
Total (S+A+F)	**29.22**	Reflect	29
Na2O	0.06	Air	9.4
K2O	0.54	Auto Clave	-0.04
Total Alkali	**0.415**	False Set	79
Moisture Content	-	Initial Set	3:10
Fineness Plus 325	97.7	Final Set	4:45
Specific Gravity	-	1 Day Strength (psi)	2230
Carbon Content	-	3 Day Strength (psi)	4130
ASTM Classification	N/A	7 Day Strength (psi)	5380
Canadian Classification	N/A	28 Day Strength (psi)	6750
Sulfur check	Ok		
LOI check	Ok		

3.2. Sand : Silica and Reactive

Commercially available standard silica sand was used for sulfate attack (ASTM C1012), composed almost entirely of naturally rounded grains of nearly pure quartz; the sand was selected such that it satisfies all the requirements of ASTM C778.

Commercially available reactive sand was used for the Alkali Silica Reaction (ASTM C1260). The sand was selected such that it satisfies all the requirements of ASTM C227.

3.3. Fly-Ash: Class C and Class F

Both Class C and F fly ash used throughout this research was provided by SRP (Salt River Project), and both the fly ashes satisfied the ASTM C618, the chemical analysis of which is provided in the table below (Table 3.3.1).

Class C fly ash is usually derived from burning of lignite or Sub-bituminous coal consists of calcium alumino-sulfate glass with quartz, tricalcium aluminate and free lime. They are usually light tan to buff in color, indicating relatively low amounts of carbon as well as the presence of some lime or calcium. Class C fly ash is also referred to as high calcium fly ash because it typically contains more than 20 % percent CaO. Class C fly ash in addition to having pozzolanic properties, also has some self-cementing properties (ability to harden and gain strength in the presence of water alone). The use of class C fly ash in concrete equals or may even increase the early strength development of concrete when compared to cement.

Class F fly ash usually derived from burning of anthracite or bituminous coal consists of alumino-silicate glass with quartz, mullite and magnetite. They are usually some shade

of gray because of the presence of unburnt carbon, with lighter shades of gray generally indicating a higher quality of fly ash. Class F also called low calcium fly ash has less than 10% CaO. Class F fly ash has pozzolanic properties, with a little or no cementing properties. The use of class F fly ash in concrete reduces the early strength development of concrete.

Table 3.3.1

Chemical analyses of fly ash used

	SRP Class F	SRP Class C
SiO2	57.68	43.5
Al2O3	22.78	20.25
Fe2O3	5.03	6.78
CaO	**6.17**	**16.44**
MgO	1.93	3.88
SO3	0.48	1.77
L.O.I.	1.07	1
Total (S+A+F)	**85.49**	**70.53**
Na2O	1.96	1.86
K2O	1.21	0.74
Total Alkali	**2.76**	**2.35**
Moisture Content	0.09	0.07
Fineness Plus 325	26.14	20.5
Specific Gravity	2.18	2.43
Carbon Content	0.74	0.91
ASTM Classification	Class F	Class C
Canadian Classification	Class F	Class CI
Sulfur check	Ok	Ok
LOI check	Ok	Ok

ASTM Classification:

- Class F, if total amount of SiO_2+Al_2O_3+Fe_2O_3 is greater than 70%
- Class C, if total amount of SiO_2+Al_2O_3+Fe_2O_3 is less than 70%

Canadian Classification:

- Class F, if CaO is less than 8%
- Class CI, if CaO is greater than 8% but less than 20%
- Class F, if CaO is greater than 20%

Other checks are:

- Sulfur check is Ok, if SO3 is less than 5%
- LOI check is OK, if LOI is less than 3
- R factor check is OK, if R factor is less than 2.5

3.4. Microstructural Analysis of Material Used

Cement:

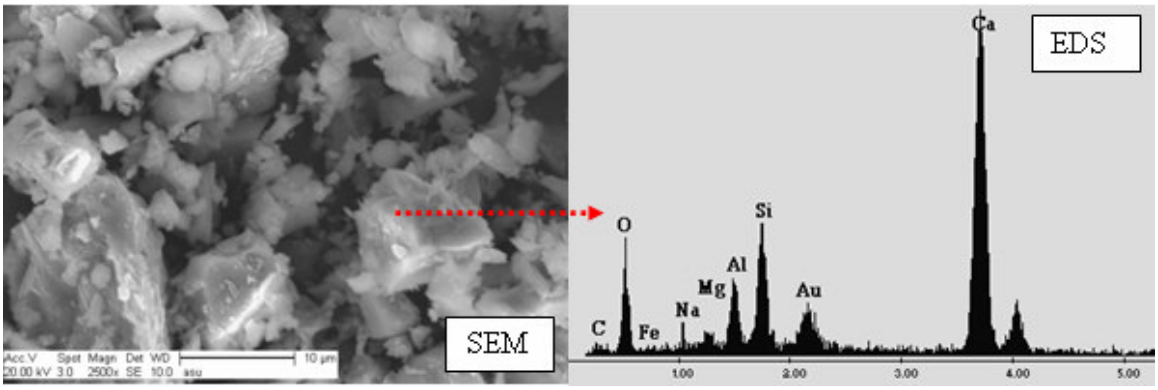

Figure.3.4.1 SEM & EDS for Cement Particles

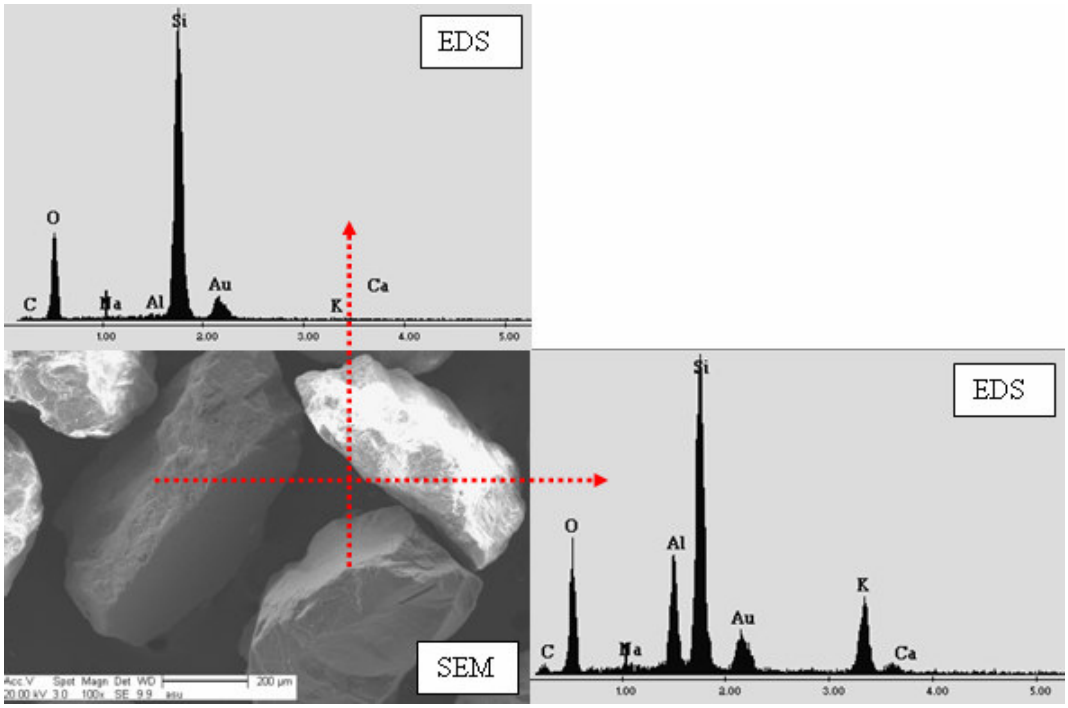

Figure.3.4.2 SEM & EDS for Silica Sand Particles used in Sulfate Attack

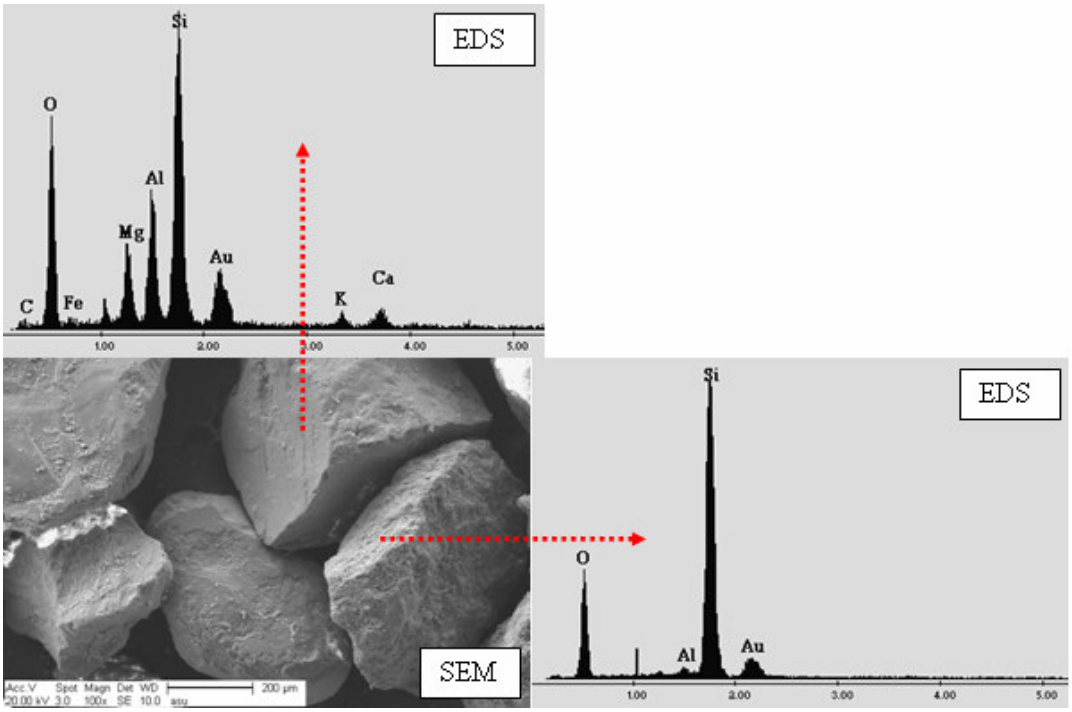

Figure.3.4.3 SEM & EDS for Reactive Sand Particles used in ASR

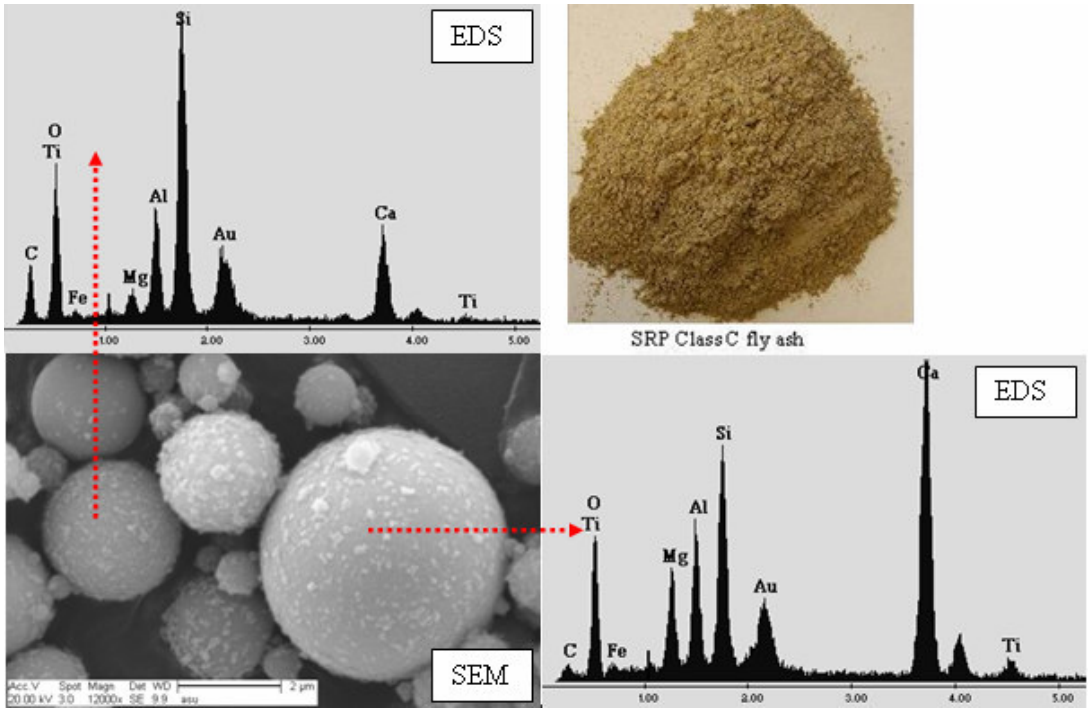

Figure.3.4.4 SEM & EDS for Class C Fly-Ash Particles

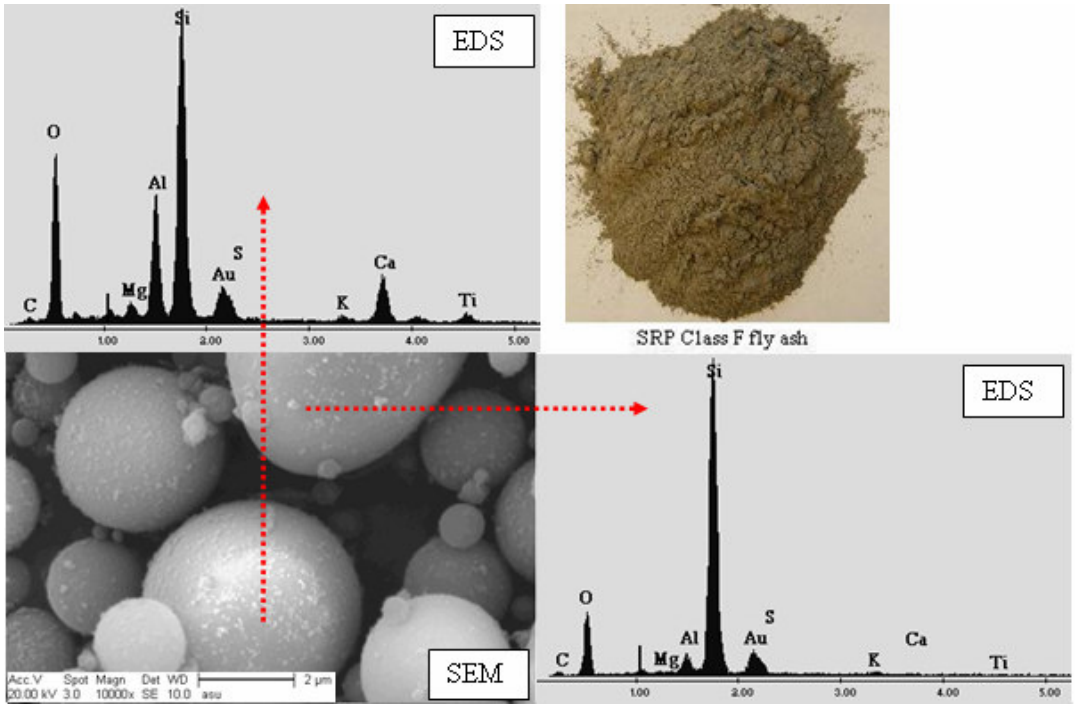

Figure.3.4.5 SEM & EDS for Class F Fly-Ash Particles

4. EXPERIMENTAL PROCEDURE

4.1. Introduction

This chapter details the procedures followed in the preparation of mortar/paste specimens. The materials used and corresponding specifications are outlined. The various test methods and test procedures are also detailed and explained. For specimens exposed to SA, a sand to cementitious material ratio of 2.75 with water to cementitious material ratio of 0.60 was used for mortar specimens (i.e. for mortar bars (1”x1”x11”) for ASTM C1012 and mortar Cylinders (2” x 6”) for ASTM C109) and a sand to cementitious material ratio of 0 with water to cementitious material ratio of 0.460 was used for the paste specimens (i.e. for paste bars (1”x1”x11”) and (0.4”x0.4”x4”) for ASTM C1012).

For the specimens exposed to ASR, a reactive sand to cementitious material ratio of 2.25 with water to cementitious material ratio of 0.47 was used for mortar specimens (i.e. for mortar bars (1”x1”x11”) for ASTM C1260). The reactive sand used in the mortar bars exposed to ASR was graded as shown in the table below.

Table 4.1.1

Grading Requirements for Aggregates for ASR

Sieve Size		Mass,%
Passing	Retained	
4.75mm(No.4)	2.36mm(No.8)	10
2.36mm(No.8)	1.18mm(No.16)	25
1.18mm(No.16)	600µm(No.30)	25
600µm(No.30)	300µm(No.50)	25
300µm(No.50)	150µm(No.100)	15

4.2. Sample Preparation

4 mortar bar specimens (1”x1”x11”) were cast for each set of mix proportion for SA and ASR, But 5-6 bar specimens of 0.4”x0.4”x4” measurement were cast for each set of mix proportion for SA since the 0.4”x0.4”x4” specimen are very weak and easily broken while de-molding or rough handling. 8 cylinders were cast for each set of mix proportion specimen for SA (compression test).

Molds were prepared in accordance with ASTM C490 except the interior surfaces of the mold were covered with releasing agents (i.e. oil in our case). The excess oil was wiped with a dry cloth so that it does not ingress the mortar/paste specimens causing additional reactions. Steel molds with two compartments which has provisions for stainless steel gage studs was used for the 1”x1”x11” specimens refer to Figure 4.2.1 and a Plexy glass molds with 4 compartments with Plexy glass studs was used for the 0.4”x0.4”x4” specimens refer to figure 4.2.2.

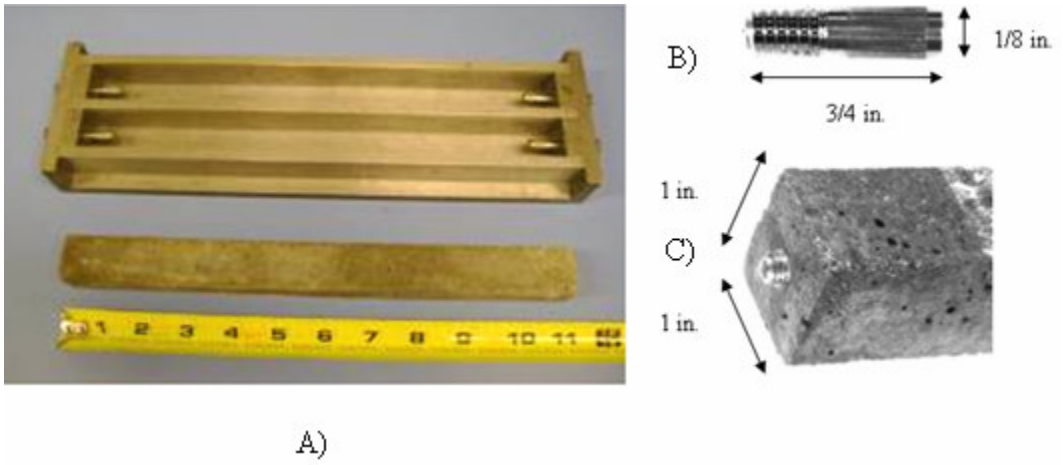

Figure.4.2.1 A) Steel mold for ASTM C 1012 test (11”), B) Steel stud (end pin), C) Steel stud held in the hardened specimen.

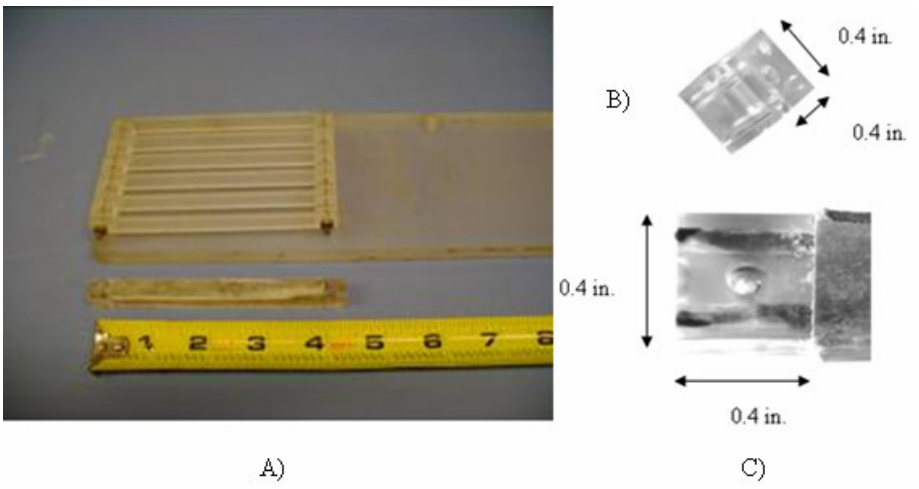

Figure .4.2.2 A) Plexy glass mold for modified test, B) Plexy glass stud (end pin) details, C) Plexy glass stud attached to the specimen.

All mortar/paste batches were mixed according to ASTM C305.The mortar/paste mixes were mixed in an electrically driven mixer and the procedure is as following the dry fine aggregates and cement were introduced in the mixer and blended for 60 seconds. Then the water was slowly added to the mixer and blended for 2 minutes to thoroughly mix all ingredients. All the molds were filled in two layers with proper compaction in between the layers. A vibration table was used to help with the consolidation of the fresh mixture in the molds; with the help of a travel the mortar/paste is level such that the surface of the specimen is smooth. In accordance to ASTM C192 to prevent evaporation of water from unhardened mortar/paste, the specimens were immediately covered with, preferably a non-absorptive, non-reactive sheet of tough, durable impervious plastic.

Figure A: mixing the materials

Figure B: casting the bars with mortar

Figure C: vibrating the cast molds

Figure D: a complete cast mortar bar

Figure.4.2.3. Mixing, Vibrating and Casting of Specimen.

Table 4.2.1

Total Number of Specimens Prepared

Total Number of Specimens Prepared			
	SA (Mortar)	SA (paste)	ASR(Mortar)
1”x1”x11” Bars	36	28	36
0.4”x0.4”x4” Bars	-	28	-
2” x 6” Cylinders	64	-	-

4.3. Solution Preparation for SA and ASR

Sodium Hydroxide Solution for ASR: 40.0 g of NaOH was dissolved in 900 ml of water, and was diluted with additional distilled water to obtain 1.0 L of solution. The volume proportion of sodium hydroxide solution to the mortar bars in a storage container was such that there were 4 ± 0.5 volumes of solution to 1 volume of mortar bars. The volume of a mortar bar was taken as 184 ml. sufficient test solution was included to ensure complete immersion of the mortar bars.

Figure.4.3.1 Sodium Hydroxide

Sulfate Solution for SA — 50.0 g of Na_2SO_4 was dissolved in 900 ml of water, and was diluted with additional distilled water to obtain 1.0 L of solution. The solution was mixed one day before use. The pH of the solution was determined before use; the solution with pH outside the range of 6.0 to 8.0 was rejected. The volume proportion of sodium sulfate solution to the mortar bars in a storage container was such that there were 4 ± 0.5 volumes of solution to 1 volume of mortar bars. The volume of a mortar bar was taken as

184 ml. sufficient test solution was included to ensure complete immersion of the mortar bars.

Figure.4.3.2 Sodium Sulfate

4.4. Storage of Specimens in solution

Storage of Specimens for SA: The container containing the specimen and sodium sulfate solution was sealed with gaffers tape to prevent evaporation from the inside. The container was stored at room temperature of 23 ± 2°C (73.5 ± 3.5°F).

Figure.4.4.1 Sample A and Sample B Specimens in Sodium Sulfate solution

Storage of Specimens for ASR: The container for storage for ASR is chosen such that it can withstand prolonged exposure to 80°C (176°F) and must be resistant to a 1N NaOH

solution. The containers containing the specimen and sodium sulfate solution was sealed with gaffers tape to prevent evaporation from the inside and the container was stored at a temperature of 80 ± 5°C (176 ± 3.6°F).

Figure.4.4.2 Specimens in Sodium hydroxide solution in Owen at 80°C

4.5. Expansion Calculation

The length change in the specimens was calculated according to ASTM C490.All the readings were taken at room temperature (the ASR samples were cooled to the room temperature before taking the reading) as we have used steel studs the temperature plays a very important role in length measurements. An interval of 1 week was maintained for the first 3 months and then the interval was increased to 2 weeks for reading between 3 – 6 months. The measurements were recorded, and then the expansion of each bar was calculated by subtracting the initial reading or the Zero reading from the measured readings at an age zero.

A standard length (11”) and modified length (4”) comparator equipped with a digital indicator and a reference steel bar was used to measure the length change of the specimens. The digital indication was graduated to read in 0.0001-in. units and it was accurate within 0.0001 in. Prior to each measurement, the digital indicator was calibrated

using the reference steel bar. The mortar/paste bars were all measured with the marked date and the direction of the sample being measured for accurately obtaining comparator readings. Figure 4.5.1 shows a mortar bar carefully positioned to measure the length change with a digital comparator.

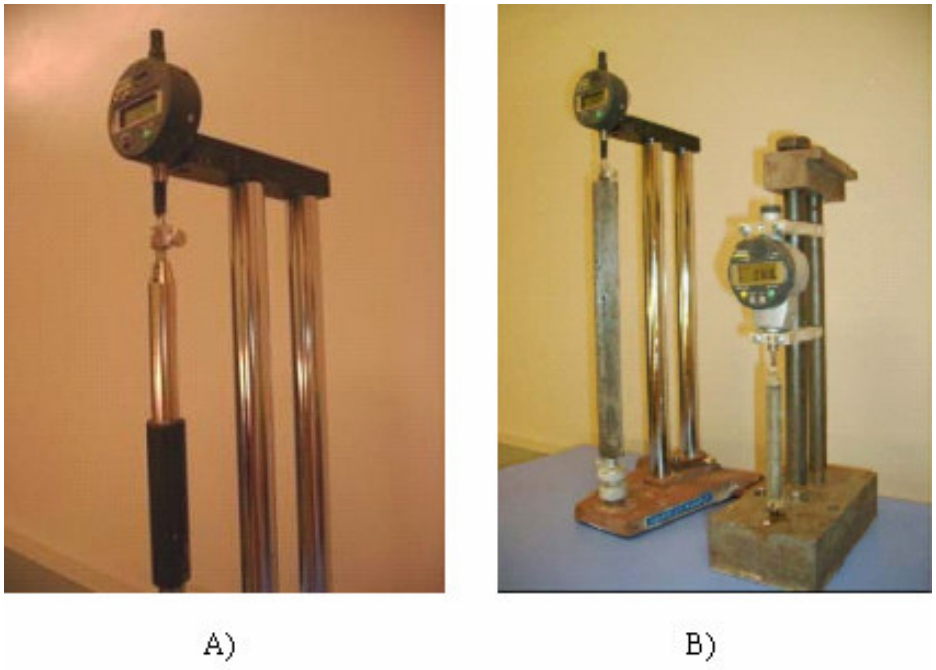

Figure.4.5.1 A) Digital comparator with standard steel rod,

B) Digital comparator with Sample A and Sample B specimen.

$$\Delta L = \frac{Lx - Li}{Lx} * 100$$

Where,

ΔL = change in length at x age, in %

Lx = comparator reading of specimen at age x – reference bar comparator reading at x age.

Li = initial comparator or zero reading of the specimen reference bar comparator reading, at the zero time.

5. SULFATE ATTACK

5.1. Introduction

Sulfate attack is among the major concrete durability and serviceability concerns in civil infrastructure systems. It is a generic name for a set of complex and overlapping chemical and physical processes caused by the reactions of numerous cement components (specially the alumina-bearing components) with sulfates originating from external or internal sources. External sources could be sulfate rich environment in the form of sodium, potassium, magnesium and calcium sulfate and the internal sources of sulfate could be either from cement or gypsum contaminated aggregates.

Different test methods have been developed to study the sulfate resistance of cementitious materials, from which ASTM C 1012 is considered the most common approach and much data is available in the literature based on the results of this test method. This test method was followed and also modified with the following objectives:

1) To study the resistance of Class C and Class F fly ashes to sulfate attack.
2) To study the effect of different level of Class C and Class F replacement (10%-40%)
3) To study the effect of Class C and Class F ashes on the compressive strength of the mortar cylinders subjected to sulfate attack.
4) To study the behavior and differences of mortar and paste specimens
5) To study the microstructure of specimens subjected to sulfate attack
6) To study the effect of specimen size (ASTM C1012 standard size sample A (1”x1”x11”) and modified size sample B (0.4”x0.4”x4”)).

7) To calibrate a model for prediction of expansion of specimens exposed to sulfate attack.

5.2. Literature review

5.2.1. Ettringite Formation

Secondary ettringite formation is considered to be the main cause of most of the expansion and disruption of concrete structures involved in the sulfate attack. However, sulfate attack is not necessarily caused by ettringite formation. When ettringite occurs homogeneously and immediately (within hours), it does not cause any significant disruptive action (Early Ettringite Formation, EEF). This type of harmless ettringite formation happens, for instance, when gypsum reacts with anhydrous calcium aluminate in the presence of water.

$$C_3A + 3(CaSO_4.2H_2O) + 26H_2O \longrightarrow C_3A.3C\bar{S}.H_{32} \quad \text{(5.2.1.1)}$$

Another example of harmless and useful EEF occurs when, under proper restraint, a calcium aluminate sulfate ($C_4A_3\bar{S}$) hydrates within few days producing ettringite uniformly distributed and then homogeneous expansion throughout the hardened concrete

$$C_4A_3\bar{S} + 6Ca(OH_2) + 8(CaSO_4.2H_2O) + 74H_2O \longrightarrow C_3A.3C\bar{S}.H_{32} \quad \text{(5.2.1.2)}$$

In such a case, the restrained expansion is advantageously transformed into a rather useful stress (0.2–0.7 MPa in shrinkage-compensated concrete and 3–8 MPa in self-stressed reinforced concretes).

On the other hand, when ettringite forms later (after several months or years) DEF (Delayed Ettringite Formation) the related heterogeneous expansion in a very rigid hardened concrete can produce cracking and spalling. The disruptive effect is due to the

non-uniform expansion localized only in the area of the concrete structure where ettringite forms. Therefore DEF, and not EEF, is associated with a damaging sulfate attack.

There are two different types of DEF related damage depending on the sulfate source- external or internal sulfate attack. External sulfate attack (ESA) occurs when environmental sulfate (from water or soil) penetrates concrete structure. Internal sulfate attack (ISA) occurs in a sulfate-free environment where the sulfate source is inside the concrete and comes from either cement with high sulfate content or gypsum-contaminated aggregate.

Internal Sulfate Attack (ISA):

Modern cements, manufactured in kilns that burn sulfur-rich fuels or organic residues - such as rubber tires - can incorporate large amounts of sulfate (up to about 2.5%) in the clinker phase, which is available for DEF formation. ISA occurs in a sulfate-free environment when the sulfate source is inside the concrete and comes from either cement with high sulfate content or gypsum-contaminated aggregate. The major factors affecting ISA are: [13, 14]

1. Sulfate Content in cement: It is noticed that concrete manufactured at room temperatures (20°C) do not show any form of ettringite-related expansion independently of the SO_3 content of the cement (2-4%). On the other hand, concrete steam-cured at 90°C show a significant expansion related to ettringite provided that the SO_3 content of the cement is relatively high (>4%).

2. Curing Temperature: When concrete is cured at elevated temperatures (>70°C) the early-formed non-destructive ettringite thermally decomposes to producing more available SO_3 because of which the ISA can aggravate.
3. Micro Cracks: plastic shrinkage, high stress in pre-stressed concrete, curing at high temperatures, & Freezing/Thawing cycles causes micro cracking in concrete, which promotes the ettringite deposition, and help them expand with the supply of water.

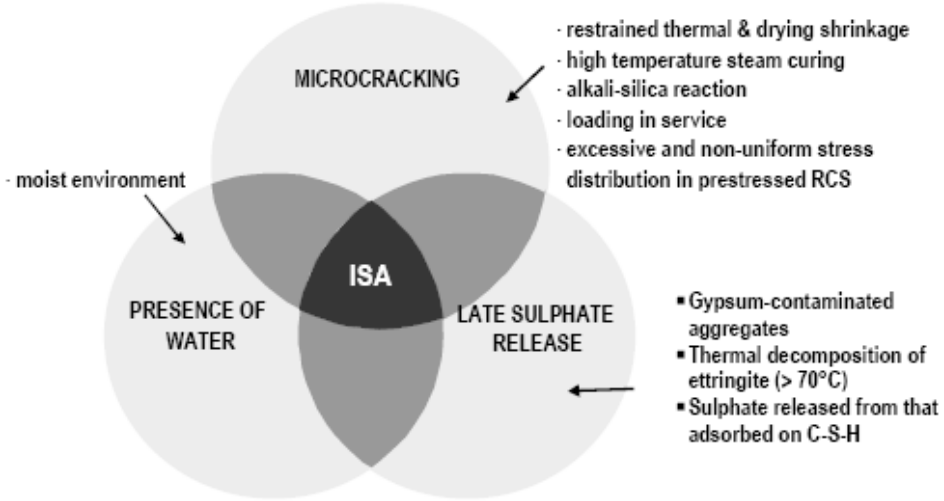

Figure.5.2.1.1 Ternary representation of ISA. [14]

External Sulfate Attack (ESA):

Also called the traditional sulfate attack is the chemical interaction of a sulfate-rich soil or water with the cement paste. Soils containing sodium, potassium, magnesium, and calcium sulfates are the main sources of sulfate ions in groundwater. For ESA to occur, the following three conditions must be fulfilled:

1. High permeability of concrete;
2. Sulfate-rich environment;
3. Presence of water. A diagrammatic representation of the holistic approach;

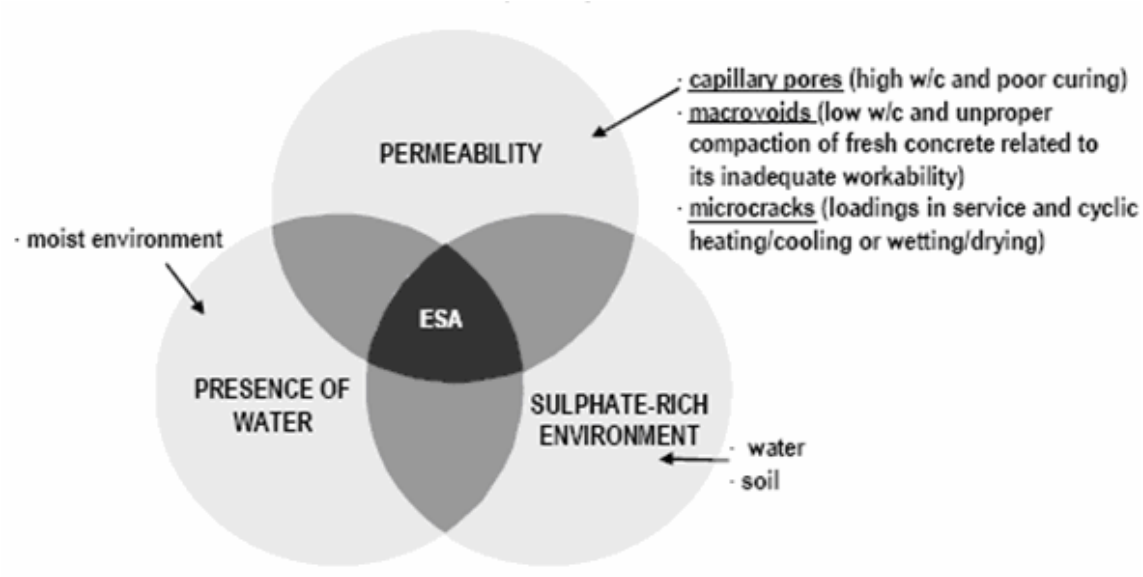

Figure .5.2.1.2 Ternary representation of ESA. [14]

The ESA damage can be divided in to 3 main chemical processes. [14]

1. Sulfate attack on calcium hydroxide (CH) and calcium silicate hydrate (CSH) in the presence of water forms gypsum.

   $$CH + CSH + H_2O \longrightarrow C\bar{S}H_2 \quad \text{(5.2.1.3)}$$

   This process may cause expansion and spalling. However, its most important feature is the loss of strength and adhesion of cement paste due to decalcification of CSH, which is responsible for the binding capacity of the cement paste. This process may occur with all the sulfate salts (Containing Na^+, K^+, etc) except calcium or magnesium sulfate.

2. Sulfate attack on calcium aluminate hydrates (CAH) and mono sulfate hydrate ($C_3A.C\bar{S}.H_{12}$) to form ettringite.

   $$CAH + C_3A.C\bar{S}H_{12} + H_2O + C\bar{S}H_2 \longrightarrow C_3A.3C\bar{S}.H_{32} \quad \text{(5.2.1.4)}$$

This process is mainly responsible for cracking and spalling as a result of expansion produced by DEF. This process may occur with all the sulfate salts (except MgSO4) including calcium sulfate.

3. Sulfate attack on CSH and CH in the presence of water and carbonate ions to form thaumasite.

$$CSH + CH + SO_4 + CO_3 + H_2O \longrightarrow CS.C\bar{S}.C\bar{C}.H_{15} \text{ ……..…..…….....} \quad (5.2.1.5)$$

The thaumasite formation is accompanied by the most severe loss of strength and adhesion, which is able to transform hardened concrete into a pulpy mass, since a significant part of C-S-H can be destroyed according to this reaction. This process may occur with every type of sulfate salts and is favored by humid atmospheres and low temperature (<10°C).

4. Sulfate attack on CSH by magnesium sulfate ($MgSO_4$) which is not directly related to ettringite formation but there is a loss of strength and adhesion of the cement paste due to decalcification of CSH.

$$CSH + CH + MgSO_4 + H_2O \longrightarrow C\bar{S}H_2 + Mg(OH)_2 + SiO_2 + xH_2O \text{ ……...} \quad (5.2.1.6)$$

5.2.2. Factors Affecting Sulfate Attack

1) Cement Type: The most important mineralogical phases of Portland cements that affect the intensity of sulfate attack are C_3A, C_3S/C_2S ratio and C_4AF. Among the hydration products, calcium hydroxide and alumina-bearing phases are more vulnerable to attack by sulfate ions. On hydration, Portland cements with more than 5% tricalcium aluminate (C_3A) will contain most of the alumina in the form of monosulfate hydrate ($C_3A.C\bar{S}.H_{12}$). If the C_3A content of cement is more than 8% the

hydration products will also contain the hydrogarnate ($C_3A.CH.H_{12}$). In the presence of calcium hydroxide, when the cement paste comes in contact with sulfate ions, both the alumina-containing hydrates are converted to ettringite ($C_3A.\ 3C\bar{S}.\ H_{32}$) causing expansion and spalling. For example in a study of two type I cements with 11.9% and 9.3% of C_3A with a C_3S/C_2S ratio of 7.88 and 2.57 respectively were investigated for sulfate deterioration it was observed that the cement with higher C_3A content had a deterioration level 2.5 times higher than the lower C_3A content. [15]

2) Cat ion Type: Sulfate attack is usually attributed to sodium, potassium, magnesium and calcium sulfate salts. Due to the limited solubility of calcium sulfate in water at normal temperatures (i.e., approximately 1400mg/l), It is noticed that sodium and potassium sulfates have a very similar sulfate attack and hence it has been studied as one by many authors hence sulfate attack can be divided in to sodium ($N\bar{S}A$) and magnesium sulfate ($M\bar{S}A$) attack. It has been reported that that the strength reduction in all blended cements exhibited superior performance in the sodium sulfate environment ($N\bar{S}A$) as compared with plain cements. However, the strength reduction was very high in all the cements exposed to magnesium sulfate solution ($M\bar{S}A$). Further, the reduction in strength in the blended cements was more than that in the plain cements. This is primarily due to the reduced calcium hydroxide (CH) content in the blended cements. [15]

It has been reported that the expansions in the specimens exposed to sodium sulfate environment ($N\bar{S}A$) was higher when compared to those specimens exposed to the magnesium sulfate solution ($M\bar{S}A$). Blended cements exhibited a better

performance in the sodium sulfate environment ($N\bar{S}A$) as compared with plain cements. However the specimens with blended cements exhibited greater expansion when compared to plain cements when exposed to magnesium sulfate solution ($M\bar{S}A$). [15]

3) C_3S/C_2S Ratio: Cements with low C_3A generally have a higher C_3S/C_2S ratio. An increase in C_3S content of the cement generates a significantly higher quantity of calcium hydroxide. The produced calcium hydroxide may directly combine with sulfate ions to produce gypsum. The gypsum reduces the stiffness and cohesiveness of the hardened cement and later gypsum also has the tendency to react with C_3A to form ettringite. For example in a study two mixes PC1 and PC2 with 7.73 % and 11.39% of C_3A and C_3S/C_2S ratio of 4.38 and 3.58 respectively were investigated for sulfate attack it was observed that larger expansions were sited in PC1 mix than PC2 mix. [16]
4) Effect of Temperature and Concentration: An increase in temperature of the solution at the early ettringite formation (EEF) stage leads to a decrease in expansion for specimens stored in the sodium sulfate solution. However, during at the delayed ettringite formation (DEF) stage the rate of expansion was similar at all temperatures. In the case of specimens exposed to magnesium sulfate solution, an increase in temperatures led to an increase of the rate of expansion.

   As the concentration of the solution increases the rate of expansion increases for the specimens stored in sulfate solution at the DEF stage. However it makes no difference at the EEF stage. In the case of specimens exposed to magnesium sulfate

solution the increase in concentration led to higher expansion both at EEF and DEF stage. [17, 18]

5.3. Experimental Results and Observations

The ASTM C 1012 test method based on the evaluation of the linear expansion of samples exposed to Sodium Sulfate Solution at room temperature was performed and the results are presented in the following. It is mentioned that “average expansion” in the following graphs means the average value for 4 or 5 similar specimens for each set of paste or mortar bars.

5.3.1. Cement Mortar Sample A (1” x 1” x11”)

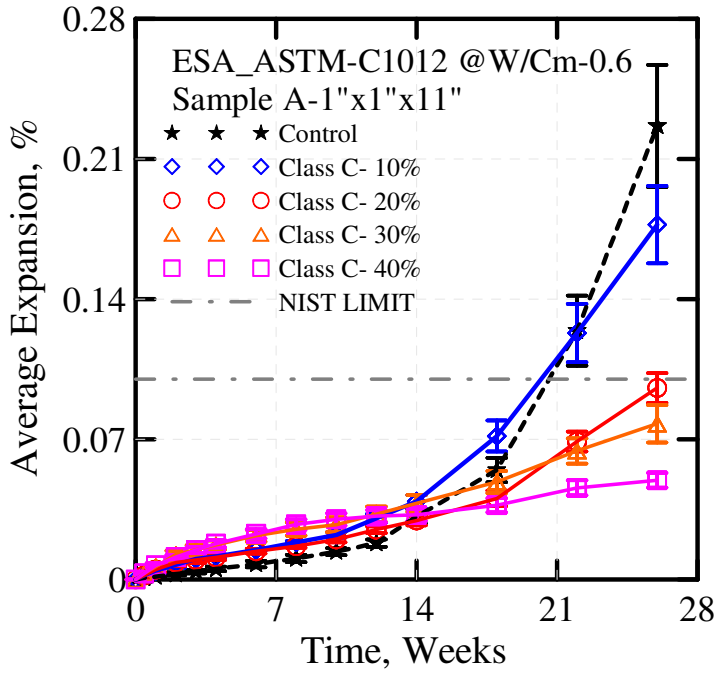

Figure.5.3.1.1 Average Expansions for Class C- Fly Ash (ESA)

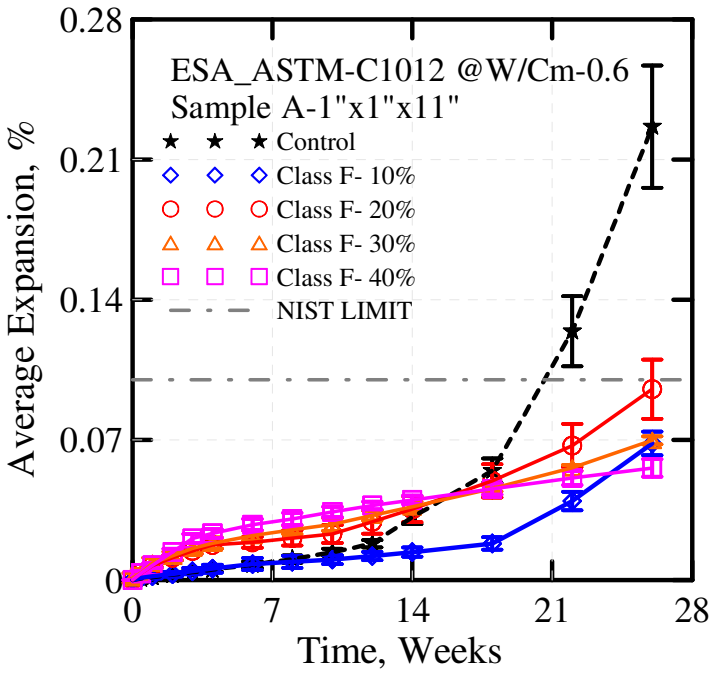

Figure.5.3.1.2 Average Expansions for Class F- Fly Ash (ESA)

Figures 5.3.1.1 and 5.3.1.2 show the comparison of control specimens with different replacement levels (i.e.10, 20, 30 & 40%) of Class C and Class F fly ash respectively.

1) It was noticed that both Class C and F fly ash replaced specimens showed much lower expansions when compared to control specimen by the end of the testing period which is being considered as 6 months.
2) Initial expansions (i.e. time being 0-14 week's) are such that, as the replacement level increases the expansion increases. Though the 10% replacement of Class F showed different trend (which was treated as a miss-fit curve).
3) It was observed that for Class C fly ash replaced specimen the replacement level has to be greater than 10% to mitigate sulfate attack, since 10% replacement specimen did not pass the NIST limit of 0.1% for 6 months, for all other replacement (i.e.20, 30 & 40%) the specimen passed the NIST limit of 0.1% for 6 months.

4) It was observed that for Class F fly ash replaced specimens the expansions of all replacement level (i.e. 10, 20, 30 & 40%) was under the specified NIST limit of 0.1% for 6 months though the 10% replacement specimens had expansion greater which were considered to be a miss fit in the experimental results.

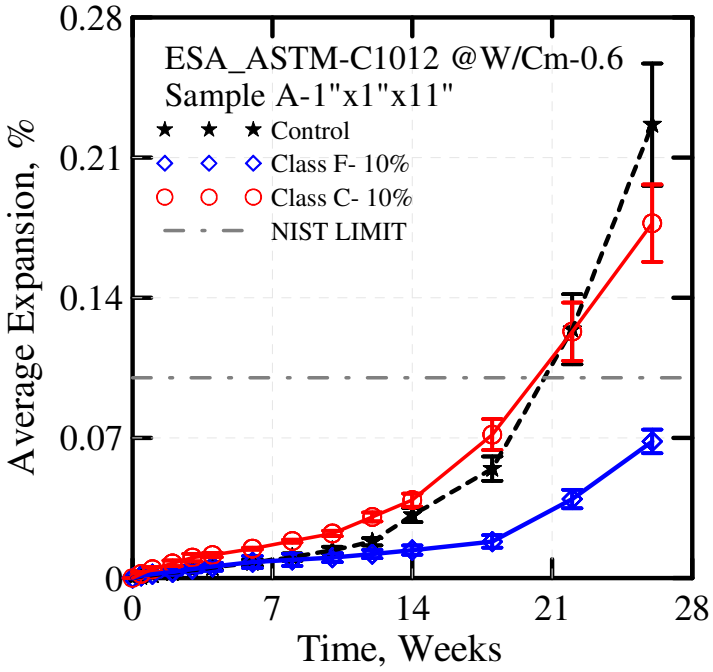

Figure.5.3.1.3 Comparison Between 10 % (Class C , F) & Control Specimen (ESA)

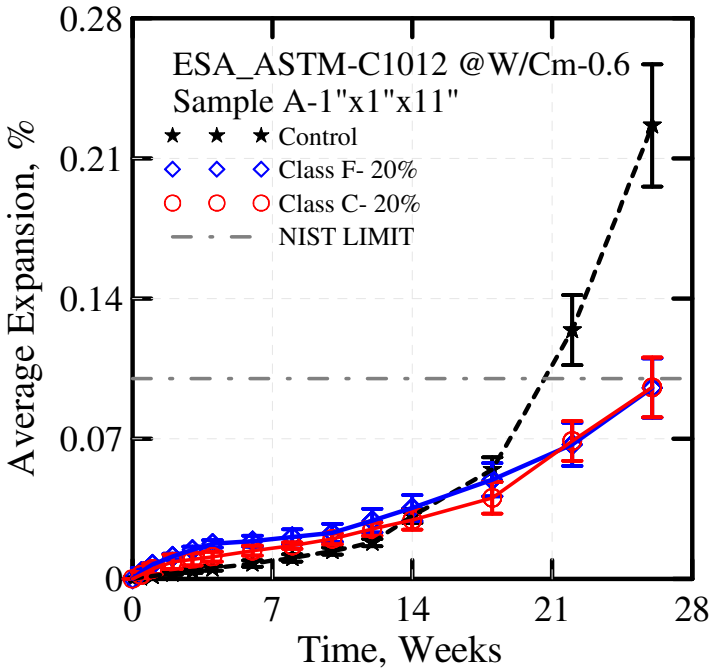

Figure.5.3.1.4 Comparison Between 20 % (Class C , F) & Control Specimen (ESA)

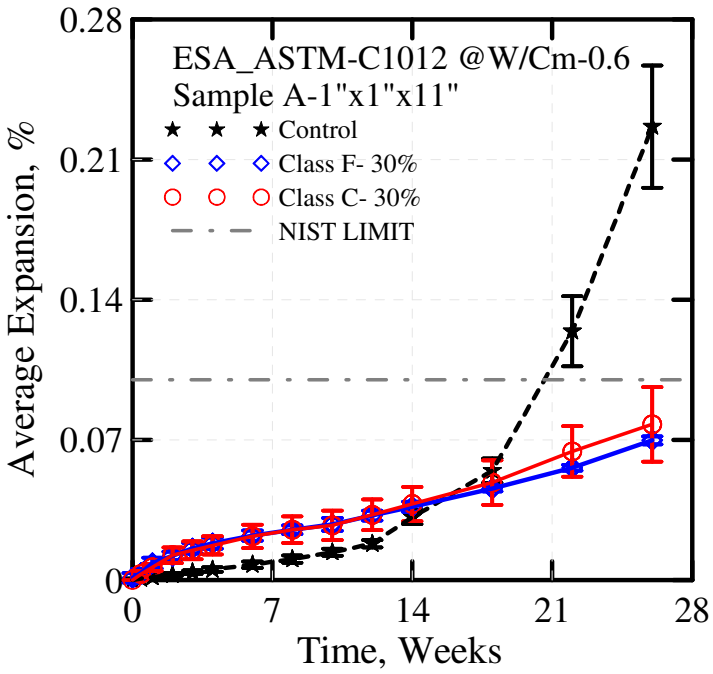

Figure.5.3.1.5 Comparison Between 30 % (Class C , F) & Control Specimen (ESA)

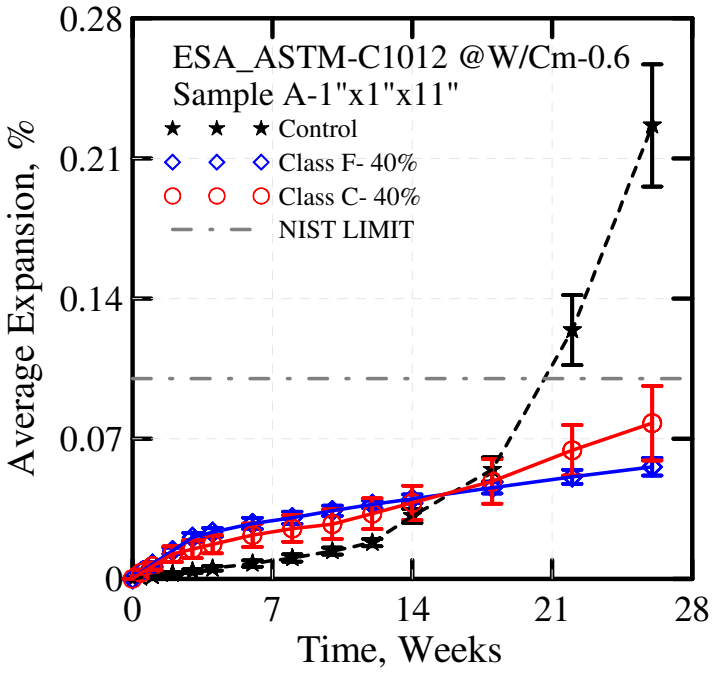

Figure.5.3.1.6 Comparison Between 40 % (Class C , F) & Control Specimen (ESA)

Figures 5.3.1.3 through 5.3.1.6 shows the comparison between Control, Class C and Class F fly ash replaced specimen with replacement levels of 10, 20, 30 & 40% respectively.

1) It was observed that for the initial period (i.e. time being 0-14 week's) Class F fly ash replaced specimen showed greater expansion when compared Class C fly ash replaced specimens Though the 10 % replacement of Class F showed different trend (which was treated as a miss-fit curve). But after the 14th week Class F fly ash replaced specimen mitigated expansions better when compared to Class C.

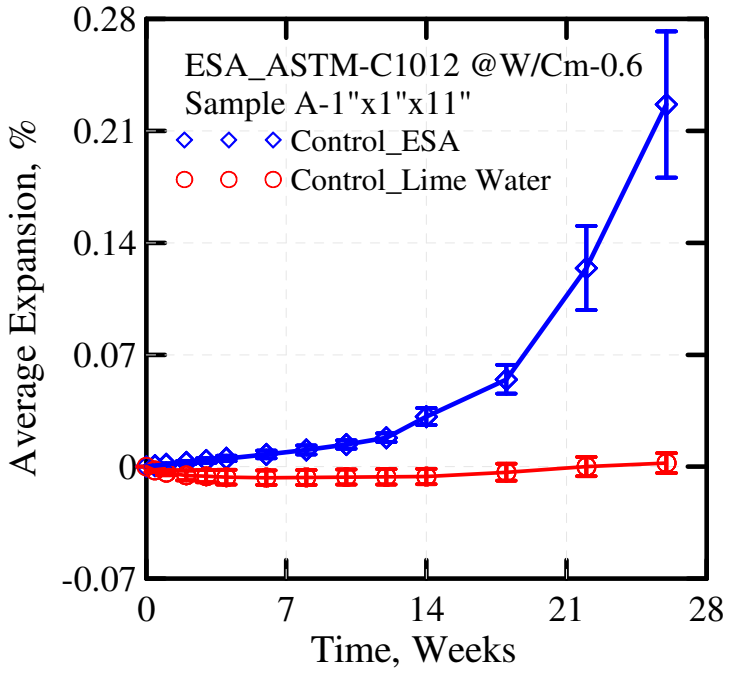

Figure.5.3.1.7 Comparison Between Control Specimen (ESA) and Lime Water

1) When specimens exposed to external sulfate attack was compared to specimens exposed to lime water, it was observed that specimens exposed to lime water did not

have any expansion this implies that the expansions caused due to external sulfate attack was solemnly due to the reaction products produced to cement chemistry.

5.3.2. Cement Paste Sample A (1” x 1” x11”)

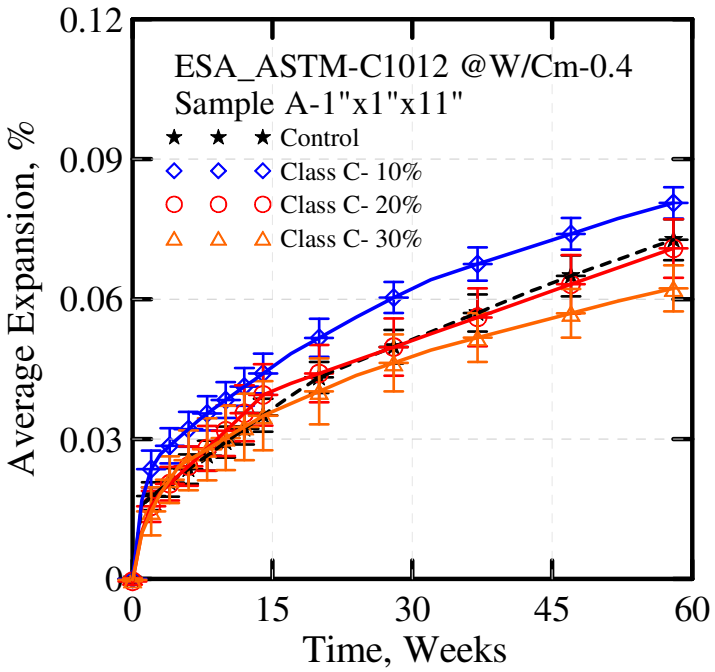

Figure.5.3.2.1 Average Expansions for Class C- Fly Ash (ESA)

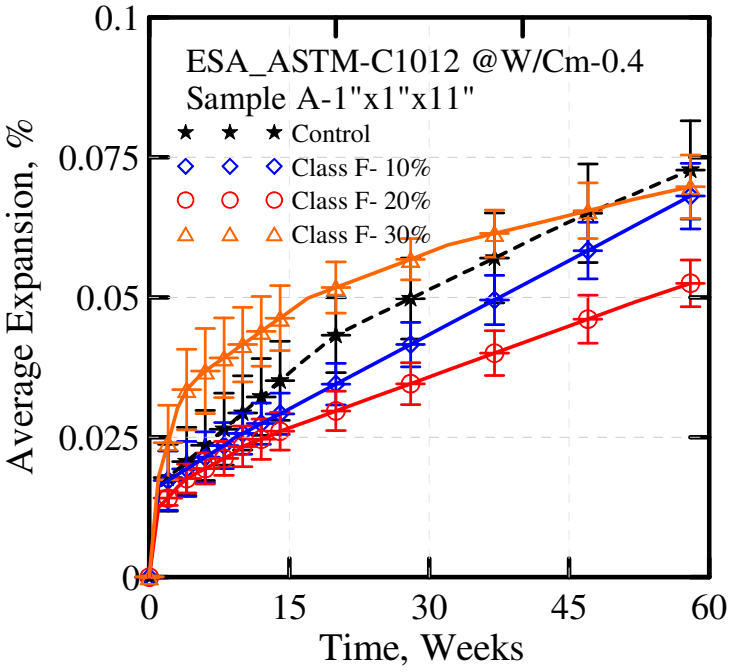

Figure.5.3.2.2 Average Expansions for Class F- Fly Ash (ESA)

Figures 5.3.2.1 and 5.3.2.2 shows the comparison of standard sized control paste specimens with different replacement levels (i.e.10, 20 & 30%) of Class C and Class F fly ash respectively.

1) It was observed that for standard sized paste Class C fly ash replaced specimen, the expansion reduced as the replacement level increased and the 10% Class C fly ash replacement specimens had greater expansions than the control specimen, this implies that addition of Class C fly ash in lower % may worsen the ability to mitigate sulfate attack.
2) When we compare the overall expansions of paste and mortar samples it was observed that the expansions in mortar specimen were much greater than the paste specimen, this is probably because of the ITZ phase in mortar and high porosity.

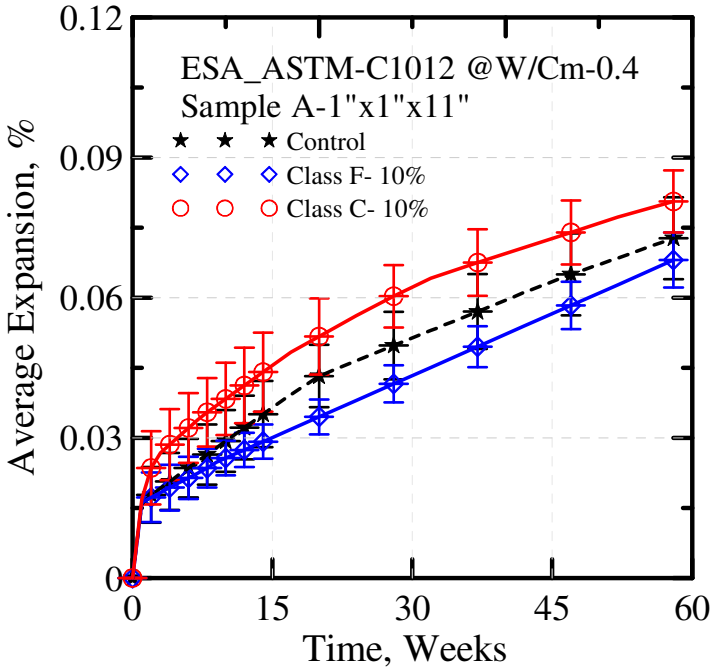

Figure.5.3.2.3 Comparison Between 10 % (Class C , F) & Control Specimen (ESA)

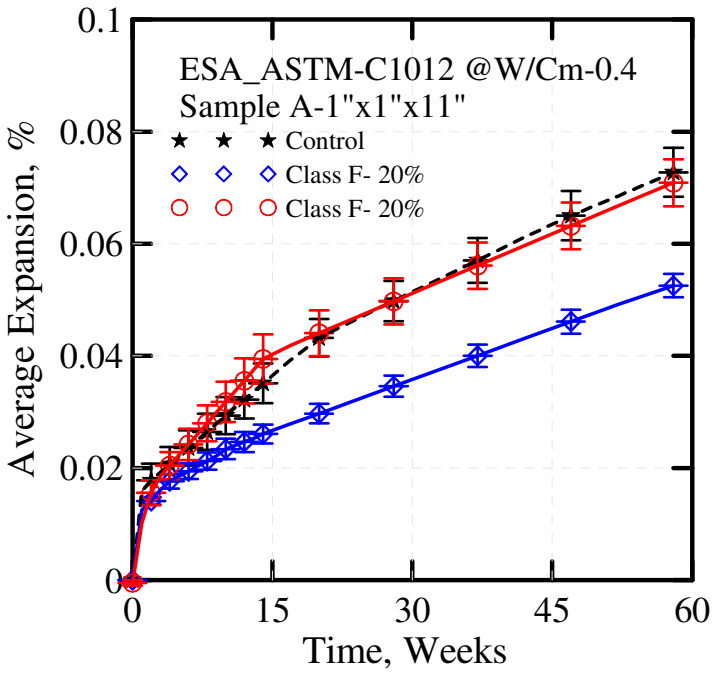

Figure.5.3.2.4 Comparison Between 20 % (Class C , F) & Control Specimen (ESA)

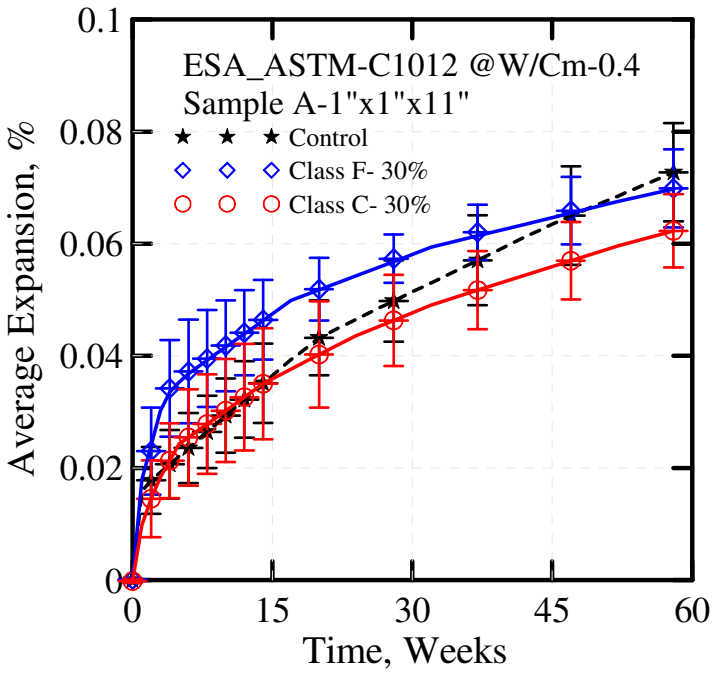

Figure.5.3.2.5 Comparison Between 30 % (Class C , F) & Control Specimen (ESA)

Figures 5.3.2.3 through 5.3.2.5 shows the comparison between standard sized Control, Class C and Class F fly ash replaced paste specimen with replacement levels of 10, 20 & 30% respectively.

1) It was observed that for standard sized paste Class F fly ash replaced specimen the expansions reduced for 10 & 20% replacement but 30% replaced specimen had greater expansion than the control specimen; this implies that replacement of Class F fly ash cannot be greater than 30% for paste specimen.

5.3.3. Cement paste Sample B (0.4” x 0.4” x 4”)

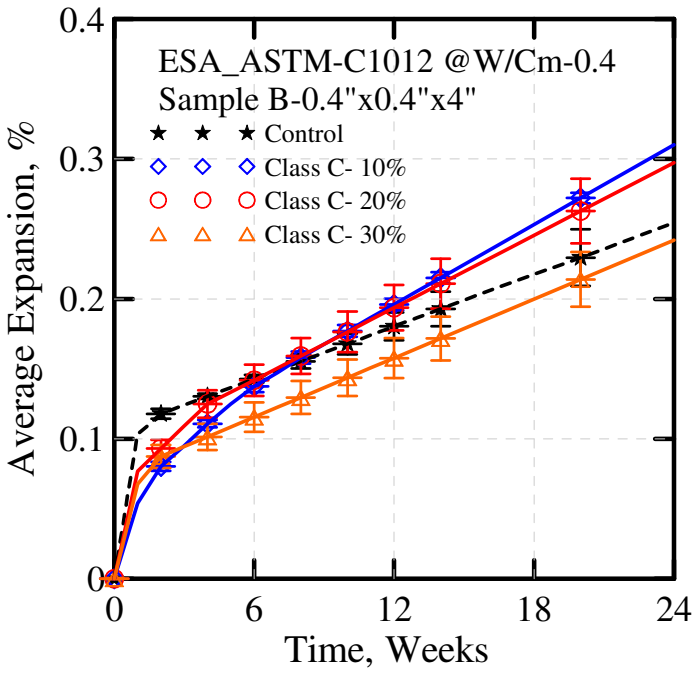

Figure.5.3.3.1 Average Expansions for Class C- Fly Ash (ESA)

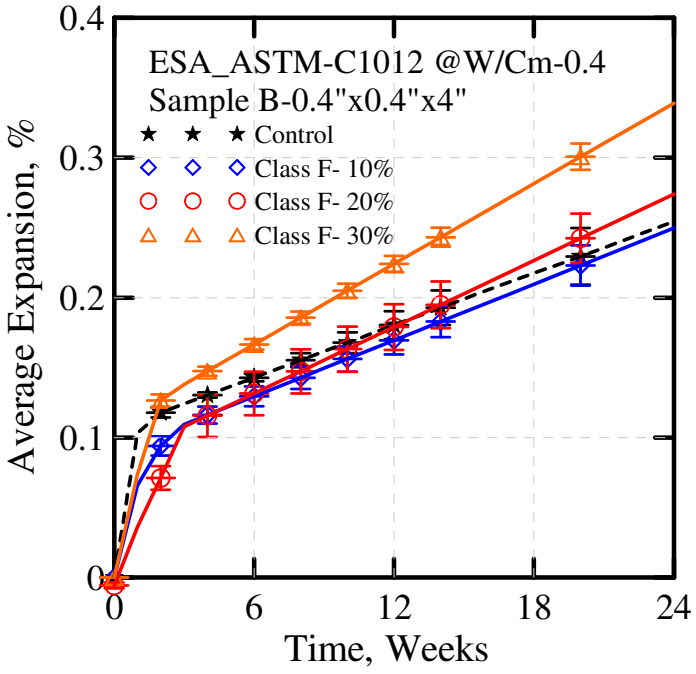

Figure.5.3.3.2 Average Expansions for Class F- Fly Ash (ESA)

Figures 5.3.3.1 and 5.3.3.2 shows the comparison of modified sized control paste specimens with different replacement levels (i.e.10, 20 & 30%) of Class C and Class F fly ash respectively.

1) It was observed that for modified sized Class C fly ash replaced specimen the expansion decreased as the replacement increased, it was noticed that 10% replacement specimen had greater expansions than the control sample, Hence Class C fly ash cannot be used as a replacement below 20%

2) It was observed that for modified sized Class F fly ash replaced specimen the expansion increased as the replacement increased, it was noticed that 20 & 30% replacement specimen had greater expansions than the control sample, Hence Class F fly ash cannot be used in greater replacement (i.e. < 20%).

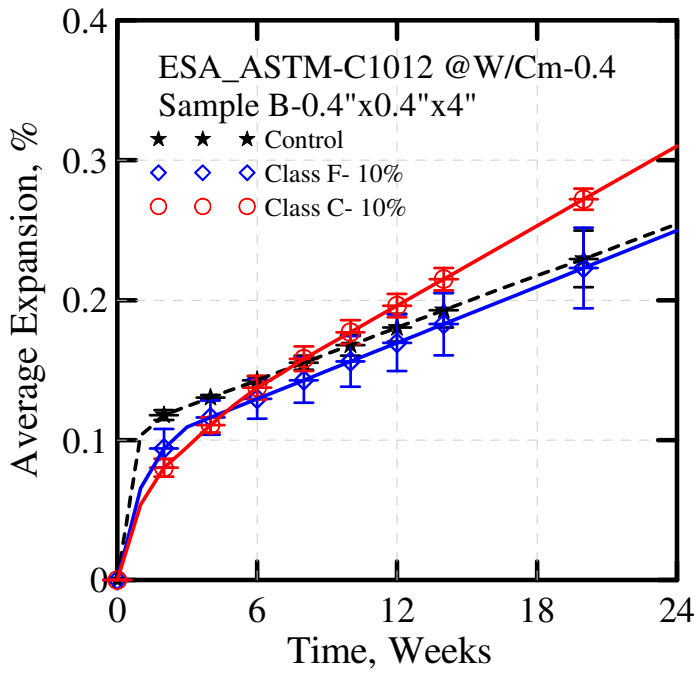

Figure.5.3.3.3 Comparison Between 10 % (Class C , F) & Control Specimen (ESA)

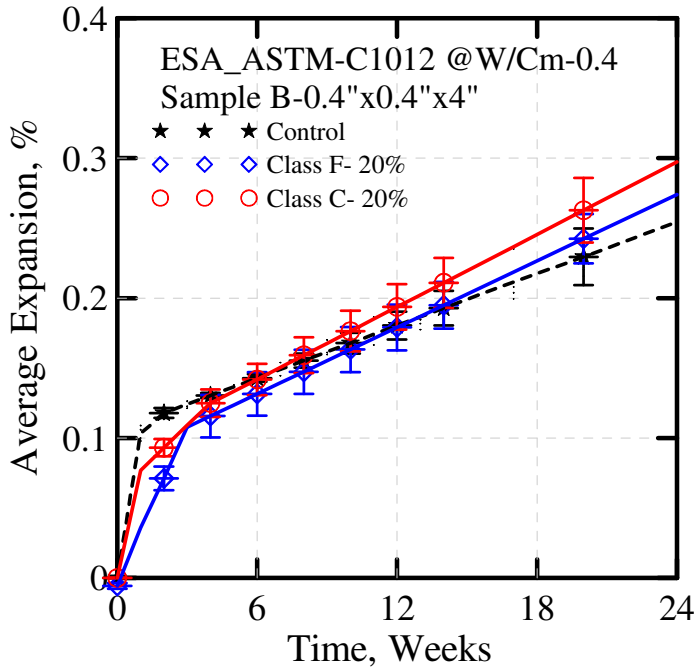

Figure.5.3.3.4 Comparison Between 20 % (Class C , F) & Control Specimen (ESA)

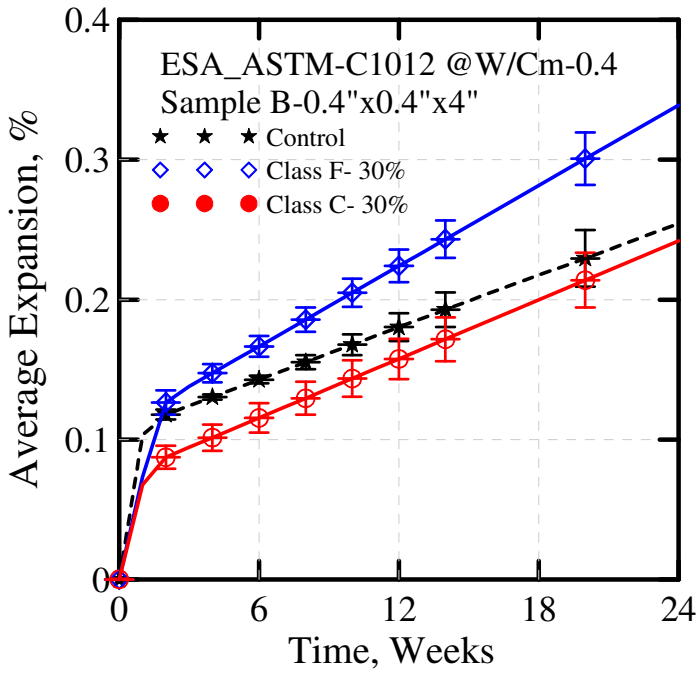

Figure.5.3.3.5 Comparison Between 30 % (Class C , F) & Control Specimen (ESA)

Figures 5.3.3.3 through 5.3.3.5 shows the comparison between modified sized Control, Class C and Class F fly ash replaced paste specimen with replacement levels of 10, 20 & 30% respectively.

1) It was observed that both standard and modified sized specimens follow the same expansion trends, in both cases Class F ash replaced specimen performed better in mitigating expansions for lower percentage levels (i.e. 10 & 20 %) whereas Class C performed better at higher replacement levels (i.e. 30%).

5.3.4. Compression Test Mortar

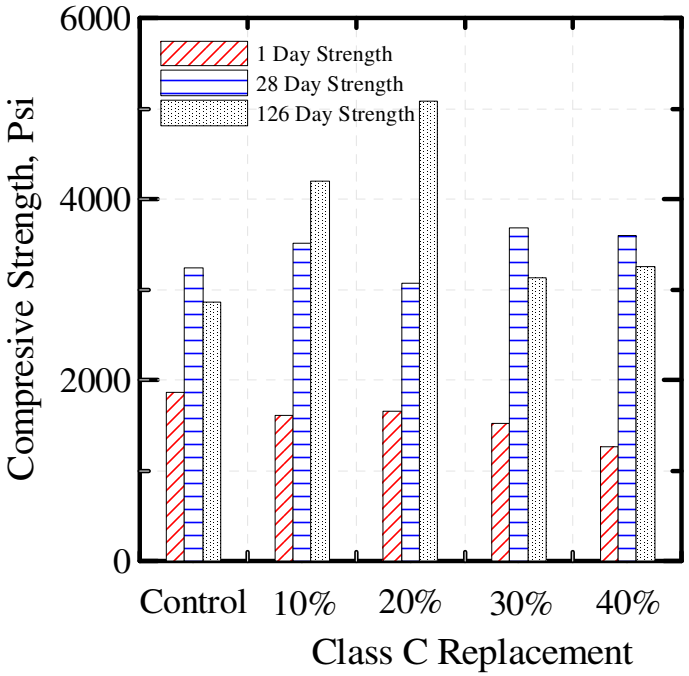

Figure.5.3.4.1 Compression Strength for Class C- Fly Ash (ESA)

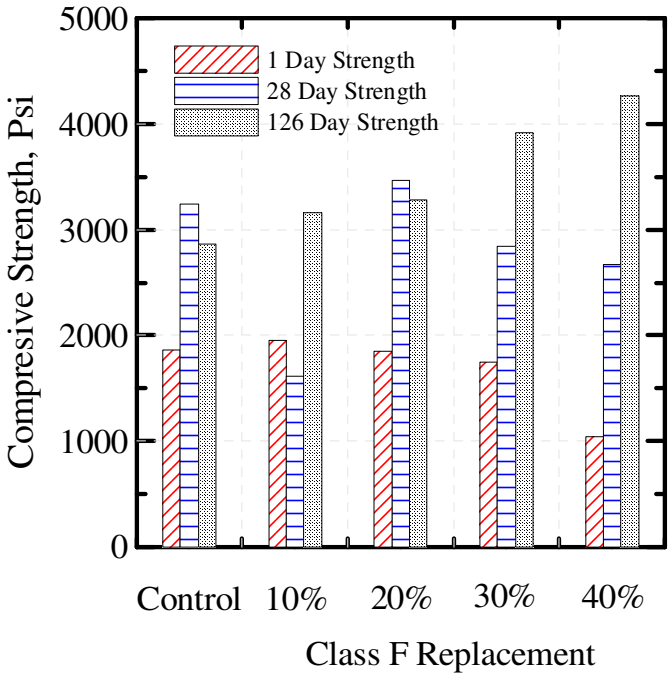

Figure.5.3.4.2 Compression Strength for Class F- Fly Ash (ESA)

Figures 5.3.4.1 and 5.3.4.2 show the comparison of compressive strength of the control specimens with different replacement levels (i.e.10, 20, 30 & 40%) for 1, 28 & 126 days of Class C and Class F fly ash respectively.

1) It was observed that the compressive strength of the control specimen increases initially (i.e. for the 28th Day) but then decreases (i.e. for the 126th Day). This reduction in strength is due to the degradation of cement matrix due to sulfate attack.
2) It was observed that the compressive strength of the Class C specimen increases with time for the 10 & 20% but the 30 & 40% replacement levels show a initial increase for the 28^{th} day but then decreases for the 126^{th} day. This behavior can be explained because of the higher calcium content in Class C fly ash, which can be deleterious in higher proportions in the cement matrix exposed to sulfate attack.

3) It was observed that the compressive strength of the Class F specimen increases with time for the 30 & 40% but the 10 & 20% replacement levels show a initial increase in compressive strength for the 28th day but then decreases for the 126th day.

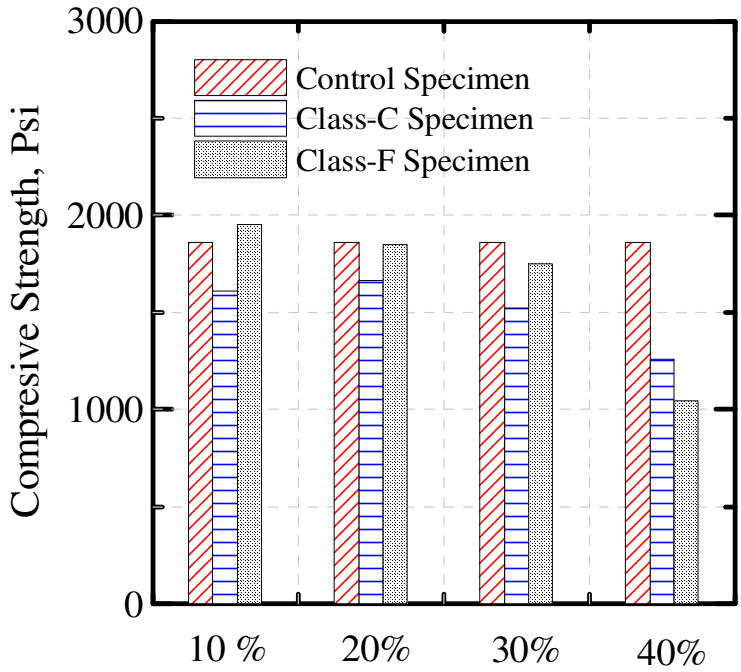

Figure.5.3.4.3 Comparison of Compressive Strength for Class F and Class C Fly Ash (ESA) for the 1st Day

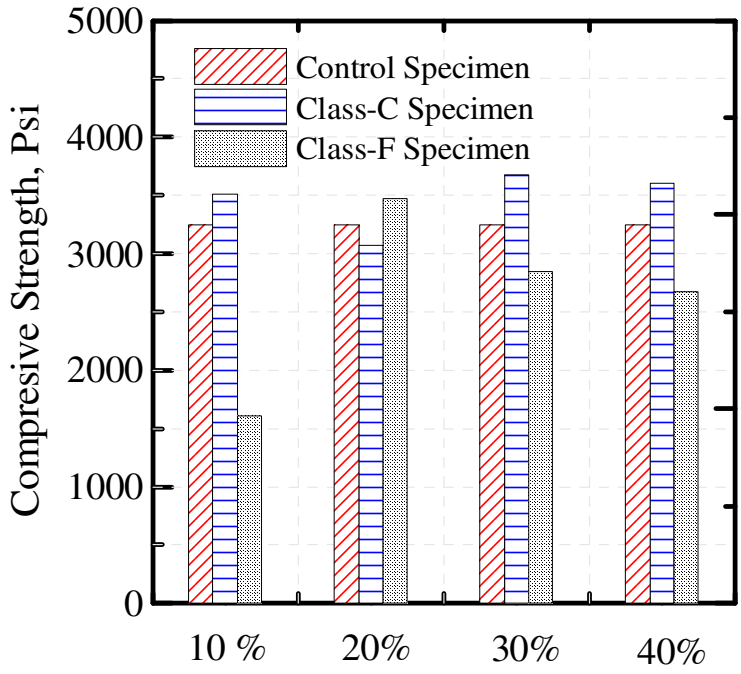

Figure.5.3.4.4 Comparison of Compressive Strength for Class F and Class C Fly Ash (ESA) for the 28th Day

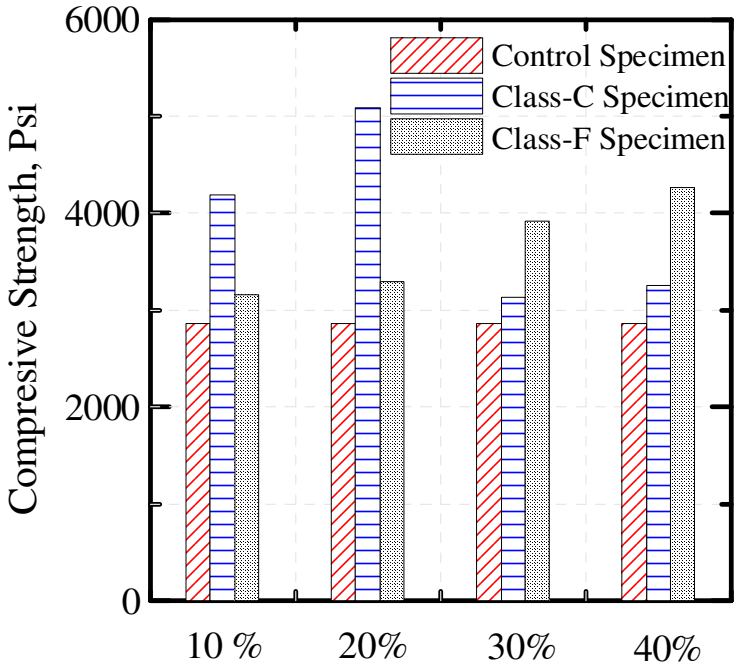

Figure.5.3.4.5 Comparison of Compressive Strength for Class F and Class C Fly Ash (ESA) for the 126th Day

Figures 5.3.4.3 through 5.3.4.5 show the comparison of compressive strength of the control specimens with different replacement levels (i.e.10, 20, 30 & 40%) of Class C and Class F fly ash for 1, 28 & 126 days respectively.

1) When compressive strengths of specimens exposed to sulfate solution and specimens cured in limewater were compared it was observed that the specimens exposed to sulfate attack had greater compressive strengths for all the curing period (i.e. 1^{st}, 28^{th} and 126^{th} day).
2) It was observed that for all replacement levels of Class C fly ash specimens the compressive strength was lesser than the control specimen strength for 1^{st} day.
3) It was observed that for 10, 20 & 30% replacement of Class F fly ash. The specimens 1^{st} day compressive strength was almost equal to the control specimens compressive strength for the 1^{st} day, but for the 40% replacement of Class F fly ash had a compressive strength much lesser than the control specimen.
4) It was observed that for all replacement levels of Class C fly ash specimens the compressive strength for 28^{th} Day was greater than the control specimen compressive strength for the 28^{th} day.

Table 5.3.4.1

Young's Modulus for Class F Fly Ash

% Replacement	E=57000$\sqrt{f'c}$ psi converted to GPa		
	1st Day	28th Day	126th Day
0	16.95 GPa	23.38 GPa	21.03 GPa
10	17.36 GPa	15.78 GPa	22.08 GPa
20	16.91 GPa	23.16 GPa	22.53 GPa
30	16.43 GPa	20.96 GPa	24.36 GPa
40	12.68 GPa	20.35 GPa	25.61 GPa

Table 5.3.4.2

Strength Activity Index of Class F Fly Ash

% Replacement	Strength Activity Index		
	1st Day	28th Day	126th Day
0	1	1	1
10	1.04821	0.49695471	1.10239
20	0.99484	1.07012341	1.14771
30	0.93917	0.87670778	1.36927
40	0.55968	0.82255143	1.48844

Tables 5.3.4.1 and 5.3.4.2 illustrate the young's modulus and strength activity index of control specimens and replacement levels (i.e.10, 20, 30 & 40%) of Class F fly ash for 1, 28 & 126 days respectively.

1) It was observed that for Class F fly ash specimen the strength activity index reduces as the percentage level of replacement increases for 1st and 28th day, but as the time increases to 126th day the strength activity increases with the increase in percentage replacement.

Table 5.3.4.3

Young's Modulus for Class C Fly Ash

% Replacement	E=57000$\sqrt{f'c}$ in psi converted to GPa		
	1st Day	28th Day	126th Day
0	16.95 GPa	23.38 GPa	21.03 GPa
10	15.75 GPa	23.27 GPa	25.45 GPa
20	16.02 GPa	21.77 GPa	28.02 GPa
30	15.34 GPa	23.84 GPa	22.01 GPa
40	13.96 GPa	23.59 GPa	22.43 GPa

Table 5.3.4.4

Strength Activity Index of Class C Fly Ash

% Replacement	Strength Activity Index		
	1st Day	28th Day	126th Day
0	1	1	1
10	0.86341	1.0808	1.46457
20	0.89326	0.94634	1.77583
30	0.81836	1.13399	1.09549
40	0.67776	1.11095	1.13745

Tables 5.3.4.3 and 5.3.4.4 illustrate the young's modulus and strength activity index of control specimens and replacement levels (i.e.10, 20, 30 & 40%) of Class C fly ash for 1, 28 & 126 days respectively.

1) It was observed that for Class C fly ash specimen the strength activity was almost equal to the control specimen for 1st and 28th day, but as the time increased to 126th day, the strength activity index for lower percentage replacement levels

5.4. SEM and EDS analysis

Microstructural studies were carried out on modified size paste specimens exposed to sulfate attack for more that one year. SEM images and EDS spectra were obtained and are presented in the following.

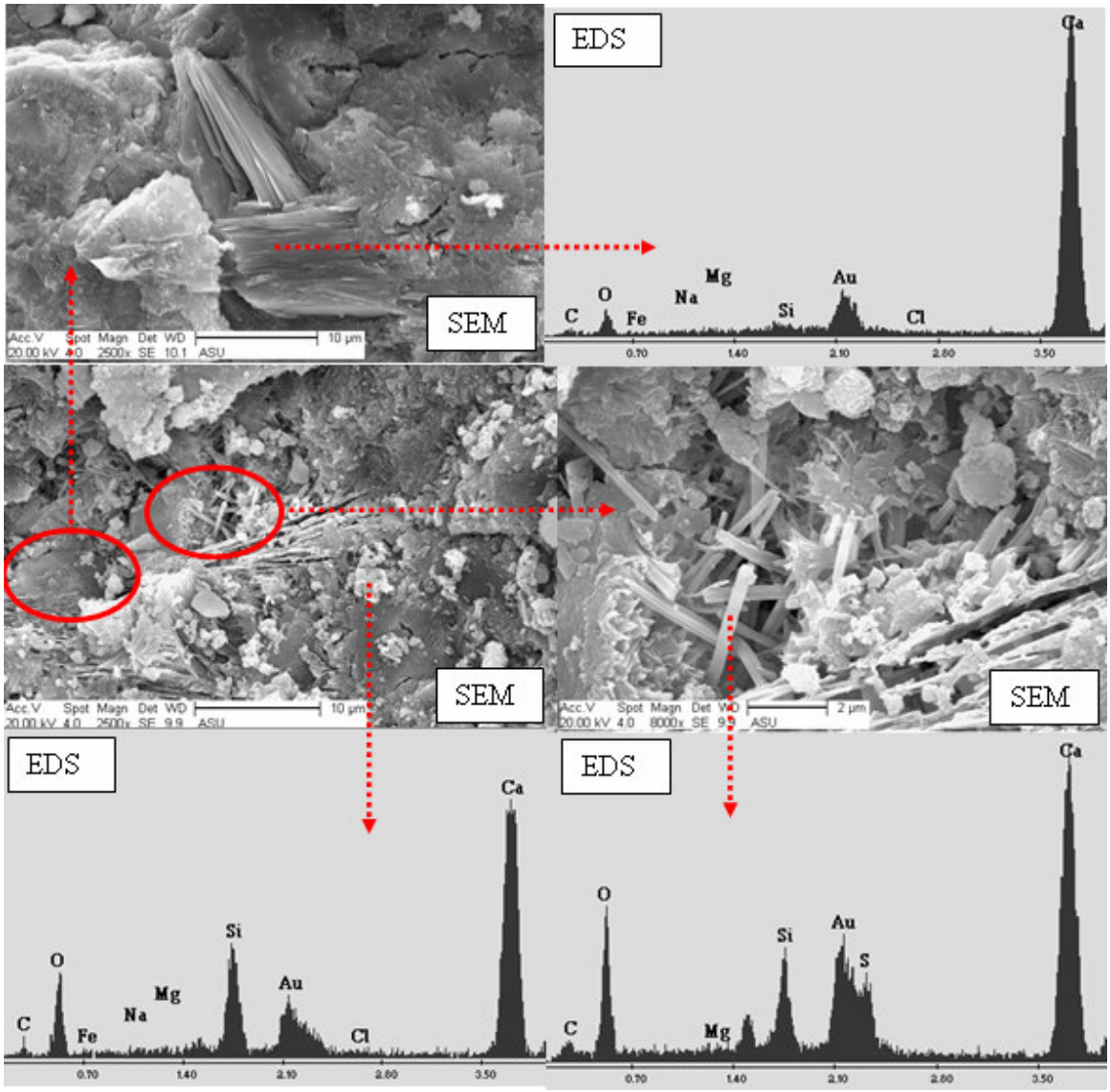

Figure.5.4.1 SEM and EDS of Control Specimen on the 80th Week (SA)

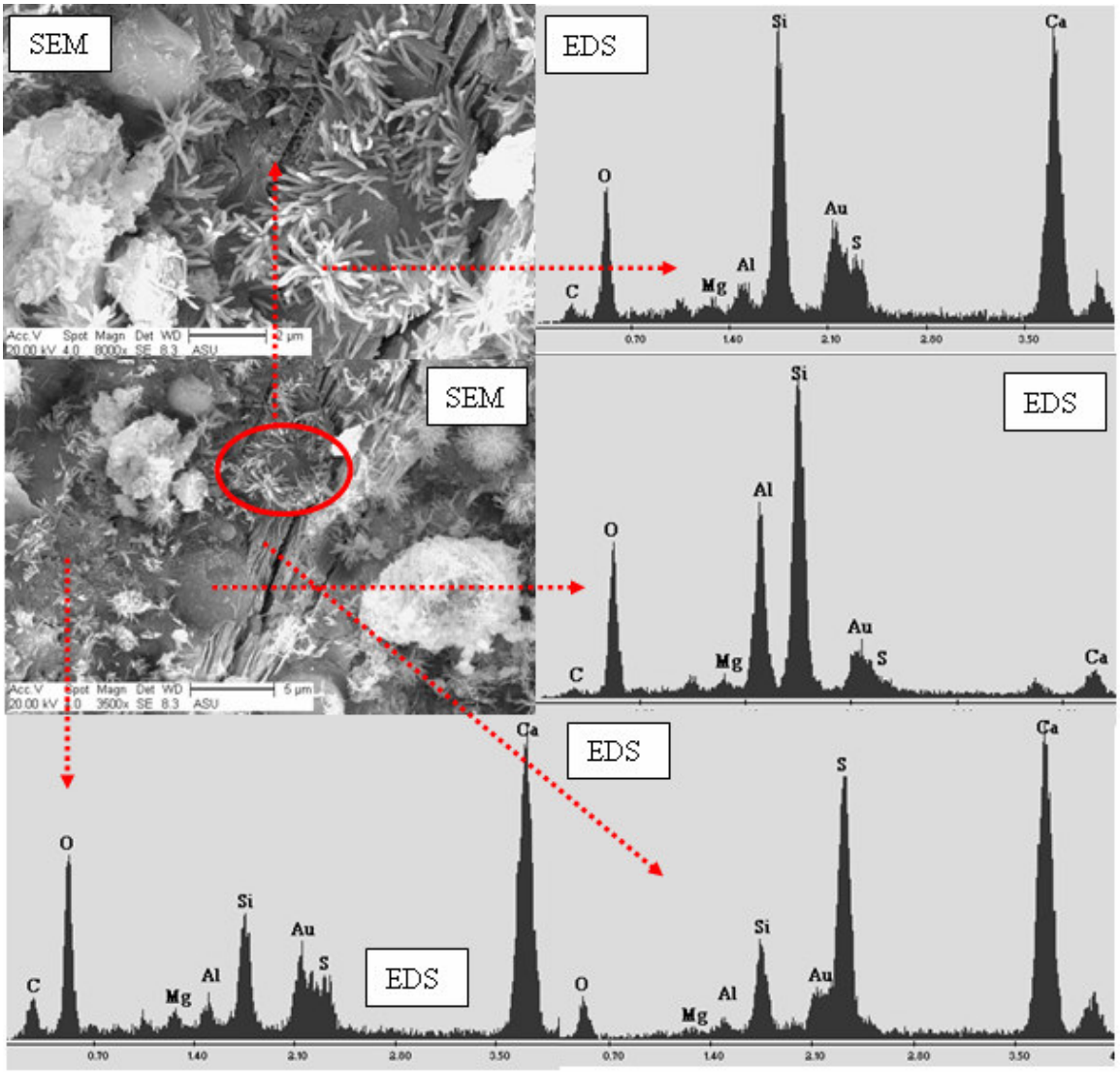

Figure. 5.4.2 SEM and EDS of Class F Specimen on the 80th Week (SA)

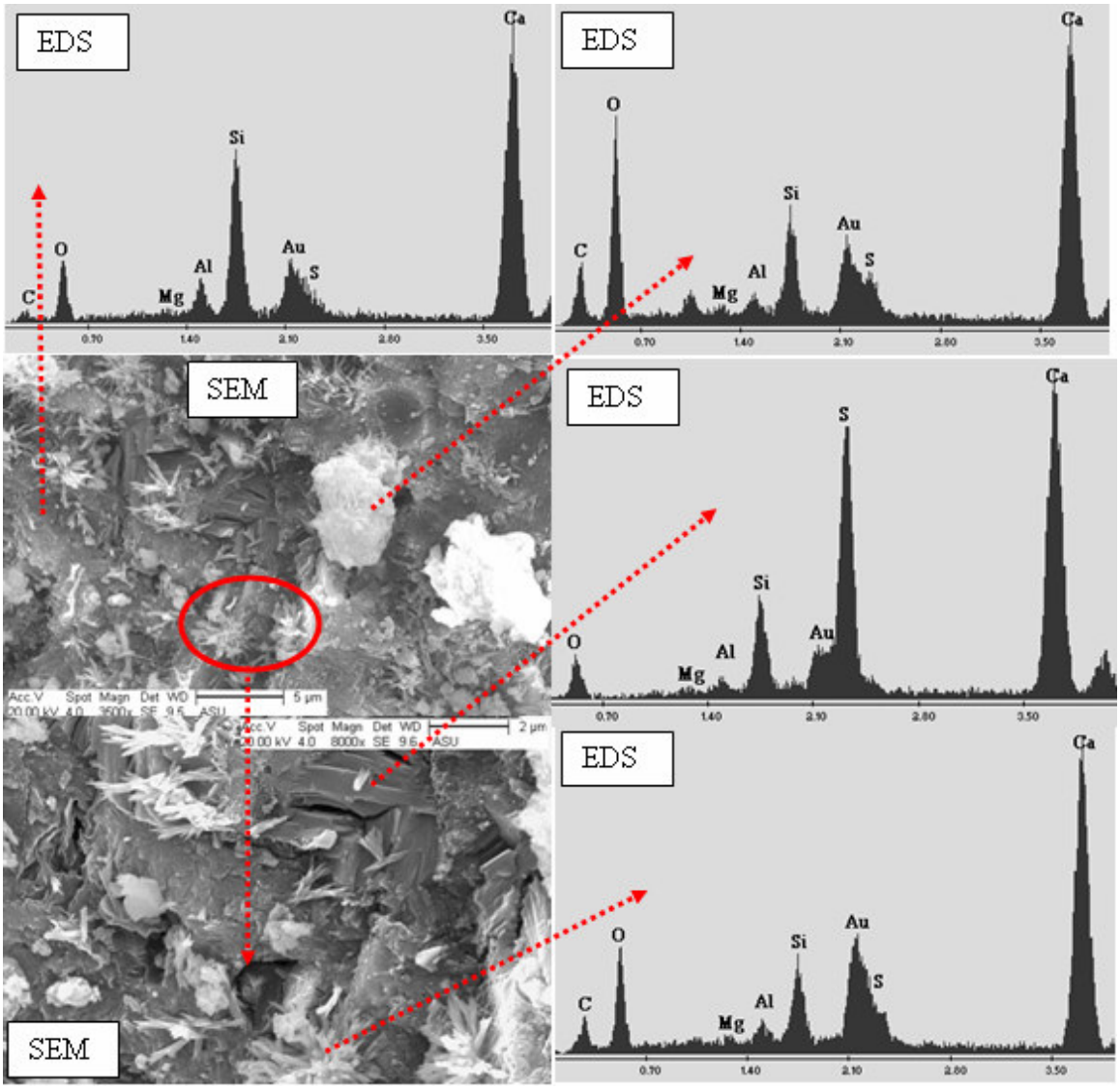

Figure. 5.4.3 SEM and EDS of Class C Specimen on the 80th Week (SA)

Figures 5.4.1, 5.4.2 and 5.4.3 show the SEM and EDS images of control, Class F and Class C specimens respectively for 80 weeks of exposure to external sulfate attack.

1) It was observed that needle like ettringite crystals were very prominent and bigger in size in control specimens compared to fly ash replaced specimen.
2) The chemical composition of the ettringite found in Class F fly ash replaced specimen was observed to be different when compared to Class C fly ash replaced and Control specimen, the amount of silica in the ettringite formed in Class F fly ash replacement specimen were much greater than the other two.
3) It was observed that fly ash specimens still had un-reacted fly ash particles after one year, Class F fly ash replacement specimen contained greater amounts of un-reacted fly ash particles when compared to Class C fly ash replacement specimen.
4) It was observed that both Class C and F fly ash replaced specimen contained gypsum and the control specimens contained portlandite.

5.5. Element Mapping Of Microstructure

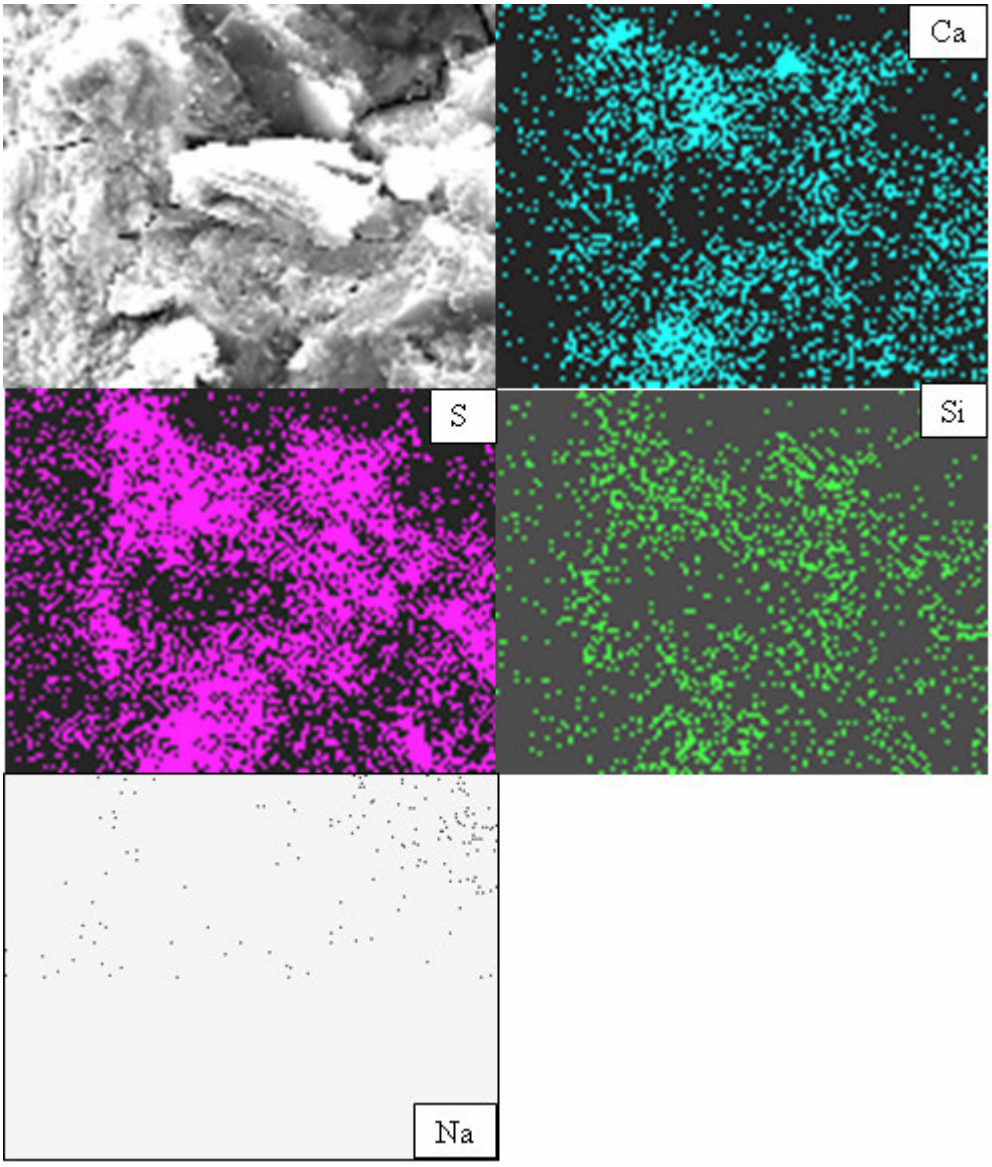

Figure.5.5.1 EDS mapping for Control Specimen on the 80th Week (SA)

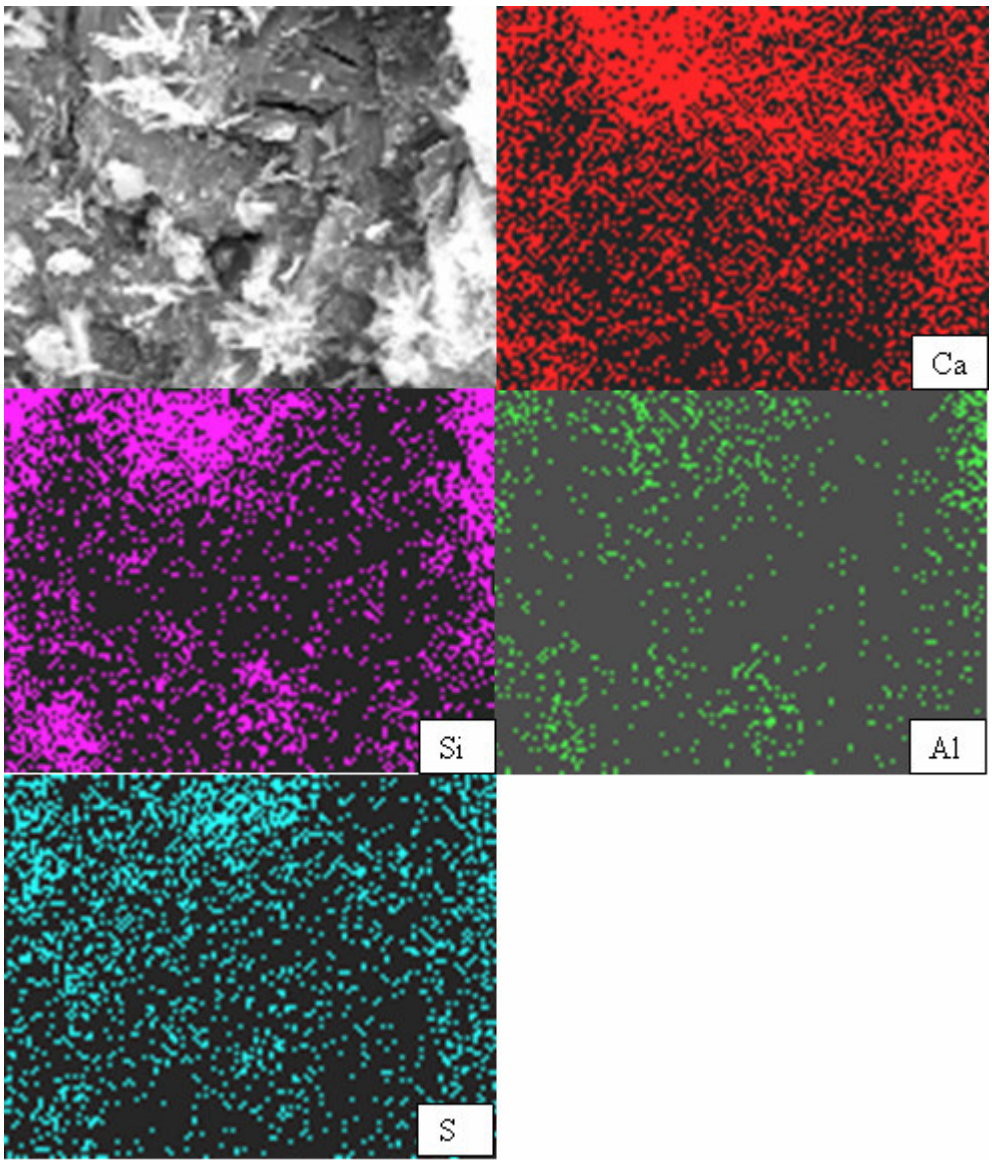

Figure.5.5.2 EDS mapping for Class C Specimen on the 80th Week (SA)

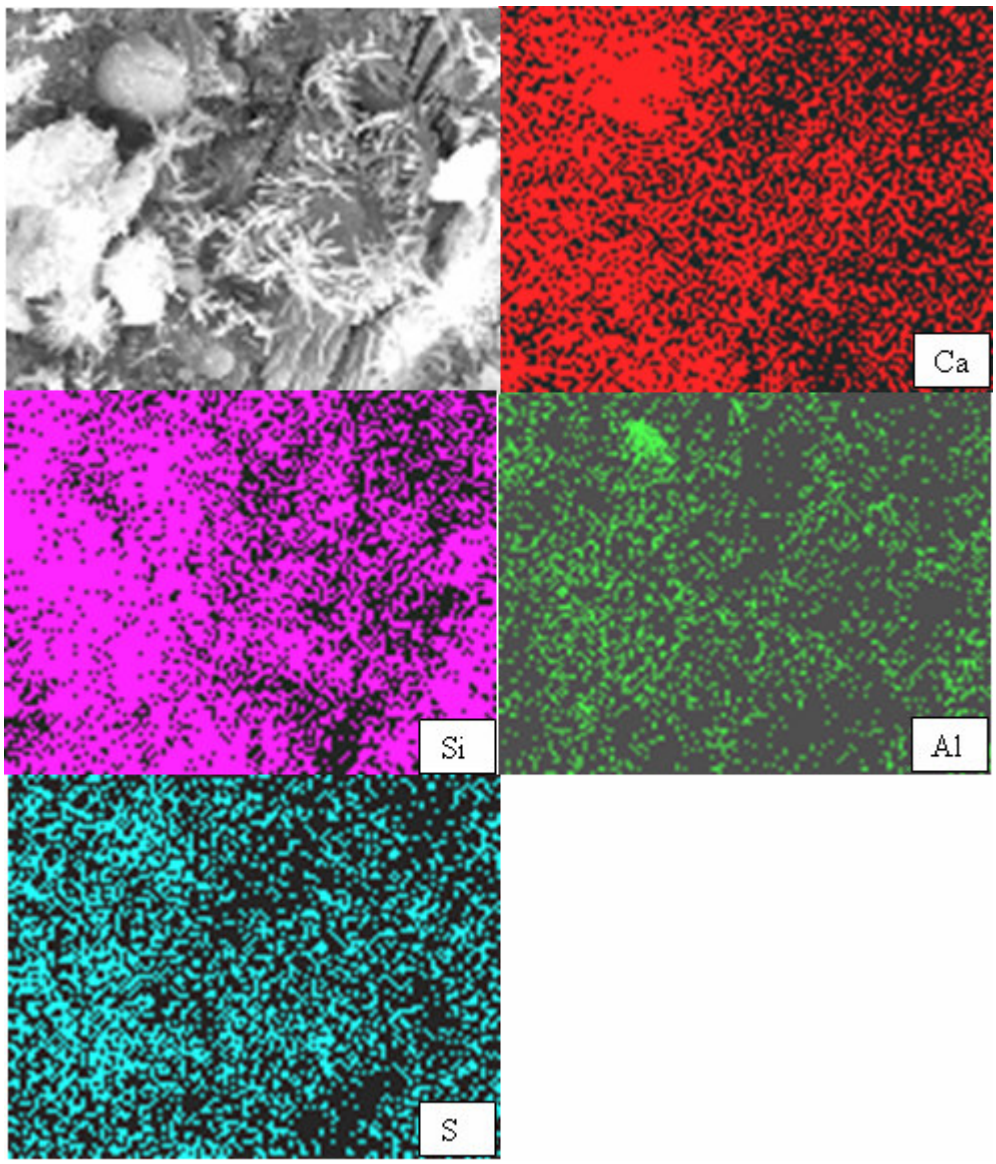

Figure.5.5.3 EDS mapping for Class F Specimen on the 80th Week (SA)

Figures 5.5.1, 5.5.2 and 5.5.3 shows the images of element mapping of control, Class C and Class F specimens respectively for 80 weeks of exposure to external sulfate attack.

1) It was observed that the concentration of sulfates in the scanned area of control specimens were much greater than the concentration of sulfates found in Class C and F fly ash replacement specimen.
2) It was observed that the concentration of calcium in Class F were greater to the concentration of calcium observed in Class C which intern was greater than the calcium found in the control specimen.
3) It was observed that the concentration of Class F was greater to the concentration of aluminum in Class C. Which was also noticed in EDS spectrums for the same specimens.

6. ALKALI SILICA REACTION –ASR

6.1. Introduction

An important aspect of concrete durability is its resistance to alkali aggregate reactions (AAR), Alkali aggregate reaction (AAR) is a chemo-physical expansive reaction in mortar or concrete between reactive mineral phases in aggregates and alkali hydroxide and/or calcium hydroxide in the pore solution from the cement paste or from external sources. The reaction can presently be divided in two types of reactions, depending on the types of minerals involved 1) Alkali-Carbonate Reaction (ACR) and 2) Alkali- Silica Reaction (ASR). [19]

1) Alkali-Carbonate Reaction (ACR) is the reaction between carbonate aggregate particles and the cement paste of Portland cement concrete/mortar. The composition of the carbonate rock involved determines which type of reaction occurs. Not all carbonate reactions are deleterious the only form of ACR known to be harmful to concrete is the "dedolomitization" reaction which may take place between argillaceous (clay-rich) dolomitic limestone aggregate particles and the high pH of the pore fluids in cement paste and the reaction involving in dedolomitization is as follows.[C]

   Dolomite+alkali hydroxide = brucite+calcium carbonate+ alkali carbonate

   $$CaMgCO_3 + 2ROH \longrightarrow Mg(OH)_2 + CaCO_3 + R_2CO_3 \quad \text{(6.1.1)}$$

   Alkali carbonate + calcium hydroxide = alkali hydroxide+ calcium carbonate

   $$R_2CO_3 + Ca(OH)_2 \longrightarrow 2ROH + CaCO_3 \quad \text{(6.1.2)}$$

   Where R may be any alkali (Sodium, Potassium)

2) Alkali silica reaction (ASR) is potentially a very disruptive reaction within concrete it is a chemical reaction between alkali hydroxide present as the principal source in the cement, some as the mineral constituents in the aggregate such as illitic clays, micas or feldspars, ground water and admixtures such as deicing salts, etc. ASR reaction produces the hydrophilic Alkali-Silica Gel (ASG) which by itself is not expansive but this gel has a very high tendency/capacity to absorb water from the pore solution making the pore solution more alkaline and causing the gels present in air voids and micro crack to expand or swell which intern cause failure of the concrete. The simplest equation which can be associated with ASR can be described as following [19, 20]

   Silicon dioxide + Alkali Hydroxide = Alkali Silica Gel + Water

   $$4SiO_2 + 2ROH \longrightarrow R_2Si_4O_9 + H_2O \quad \text{(6.1.3)}$$

   Where R may be any alkali (Sodium, Potassium)

During the cement hydration a certain amount of alkali ions can be released and carried into the pore solution. When fly ashes are used in cement as SCM, they reduce the available alkalies in the pore solution, which is called the dilution effect. Fly ashes do contain some alkalies in them but these are mainly held in glassy structure and are not readily available. Typically, only 16- 20 % of the total alkalis in fly ashes are water soluble. [A]

In this thesis no distinction is made between ACR and ASR. When we use the term ASR it is the effect of specimens exposed to NaOH solution according to ASTM C1260.

The aim of this work was

1) To study the resistance of Class C and Class F fly ashes as a SCM to ASR.
2) To study the effect of different level of Class C and Class F replacement (20%-40%)
3) To study the microstructure of specimen subjected to ASR.

6.2. Literature Review

Many results have been published from the experimental data on ASR and the mitigation methods. ASTM C 1260 and C 1293 have been traditionally used for short term and long-term test of ASR, respectively.

6.2.1. Proposed Theories of ASR

Though the exact mechanism of ASR reaction is not very well understood many theories have been proposed by different researchers and in the literature review they have been identified as following.

The hydroxyl ions (OH^-) attacks the reactive aggregate and provokes its dissolution, this dissolved silica reacts with alkalis (Na^+ or K^+) to form alkali-silica gel (ASR Gel).

1) The expansion of concrete is due to the osmotic pressure generated by alkali silica gels, which are confined within a semi permeable membrane of cement paste [25].
2) The expansion is a consequence of the formation and subsequent widening of cracks due to mechanical pressure exerted by the reaction products [26].
3) The expansion of concrete depends on the type of reaction products, i.e. swelling alkali-silica gel or non-swelling lime-alkali-silica gel. Expansion will occur only when the swelling alkali-silica gel is formed. The Ca++ ion concentration in concrete controls the formation of the type of reaction products [27] [28].

4) Different theory has been proposed by Chatterji, the main points of which are delineated as follows: i) During the reaction, OH^-, Na^+, K^+ and Ca^{++} ions penetrate reactive grains. The rate of penetration is determined by the size of the ions in solution. ii). More Ca++ ions are left in the liquid phase because their size is larger. iii) During the penetration, some fraction of the silica is set free to migrate away from its original site. (iv) The concentration of Ca++ in the environment controls the rate at which dissolved silica diffuses out of the grains. (v) An expansion occurs if more materials penetrate a reactive grain than silica migrates out of the grains.[29]

6.2.2. Pessimum Effect and Aggregate Size Effect

An interesting feature of ASR is that expansion, which depends on the amount of reactive silica in the aggregate, usually shows a maximum value at some intermediate proportion of the reactive silica. At low levels of reactive silica increasing the amount increases the expansion, but at some amount the expansion peaks, and at high levels of reactive silica increasing the amount decreases the expansion. This is termed a pessimum effect, because expansion is greatest, or pessimum, at this intermediate proportion of reactive silica. [21]

A similar feature is observed with particle size of the reactive aggregate. Large sized particles (say, centimeters in diameter) are slow to react and produce little expansion, at least at early ages. Crushing the same material to sand size (millimeters in diameter) speeds up the reaction and produces more expansion at early ages. Grinding the same material to a powder (micrometers in diameter) fundamentally changes the chemical reaction, producing calcium silicate hydrate (a normal hydration product of Portland

cement), which has little tendency to adsorb water and swell, instead of alkali silica gel, so expansion is reduced. Materials that are reactive as sands are pozzolanic as powders. [21]

6.2.3. Effect of SCM and Its Composition on ASR

The utilization of supplementary cementing materials (SCM) example fly ash, silica fume etc. is one of the most popular ways to minimize the deleterious expansions due to alkali–silica reaction (ASR). The precise mechanisms by which SCM suppresses expansion are poorly understood, and the role of SCM has been variously attributed to the following:

(1) Reduction in pore solution alkalinity

(2) Reduced availability of calcium

(3) Refined pore structure leading to reduced ionic mobility and water permeability. Pore solution studies have shown the effect of SCM on the alkalis available in solution to vary depending on the composition of the ash, level of replacement, age of sample, and alkali content of the cement. [23]

The hydration products of cement-fly ash systems to bind alkalis is a function of the CaO content of the fly ash, the binding increasing as the calcium content decreases. However, concerning the long-term effectiveness of SCM against ASR, there are reports stating that no deleterious expansion has been observed at the Lower Notch dam, Northern Ontario (Canada), built with a reactive argillite and 20% fly ash, after more than 20 years, some dams built in Britain more than 50 years ago with reactive aggregates and SCM are still in excellent condition. [19]

6.2.4. Effect of Cement composition on ASR

Alkali oxides such as K_2O and Na_2O are identified as the most significant contributors to ASR expansion with a less strong correlation to SO_3 content. The sodium and potassium in cement are present as sulfate phases or contained within the aluminate and silicate phases of the anhydrous cement. More than half of the alkalis not in sulfate form are found in the C3A, C3S and ferrite in the cement higher concentrations of alkalis (K or Na) in the pore water solution encourage greater swelling capacities in the gel. The concentration of sodium and potassium compounds and hydroxyl ions is dependent on the quantity of sodium and potassium compounds in the anhydrous Portland cement. The hydroxyl ion concentration in the pore solution of concrete made with high alkali cement may be ten times as high as that made with low alkali cement. [30]

Studies have shown that free $Ca(OH)_2$ is a requirement for ASR to occur, although the reactive silica may continue to dissolve without free Ca(OH)2. There appears to be a correlation between the C/S ratio of C-S-H in portland-cement pastes and potential deterioration from ASR. Binding C-S-H compounds with lower C/S ratios (or cements with lower C3S/C2S ratios) are not as susceptible to deterioration as higher C/S ratio C-S-H compounds and higher silica content binders may increase the resistance to ASR deterioration. Therefore, cements with lower C3S/C2S ratios produce C-S-H compounds with lower C/S ratios, which are not as susceptible to generating and sustaining ASR attack. [30]

6.3. Experimental Results

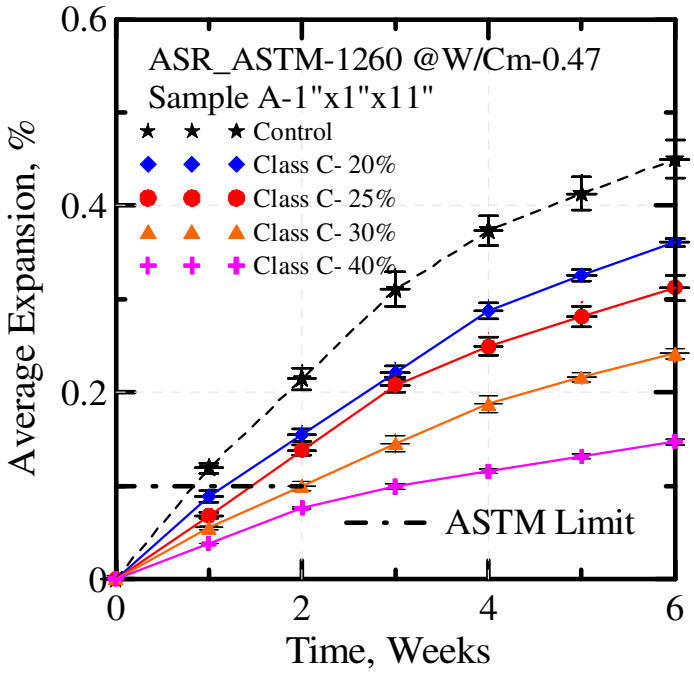

Figure.6.3.1 Average Expansions for Class C- Fly Ash (ASR)

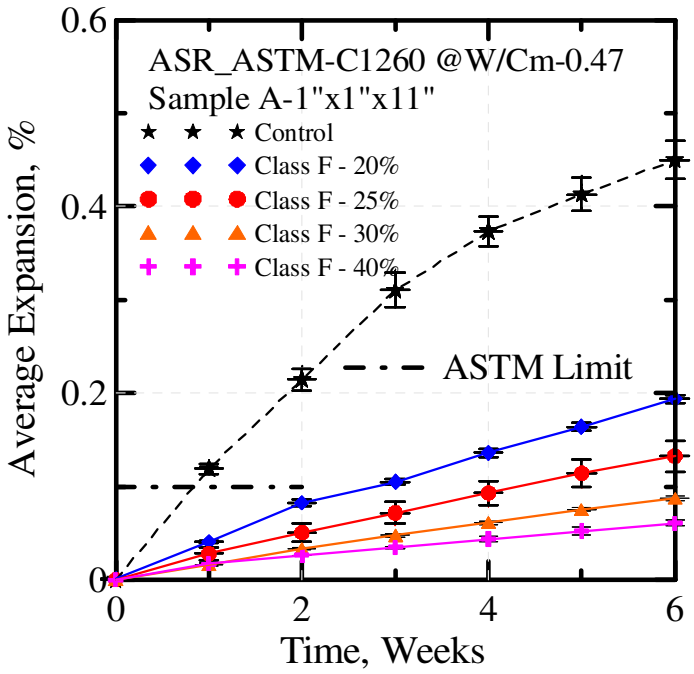

Figure.6.3.2 Average Expansions for Class F- Fly Ash (ASR)

Figures 6.3.1 and 6.3.2 show the comparison of control specimens with different replacement levels (i.e.20, 25, 30 & 40%) of Class C and Class F fly ash respectively.

1) It was observed that both Class C and F fly ash specimen for all replacement levels (i.e.20 – 40%) showed a lower expansion when compared to Control specimen throughout the exposure time.
2) It was also observed that as the amount of flyash was increased in both Class C and Class F fly ash specimen the overall expansion decreases.
3) It was observed that though both fly ash samples mitigated ASR, class F specimen seems to show a much better resistant to ASR when compared to class C specimens.

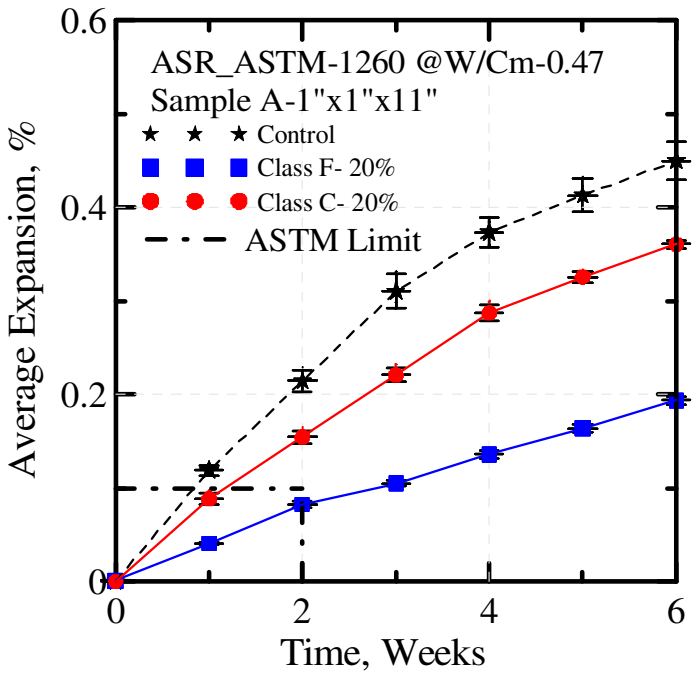

Figure. 6.3.3 Comparison Between 20 % (Class C , F) & Control Specimen (ASR)

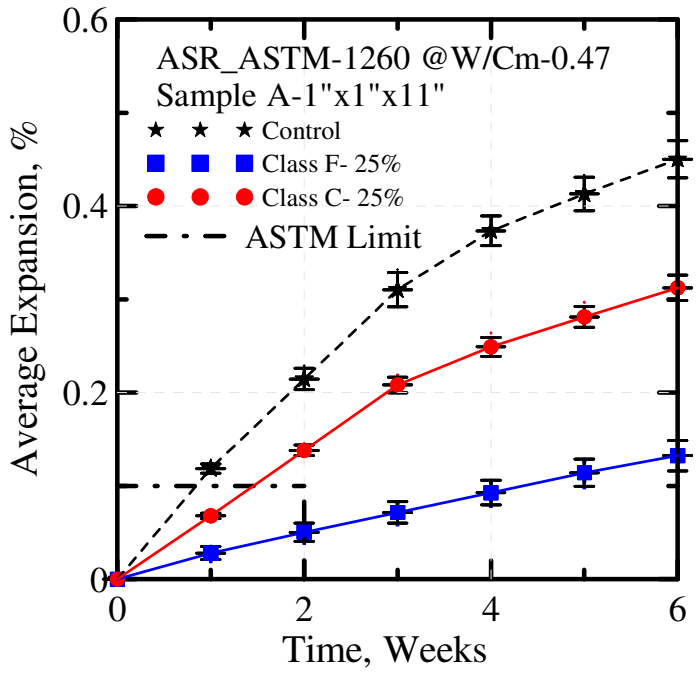

Figure.6.3.4 Comparison Between 25 % (Class C, F) & Control Specimen (ASR)

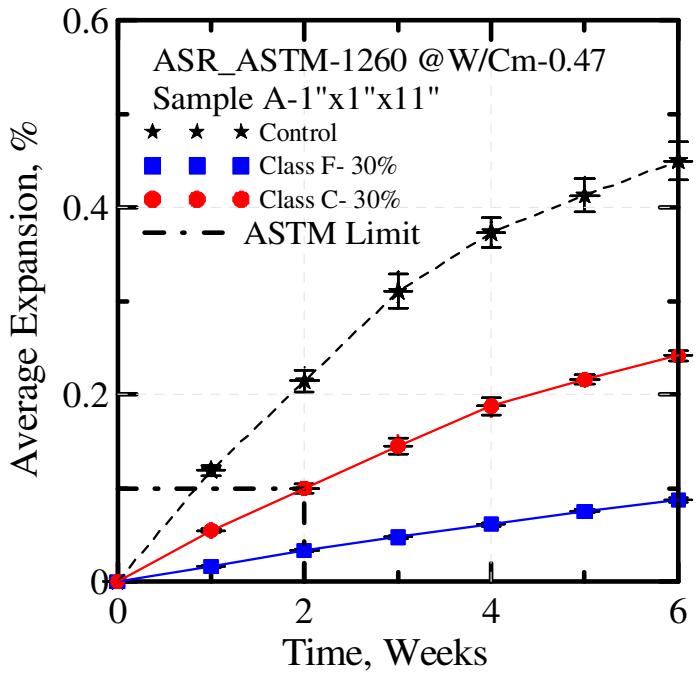

Figure. 6.3.5 Comparison Between 30 % (Class C, F) & Control Specimen (ASR)

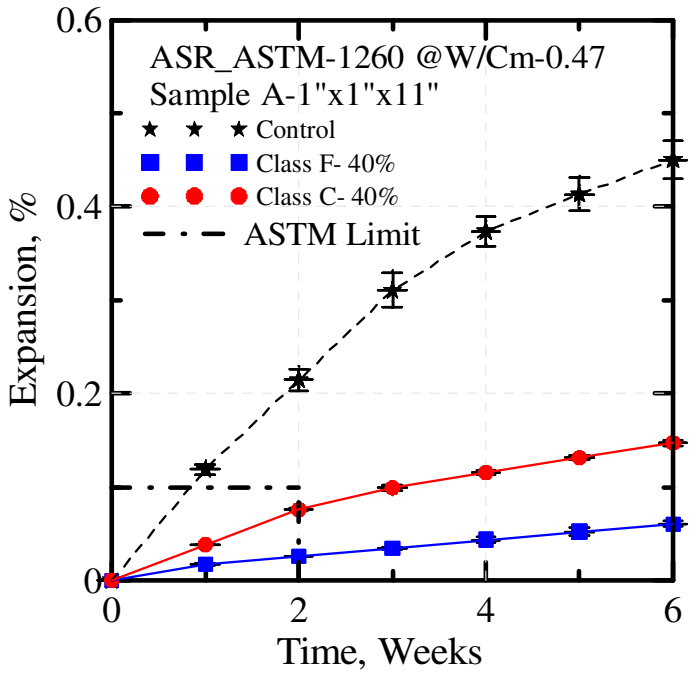

Figure. 6.3.6 Comparison Between 40 % (Class C, F) & Control Specimen (ASR)

Figures 6.3.3 through 6.3.6 shows the comparison of expansion for the control specimens with different replacement levels (i.e.20, 25, 30 & 40%) of Class C and Class F fly ash respectively.

1) It was observed that for Class C fly ash specimen lower replacements (20 & 25 %) was not useful in mitigating ASR because the specimen showed greater expansions than the specified ASTM limit of 0.1 % expansion for 2 weeks exposure time. If class C needs to be used as a replacement in concrete/ mortar a minimum replacement of 30 % is required to mitigate ASR.
2) It was observed that for Class F fly ash specimen all replacement level's (i.e. 20 to 40%) showed lesser expansions than the specified ASTM limit of 0.1 % expansion for 2 weeks of exposure time.

6.4. SEM and EDS Analysis

Microstructural studies were carried out on control & 30%Class F fly ash specimens exposed to sodium hydroxide solution @ 80°C for 7, 14 & 28 days. SEM images and EDS spectra were obtained and are presented in the following.

6.4.1. Microstructural Analysis for 7 Days of Exposure

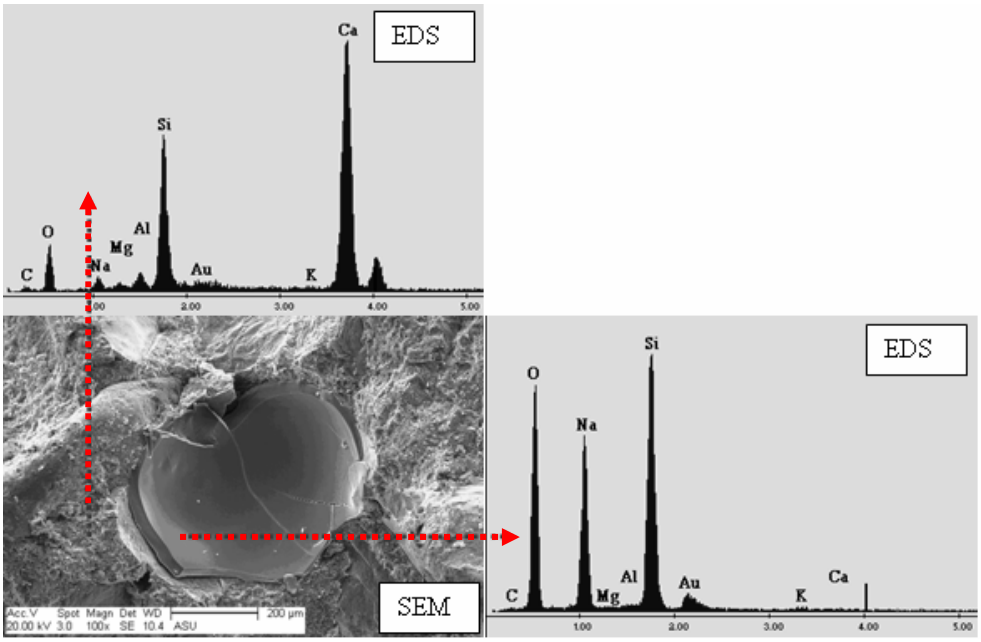

Figure. 6.4.1.1 SEM and EDS of Control Specimen on the 7th Day (ASR)

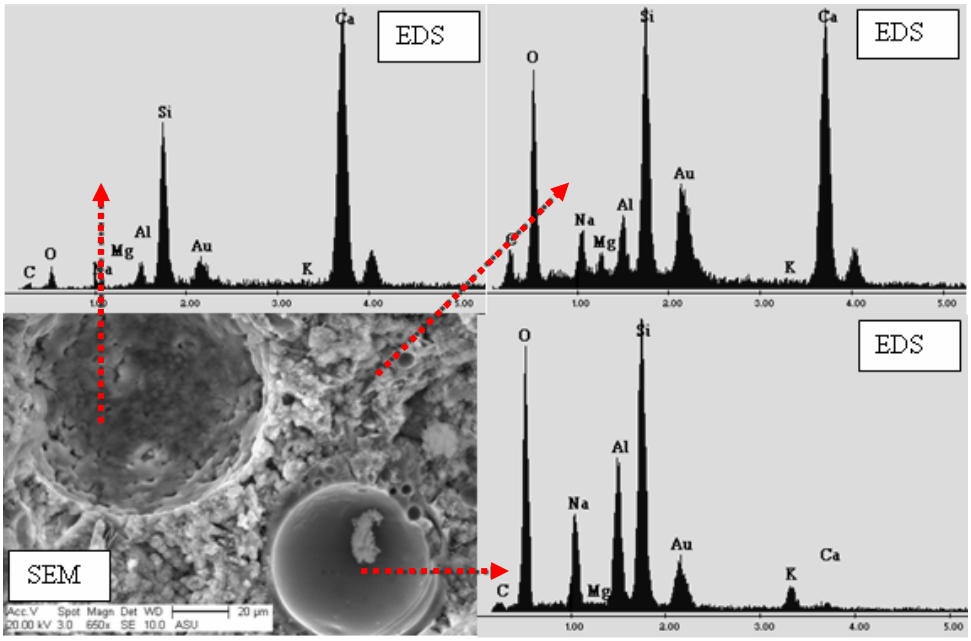

Figure. 6.4.1.2 SEM and EDS of Fly Ash Specimen on the 7th Day (ASR)

Figures 6.4.1.1 and 6.4.1.2 show the SEM images and their EDS spectra of control and fly ash specimen respectively for an exposure time of 7 days.

1) It was observed that the pore size (i.e. Radius of the pore) found in control specimen were almost 200µm where as the pore size in fly ash specimen were of 30 µm.
2) In control specimen prominent ASR gel was found but in the fly ash specimen the ASR gel layer formed were found in very small pores and were very thin.
3) Thin cracks were observed in control specimen were as the matrix of fly ash specimen were dense and crack free.
4) The composition of ASR gel in control specimen shows greater amounts of sodium were as in fly ash specimen aluminum was found in greater quantity compared to sodium.

6.4.2. Microstructural Analysis for 14 Days of Exposure

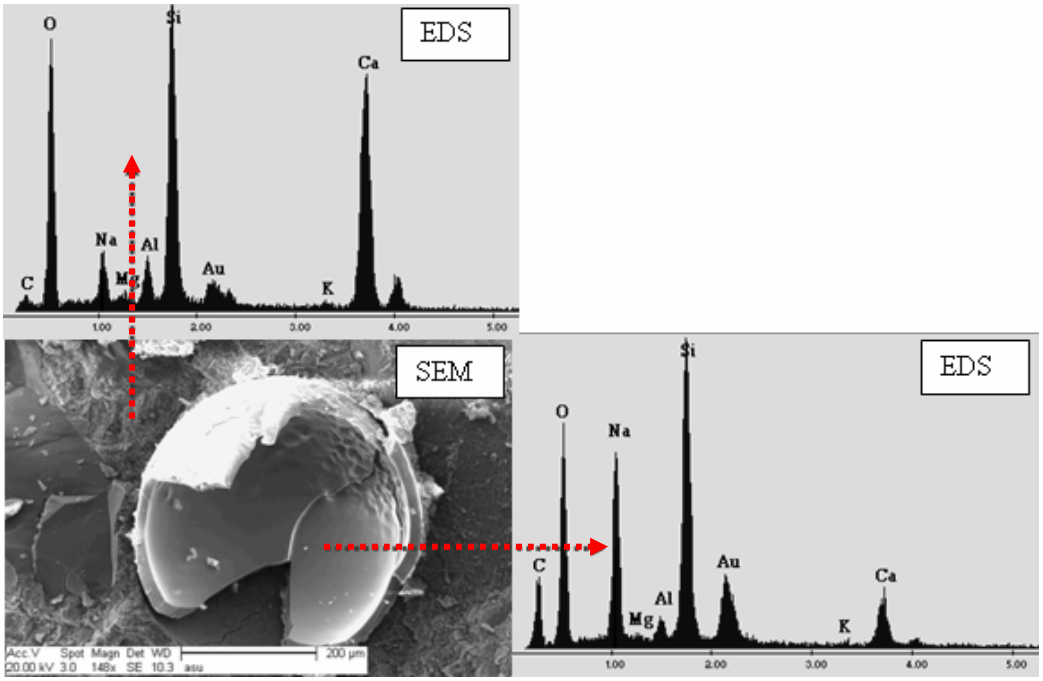

Figure. 6.4.2.1 SEM and EDS of Control Specimen on the 14th Day (ASR)

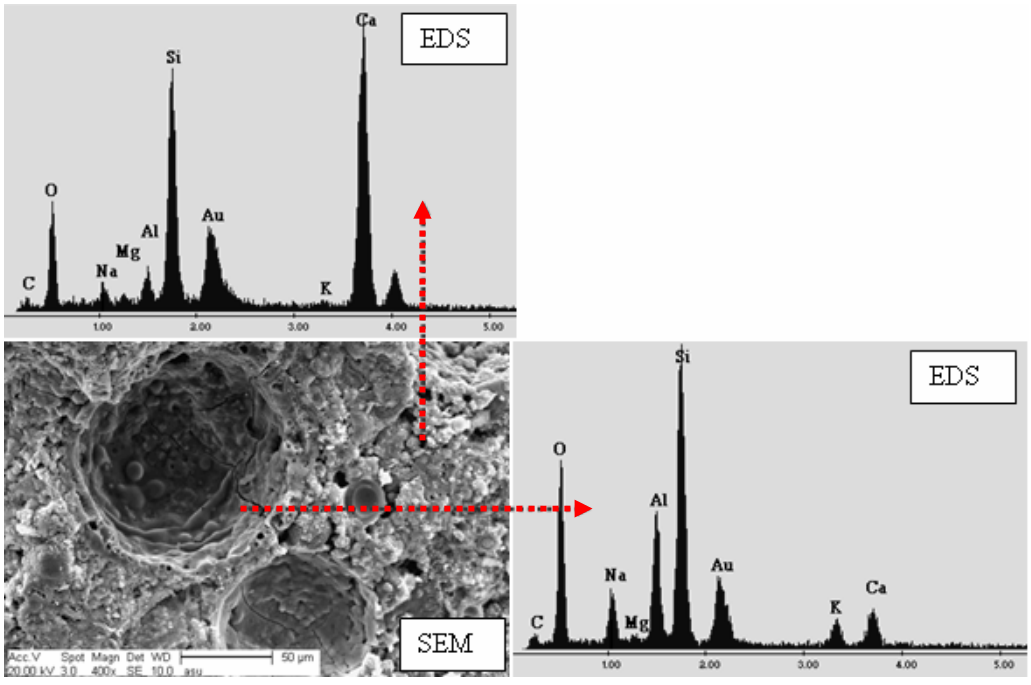

Figure. 6.4.2.2 SEM and EDS of Fly Ash Specimen on the 14th Day (ASR)

Figures 6.4.2.1 and 6.4.2.2 show the SEM images and their EDS spectra of control and fly ash specimen respectively for an exposure time of 14 days.

1) It was observed that the pore size (i.e. Radius of the pore) found in control specimen remained the same where as the pore size in fly ash specimen were bigger compared to the 7 days of exposure.
2) It was observed that for both control and fly ash specimen the ASR gel formed for the 14^{th} day was much thicker than the ASR gels formed on the 7^{th} day.
3) The cracks observed for both control and fly ash specimen were wider for the 14^{th} day compared to the cracks found on the 7^{th} day.
4) The composition of ASR gel in control specimen shows greater amounts of sodium for the 14^{th} day compared to the 7^{th} day, but in the fly ash specimen it was almost the same.

6.4.3. Microstructural Analysis for 28 Days of Exposure

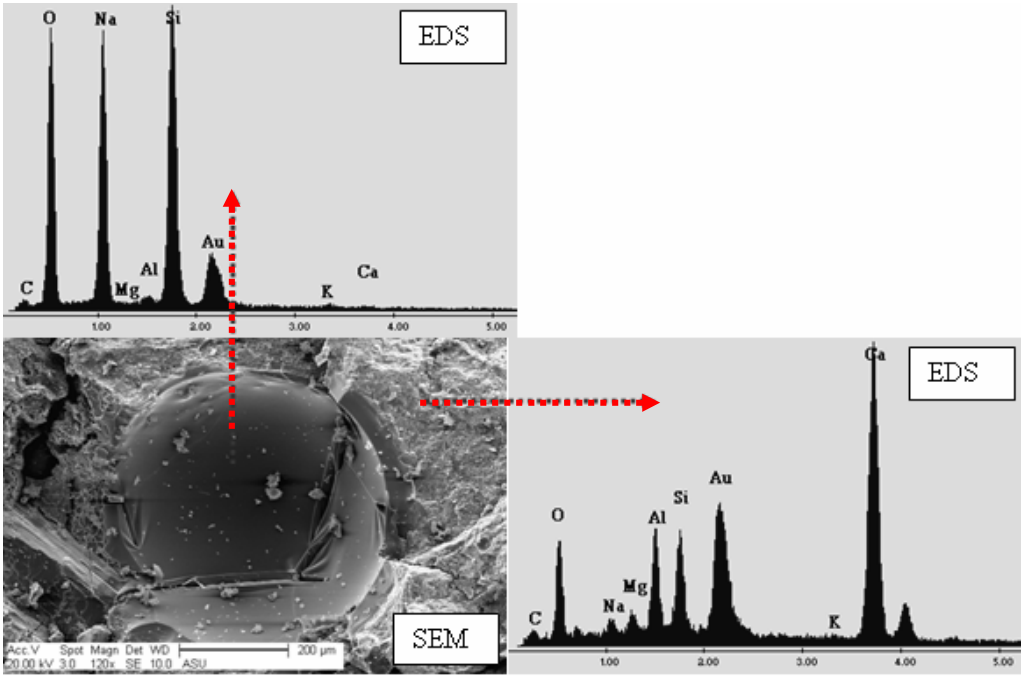

Figure. 6.4.3.1 SEM and EDS of Control Specimen on the 28th Day (ASR)

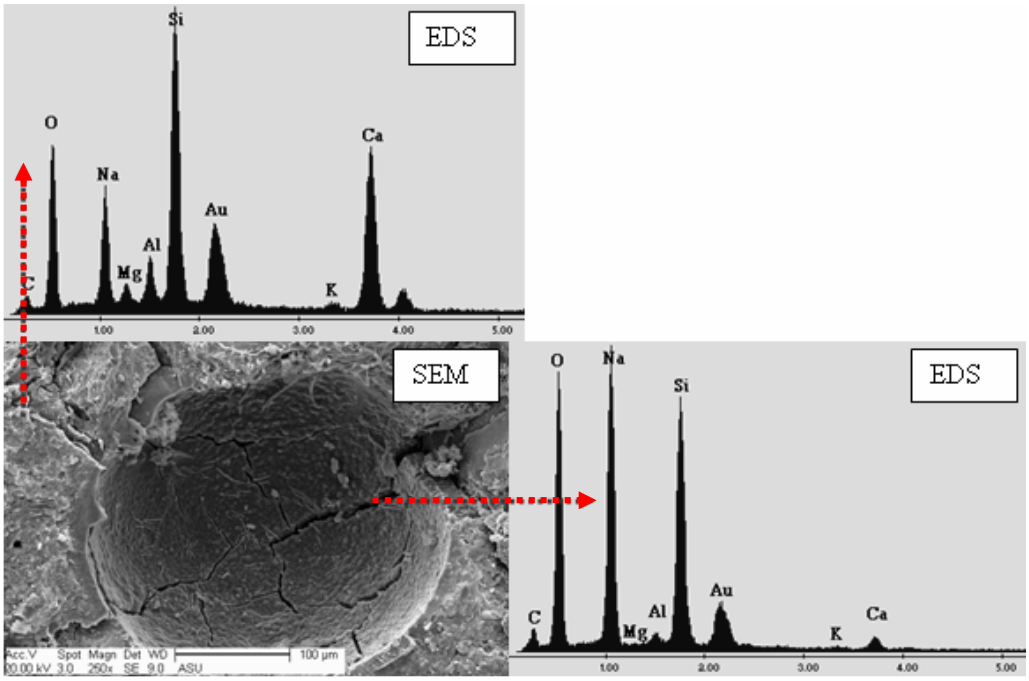

Figure. 6.4.3.2 SEM and EDS of Fly Ash Specimen on the 28th Day (ASR)

Figures 6.4.3.1 and 6.4.3.2 show the SEM images and their EDS spectra of control and fly ash specimen respectively for an exposure time of 28 days.

1) It was observed that the pore size (i.e. Radius of the pore) found in control specimen remained almost the same where as the pore size in fly ash specimen were bigger compared to the 7 & 14 days of exposure.
2) It was observed that for both control and fly ash specimen the ASR gel formed for the 28^{th} day was much thicker than the ASR gels formed on the 7^{th} & 14^{th} day.
3) The cracks observed for both control and fly ash specimen became very prominent and wider for the 28^{th} day compared to the cracks found on the 7^{th} & 14^{th} day.
4) The composition of ASR gel in control and fly ash specimen shows greater amounts of sodium when compared to the 7^{th} & 14^{th} day.

6.4.4. Different Structures observed on the 28th Day

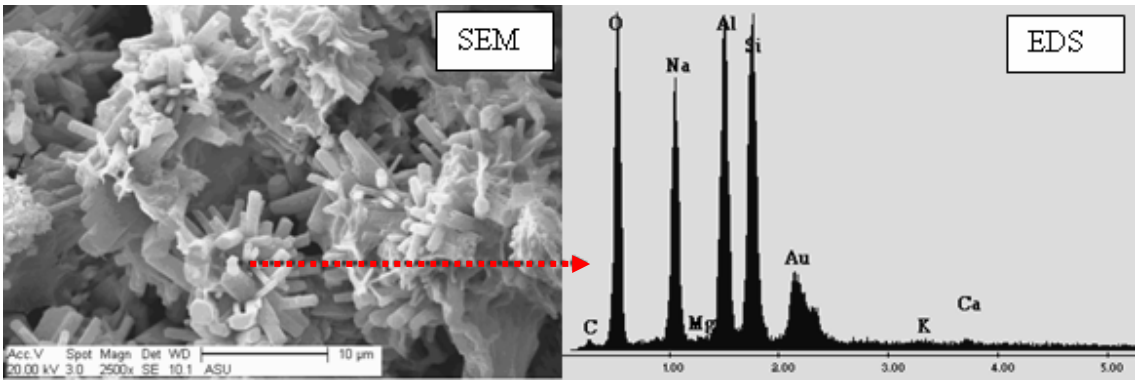

Figure. 6.4.4.1 SEM and EDS of Control Specimen on the 28th Day (ASR)

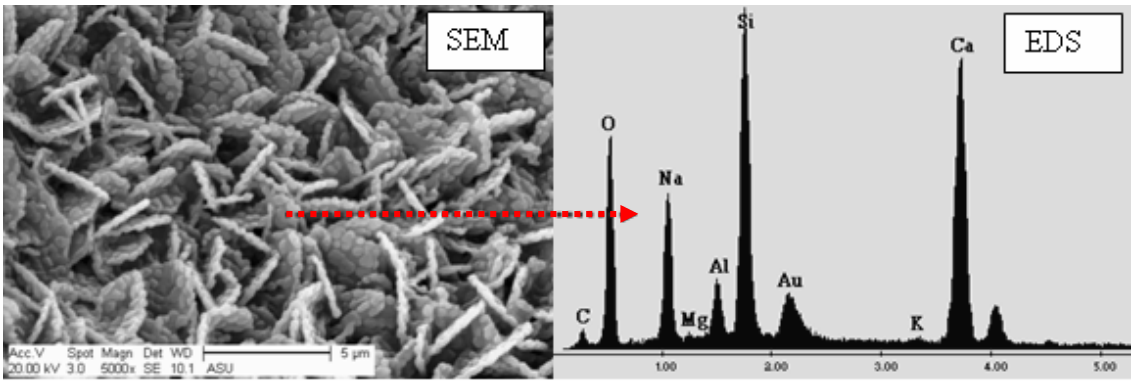

Figure. 6.4.4.2 SEM and EDS of Fly Ash Specimen on the 28th Day (ASR)

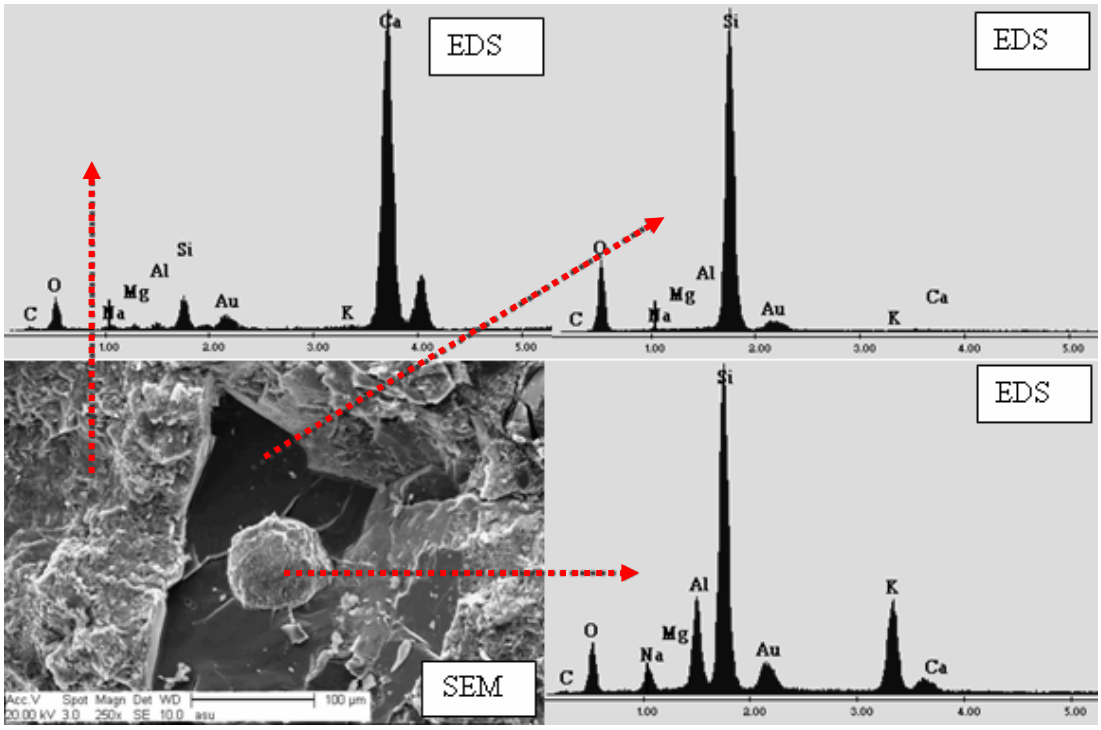

Figure. 6.4.4.3 AAR in Control Specimen on the 28th Day

Figures 6.4.4.1, 6.4.4.2 and 6.4.4.3 show the SEM images and their EDS spectra of control and fly ash specimen as mentioned for an exposure time of 28 days.

1) In control and fly ash specimens for the 28th day exposure, different kinds of crystals were observed with almost equal amount of (Sodium (Na), Silica (Si), Aluminum (Al) and Oxygen (o)) as ASR gels.
2) In control specimens for the 28th day, we could observe Alkali Aggregate Reaction (AAR) where the alkali's (i.e. Na, sodium in our experiment) penetrated the aggregate and caused the aggregate to crack, Other than the alkali silica gel pressure in the pore this could be one of the means of expansion of specimen.

7. MODELING

7.1. Introduction

A majority of the durability issues in concrete structures deal with the diffusion of one or several different ions into the material. Very few durability models are currently applicable to external sulfate attack. Portland cement-based materials subjected to attack from external sulfates may suffer from two types of damage: loss of strength of the matrix due to degradation of C-S-H, and volumetric expansion leading to cracking. Loss of strength has been linked to decalcification of the cement paste hydrates upon sulfate ingress, especially of C-S-H, while cracking and expansion are attributed to formation of expansive compounds such as gypsum or ettringite. [33]

An empirical relationship between ettringite formation and expansion is the basis for many models where the expansive strain is linearly related to the concentration of ettringite. This approach has been incorporated in the 4SIGHT program which predicts the durability of concrete structures, as well as in a model that calculates the service life of structures subjected to the ingress of sulfates by sorption or mechanical and transport properties [37]. The work presented here uses a simplified model of the previously developed model by R. Tixier and B. Mobasher at Arizona state University [33], [34] for predicting the degradation of cementitious materials exposed to sulfate attack, the literature relevant to sulfate attack modeling was reviewed and the material parameters for the model were identified. Finally, the model predictions were compared to experimental expansion data.

7.2. Simplified Model

The simplified model is presented to compute the rate of degradation and expansion potential using a series solution approach. The model is based on the diffusion-reaction moving boundary approach and several mechanisms for the reaction of calcium aluminates with sulfates to form expansive ettringite are considered. There are three major input parameters categorized under the main categories of 1) Initial Material Parameters, 2) Size & Shape of members, and 3) Exposure & Environmental Loading. The input parameters are used to estimate physical parameters such as the diffusivity, strength, concentration of available calcium aluminates, and the volumetric proportions due to chemical reactions. A schematic representation of the same is presented in the Figure 7.2.1.

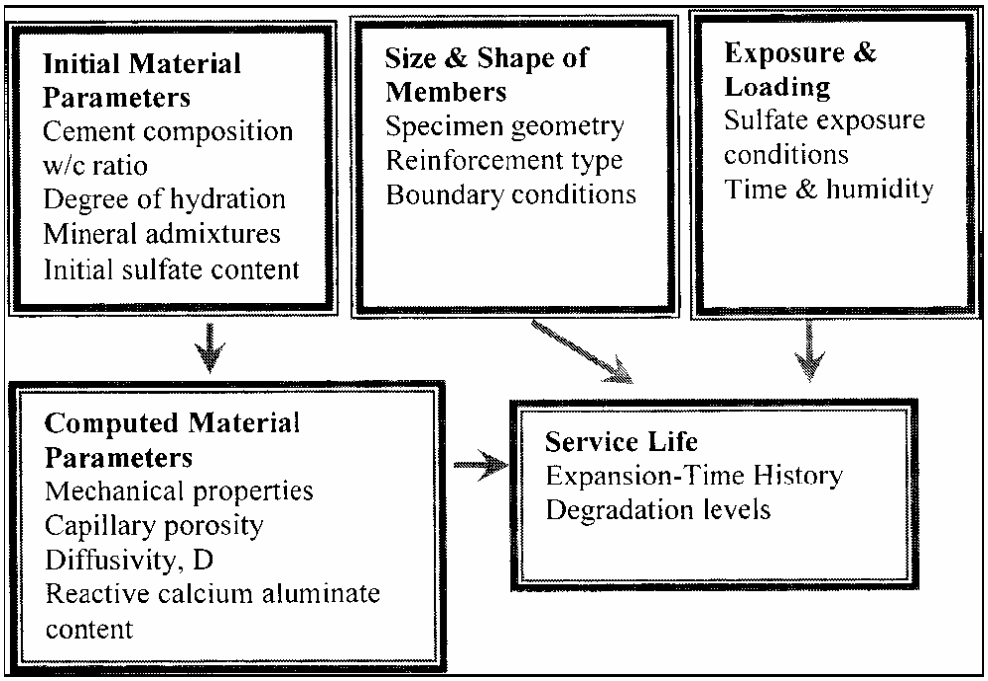

Figure. 7.2.1 The schematics of the model for sulfate attack [35]

Three distinct but coupled problems of sulfate diffusion, calcium aluminate depletion, and crack front propagation are treated as a moving boundary problem as shown in Figure 7.2.2. As the time parameter increases, the sulfates diffuse, and then react with aluminates, resulting in hydration products which expand and potentially cause cracking.

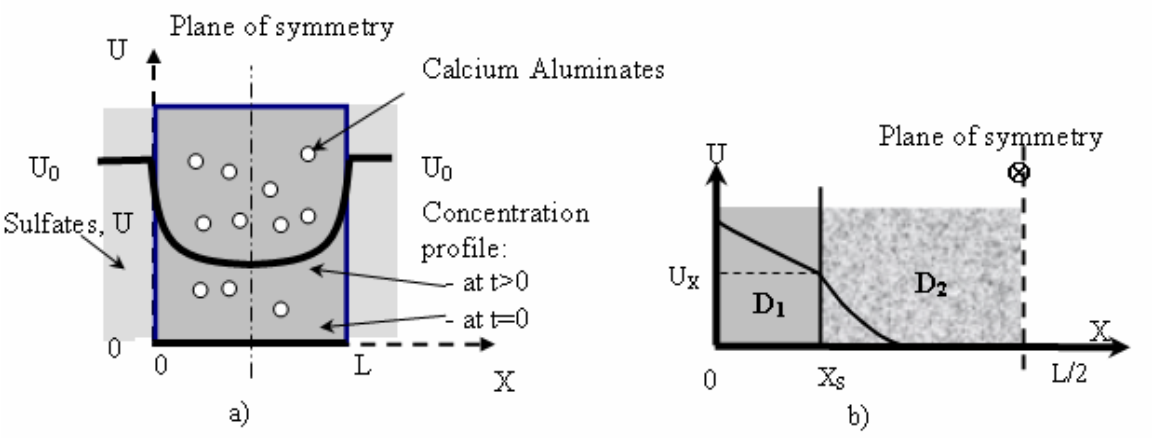

Figure. 7.2.2. a) Sulfate concentration profile in a specimen of length L subjected to sulfates from at times t=0 and t>0. b) The variation of concrete diffusivity as a function of crack front located at X=Xs [35]

It is assumed that the calcium aluminates may be a blend of three different phases of tricalcium aluminate, tetra calcium alumino hydrate, and monosulfate with parameter γ_i representing the proportion of each phase. The cement chemistry notation is used with (C=CaO, S=SiO_2, A=Al_2O_3, H=H_2O, and $\bar{S}$=SO_3). The total calcium aluminate phase is then introduced as: "C_a" (C_a= $\gamma_1 C_4AH_{13}$ + γ_2 $C_4A\bar{S}H_{12}$ + $\gamma_3 C\bar{S}H_2$). Each of these compounds may react with the ingression of sulfates (represented in the form of gypsum) according to stoichiometric amounts defined in equations 7.2.1-7.2.3:

$$C_4AH_{13} + 3\,C\bar{S}H_2 + 14H \longrightarrow C_6A\bar{S}_3H_{32} + CH \quad \text{(7.2.1)}$$

$$C_4A\,\bar{S}\,H_{12} + 2\,C\bar{S}H_2 + 16H \longrightarrow C_6A\bar{S}_3H_{32} \quad \text{(7.2.2)}$$

$$C_3A + 3C\bar{S}H_2 + 26H \longrightarrow C_6A\bar{S}_3H_{32} \quad \text{(7.2.3)}$$

These reactions are lumped in a global sulfate phase-aluminate phase reaction as:

$$C_a + q\bar{S} \longrightarrow C_6A\bar{S}_3H_{32} \quad \text{(7.2.4)}$$

Where $q\bar{S} = (3\gamma_1 + 2\gamma_2 + 3\gamma_3)C\bar{S}H_2$ represents the weighted stoichiometric coefficients of the sulfate phase. For any of the individual reactions described above, the volumetric change due to the difference in specific gravity can be calculated.

$$\frac{\Delta V_P}{V_P} = \frac{\left(m_V^{C_6A\bar{S}_3H_{32}}\right)^{-1}}{\left(m_V^{P_i}\right)^{-1} + a\left(m_V^{C\bar{S}H_2}\right)^{-1}} - 1 \quad \text{With } m_V^k = \frac{d^k}{M^k} \quad \text{(7.2.5)}$$

Where d^k, M^k and m_v^k are respectively the density, molar mass and molar volume of a given compound k. The concentrations of the aluminate and the sulfate phases are represented as two parameters U and C.

$$U = U_{SO_4} \text{ and } C = U_{CA} \quad \text{(7.2.6)}$$

The coupled differential equation for the penetration of sulfates and their reaction with the calcium aluminate phase is represented as a first order diffusion reaction equation and represented as:

$$\frac{\partial U}{\partial T} = D\,\frac{\partial^2 U}{\partial X^2} - KUC \quad \text{(7.2.7)}$$

$$\frac{\partial C}{\partial T} = -\frac{kUC}{q} \quad \text{(7.2.8)}$$

Equation 7.2.7 represents the rate of change of concentration of sulfates as a function of sulfate diffusivity and also the rate of reaction of sulfates presented as the parameter k. Equation 7.2.8 represents the rate of reaction of Aluminate phase and since they are assumed to be stationary in space, there is no diffusion of this phase considered. Therefore, the change of aluminates is considered as a function of time only. It is possible to obtain a series based solution by making simplifying assumptions regarding the interaction of Sulfates and the Aluminate phases. If we assume that there is sufficient amount of aluminates present so that there is no depletion of this phase, one can correlate the rate of reaction of the Sulfates with the Aluminate phase into a single material constant, *k,* representing the rate of depletion of sulfates. The higher this value the more readily available the reaction of aluminates will be. Furthermore it is assumed that the diffusivity remains constant and is not affected by the cracking (i.e. $D_1 = D_2$) refer to figure 7.2.2. b) Equation 7.2.7 can be simplified as a single variable second order partial differential equation represented as Equation 7.2.9 and its series solution is represented as equation 7.2.10 (Taken from the Crank's Book)

$$\frac{\partial U}{\partial T} = D\frac{\partial^2 U}{\partial X^2} - kU \quad \text{..... (7.2.9)}$$

$$\frac{U}{U_0} = 1 - \frac{4}{\pi}\sum_{m=0}^{\infty}\frac{1}{n(k+\nu)}\sin\left(\frac{n\pi X}{L}\right)\left(k+\nu\exp\left[-T(k+\nu)\right]\right) \quad \text{..... (7.2.10)}$$

$$n = 2m + 1\ ,\nu = D\left(\frac{n\pi}{L}\right)^2 \quad \text{..... (7.2.11)}$$

Computation of expansion in a sample using the simplified series solution algorithm is as follows. The solution for the series expansion of sulfate distribution is

obtained as a function of time for a given diffusivity and rate of reaction (D, and k= finite amount). The baseline case for the same expression is also solved using an assumption of k=0 (representing no Sulfate depletion due to reaction). The baseline represents the case for the amount of sulfates that would have penetrated if there were no reactions. The difference between the two levels is the amount of reacted sulfates as defined by Equation 7.2.12. The average values of sulfates penetrated are obtained by integrating the U/U_0 values over the entire depth of the specimen. This level (average value of U/U_0) is multiplied by the initial sulfate concentration at the surface (ex. U_0= 0.35moles/Lit, input) to find the concentration of reacted sulfates. Stoichiometric and molar volume relations are used to convert reacted sulfates to reacted aluminates, and ettringite formed. Volumetric changes are related to linear expansion values. The total calcium aluminate phase is divided into reacted and unreacted amounts and represented respectively as C_{ar} and $C_{au}(x,t)$ according to:

$$C_{ar}(x,t)=C_a-C_{au}(x,t) \quad \text{..... (7.2.12)}$$

Using a rule-of-mixtures approach, one can relate the expansive nature of the products with the prescribed specific gravity of the compounds. In the present approach, calculations of the volumetric changes between reactants and products were conducted by assuming that ettringite was the only product obtained. Once the amount of reacted calcium aluminates into ettringite as a function of time and space are obtained, they can be related to the volumetric strain and the volume changes. It is furthermore assumed that the crystallization pressure of products of reaction results in a bulk expansion of the solid. The constitutive response of the matrix and the expansive stresses are calculated

from the imposed volumetric strain. The expansive strains are used in the constitutive stress crack width response and an elastic equivalent stiffness is defined to account for the reduced stiffness of the sample. An averaging scheme is used the corresponding expansion based on the molar volumes is defined as:

$$\varepsilon_V^t(x,t)=\varepsilon_V^0(x,t)\text{-f }\Phi=C_{ar}\sum_P\left(\frac{\Delta V}{V}\right)_P\text{-f }\Phi \quad \text{..... (7.2.13)}$$

According to equation 7.2.13, the volumetric strain is directly proportional to the volumetric change due to the reaction products and adjusted by a shift factor representing the total capillary porosity (Φ). Parameter *f* is defined as the fraction of capillary porosity available for the dissipation of the expansion products. The magnitude of the shift (delay) in the expansion is due to the amount of capillary porosity.

As the expansive pressures generate, localized tensile stresses are imposed on the internal pore structure of the body. These tensile stresses are assumed to be applied to a sample under end restrain. While a proper representation of the closing pressure profile that normally exists in the cement based materials is needed in the formulation, in the present case, it is assumed that the internal expansive pressures relieve the generation of closing pressures in the vicinity of cracks. The toughening behavior, which is an inherent component of failure in cement-based materials, is therefore lost due to the existence of internal pressures due to the chemical reactions. The proposed procedure is based on a simplified bridging tractions formulation. The first step is to utilize a stress crack width relationship model. A simple uniaxial tensile stress-strain law proposed by Sakai and Suzuki [36] is used to represent the constitutive response and represented in Equations 7.2.14 and 7.2.15. The material is assumed to be linear elastic up to the peak stress, and

follows a strain softening rule for the descending part this approach represents the stress across the crack ligament as a function of both the crack opening and also the crack ligament length. By assuming various functional relationships, models of the decreasing stress as a function of crack opening are represented. For example, the responses for both stress crack opening and crack opening vs. position can be expressed as equations 7.2.14 and 7.2.15 respectively. Parameter l_b in this case is equivalent to the stable crack growth length Δa_c.

$$\sigma_b = \sigma_b^0 \left[\left(\frac{x}{l_b} \right)^q \right]^{x_d} \quad \text{..... (7.2.14)}$$

$$u_b(x) = u_b^0 \left(\frac{x}{l_b} \right)^n \quad \text{..... (7.2.15)}$$

The deformation at peak stress is obtained as: $w_0 = \varepsilon_p \; x \; H$, where H is the gage length of the specimen, and ε_p is the strain at peak. The post peak response is assumed to be by means of a power curve with its coefficients defined as *n, q,* and n_d. In the present model, effect of shape of tensile stress crack opening profile was not studies and constant parameters representing w_0= 0.38, q= 0.5, and n_d = 1.5 were used. It is furthermore assumed that the unloading is elastic and the modulus in the post-peak region is obtained through as an average of the points within the damages zone and undamaged zones:

$$E = \frac{\sigma_b}{\varepsilon - \varepsilon_p} \qquad \bar{E} = \frac{1}{A} \int_A E dA \quad \text{..... (7.2.16)}$$

For a prismatic specimen subjected to sulfate ingress from all sides, a uniaxial condition is used, and the stiffness is averaged across the cross section using Equation 7.2.16. Furthermore, it is assumed that normal strain is the primary mode of deformation

and no curvature is induced throughout the cross section. The averaged expansion is obtained using an averaging algorithm:

$$\text{Absolute expansion} = \Delta_i = \sigma_r \left(\frac{1}{E_{avg}} - \frac{1}{E_0} \right) \quad (7.2.17)$$

$$\text{Overall expansion} = \Delta = \sum_{i=1}^{n} \Delta_i \quad (7.2.18)$$

Parameter E_{avg} is the average instantaneous modulus over the cross-section, Parameter σ_r is assumed to be a constant uniform residual stress in the specimen due to past history before sulfate attack such as a uniform shrinkage. In the present approach it is assumed as 2-10 MPa, and may be viewed as the scaling parameter used to relate the changes in the stiffness of the sample to the expansion levels observed in experiments.

7.3. Parameters used for Modeling

The replacement of fly ash changes the C_3A content and unit weight of paste/ mortars as mentioned in the tables 7.3.1 and 7.3.2 respectively.

Table 7.3.1

Parameters Considered For Paste Specimen.

Replacement Level , W/Cm - 40 %	Unit weight of mortar	C_3A Content in %
0 % Fly ash , 100% Cement	2.5	5
10 % Fly ash, 90% Cement	2.4	4.5
20 % Fly ash, 80% Cement	2.2	4
30 % Fly ash, 70% Cement	2.0	3.5

Table 7.3.2

Parameters Considered For Mortar Specimen

Replacement Level , W/Cm - 60 %	Unit weight of mortar	C_3A Content in %
0 % Fly ash , 100% Cement	2.10	5
10 % Fly ash, 90% Cement	2.00	4.5
20 % Fly ash, 80% Cement	1.80	4
30 % Fly ash, 70% Cement	1.60	3.5
40 % Fly ash, 60% Cement	1.40	3

7.4. Results of Standard Size Mortar Specimen

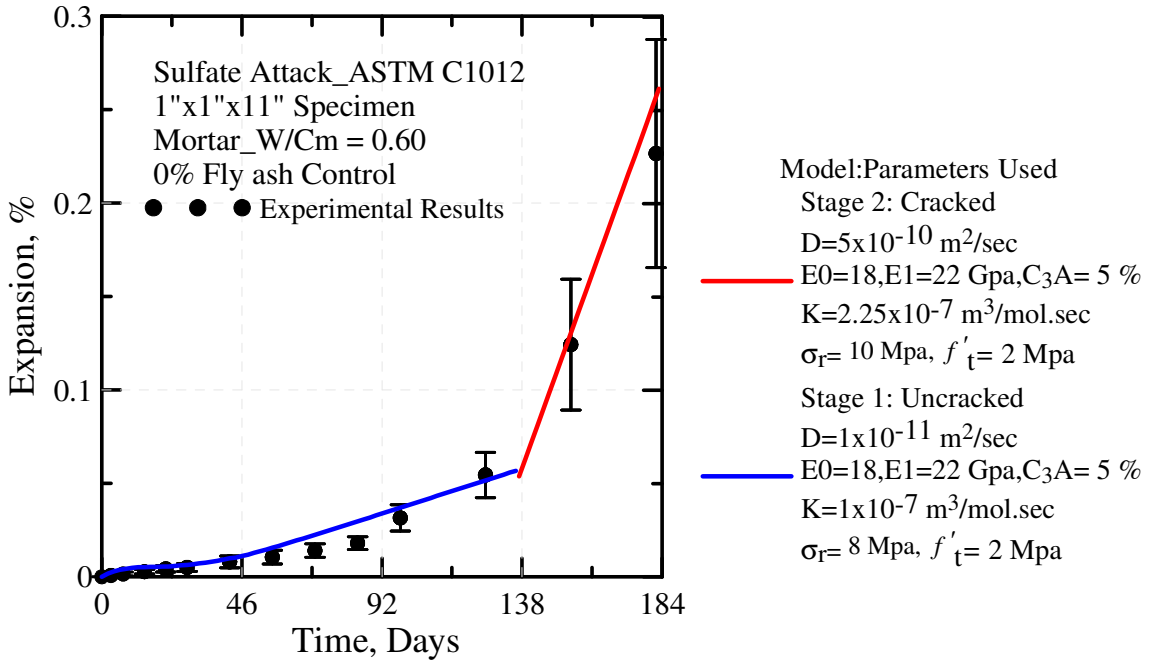

Figure. 7.4.1 Modeling for 0 % Fly Ash Control - Mortar Specimen

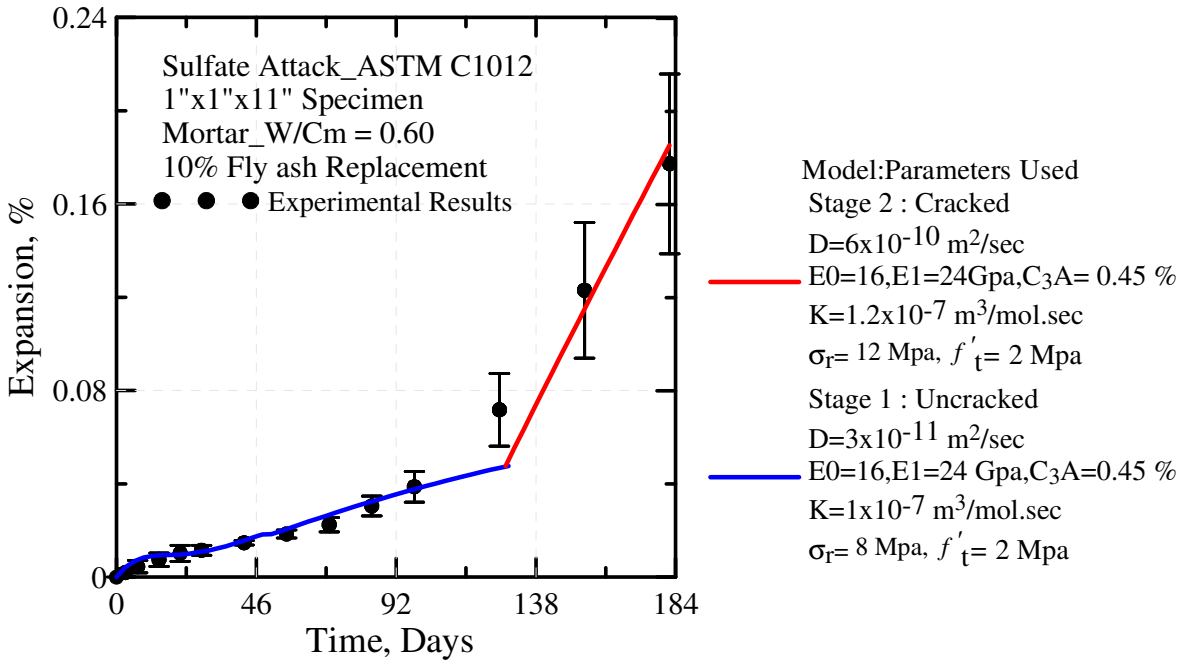

Figure. 7.4.2 Modeling for 10 % Fly Ash - Mortar Specimen

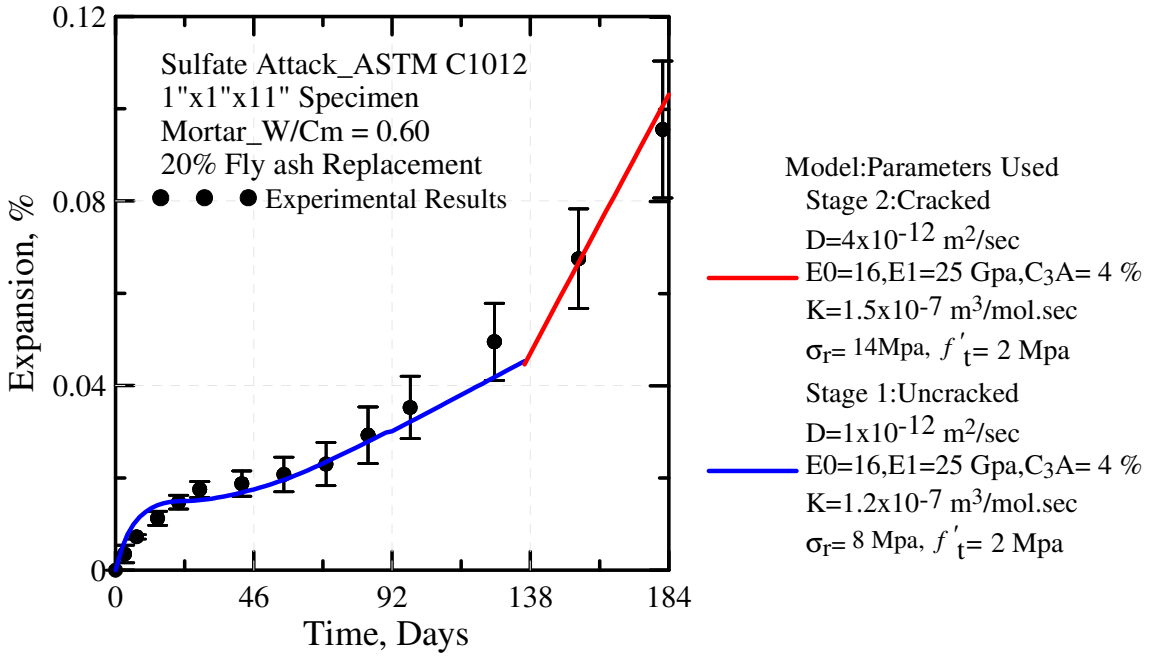

Figure. 7.4.3 Modeling for 20 % Fly Ash - Mortar Specimen

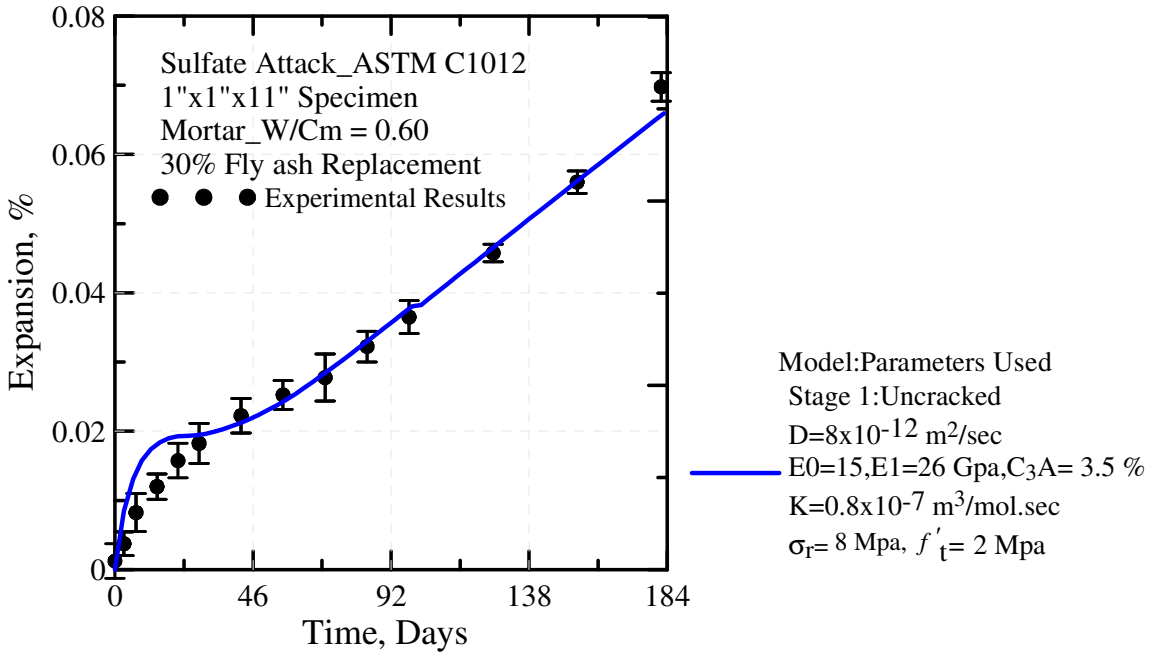

Figure. 7.4.4 Modeling for 30 % Fly Ash - Mortar Specimen

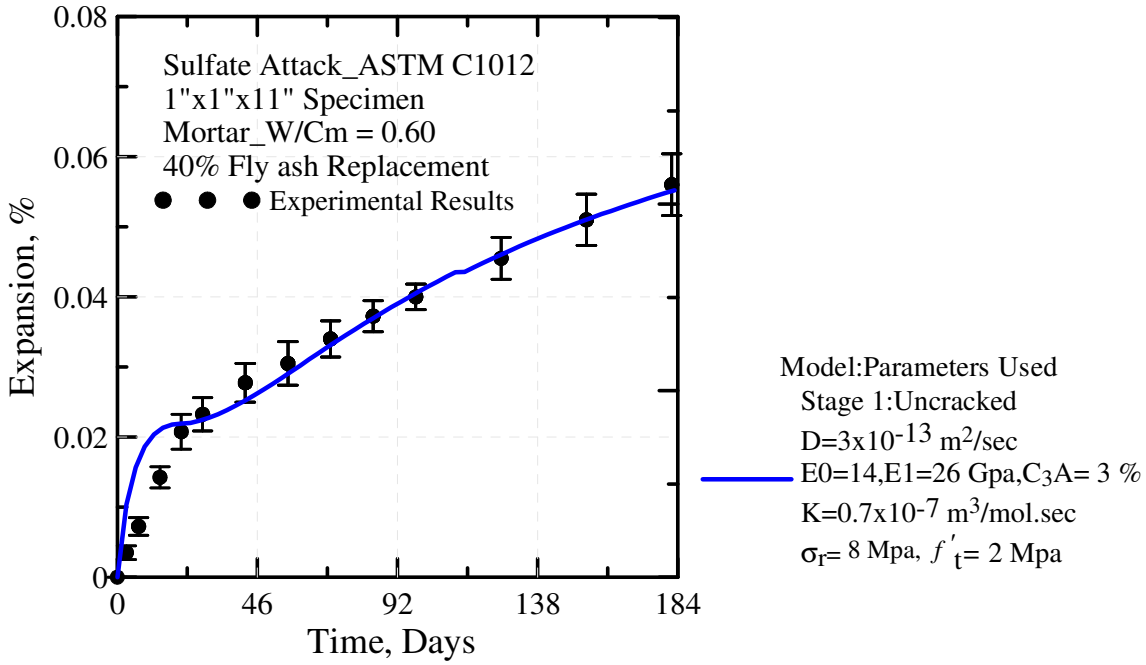

Figure. 7.4.5 Modeling for 40 % Fly Ash - Mortar Specimen

Figures 7.4.1 through 7.4.5 shows the comparison between experimental and simulation data for 0% (Control), 10, 20, 30 & 40% fly ash mortar specimen respectively.

1) Cracking was observed only in control, 10 % and 20 % replacement specimens.
2) In control specimens the diffusivity changed by 50 times with the addition of fly ash it was noticed that, though cracking was observed the diffusivity decreased to 25 times in the 10 % specimen and 4 times in the 20 % specimens.
3) The change in rate constant of reaction between sulfates and aluminates (i.e. K) noticed after cracking in control, 10% & 20% is assumed to be because of the greater surface area exposed to sulfate solution after cracking.
4) The residual hydrostatic expansive stresses (i.e.$\sigma_{r)}$ in the pore microstructure increased from 8Mpa – 10 Mpa, when cracking was observed in control, 10% & 20% mortar specimens.

5) For mortar specimens it was observed that the Young's modulus of material at exposure time (t < 28 days) (i.e. E0) decreased with the increase in the fly ash replacement. It was observed that E0 decreased from 18 Mpa for the control specimen to 14 Mpa for the 40 % fly ash specimen.
6) For mortar specimens it was also observed that the Young's modulus of material at exposure time (t > 28 days) (i.e. E1) increased with the increase in the fly ash replacement. It was observed that E1 increased from 22 Mpa for the control specimen to 26 Mpa for the 40 % fly ash replacement specimen.
7) In general it was observed that for all mortar specimens it was noticed that the rate constant of reaction between sulfates and aluminates (i.e. K) decreased with the increase in fly ash replacements.

7.5. Results of Standard Size Paste Specimen

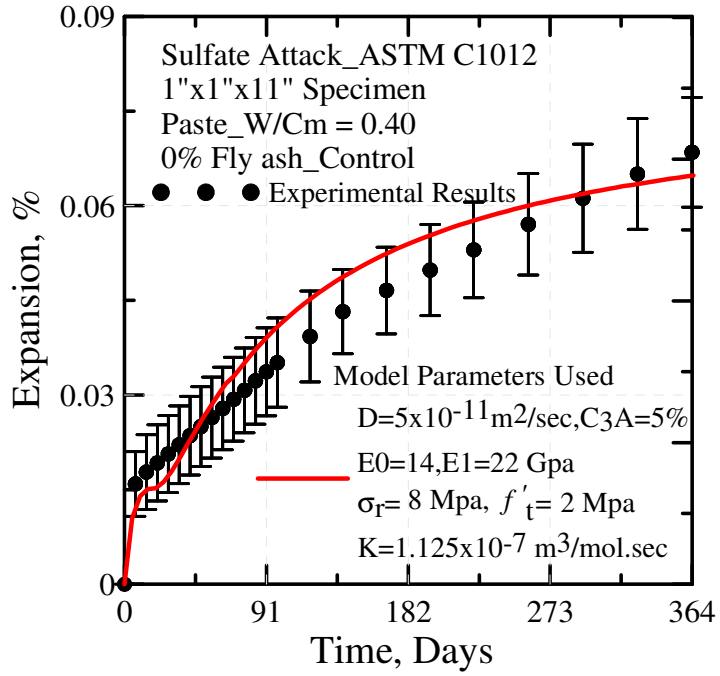

Figure. 7.5.1 Modeling for Control Paste Sample-A Specimen

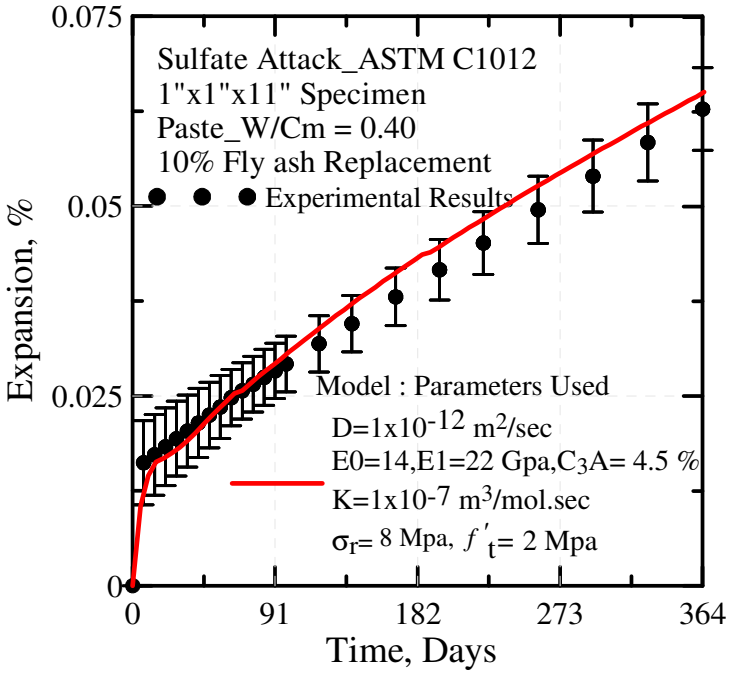

Figure. 7.5.2 Modeling for 10 % Fly Ash Replacement Paste Sample-A Specimen

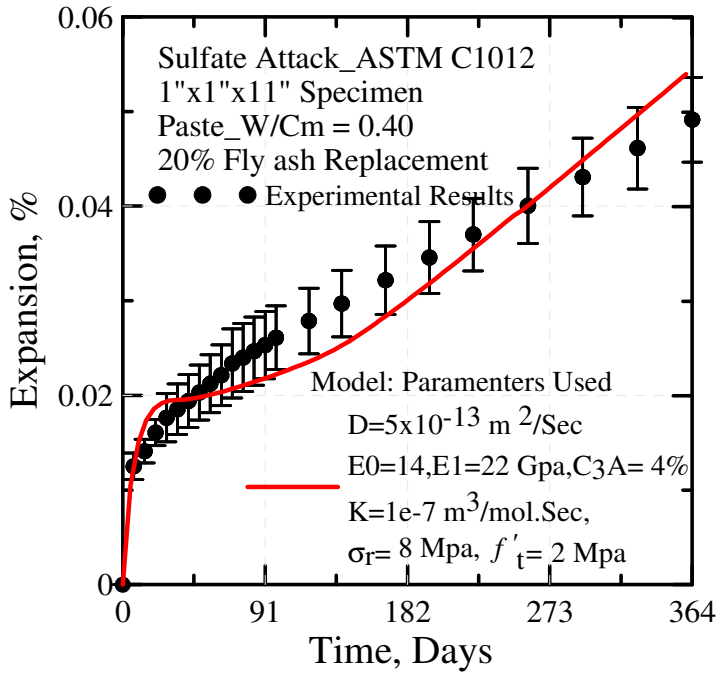

Figure. 7.5.3 Modeling for 20 % Fly Ash Replacement Paste Sample-A Specimen

Figures 7.5.1, 7.5.2 and 7.5.3 show the comparison between experimental and simulation data for 0% (Control), 10 and 20% fly ash paste specimen respectively.

1) It was observed that only by changing the amount of fine aggregates, the model could simulate expansions in agreement with the experimental results.
2) There was a greater change in diffusivity observed in paste specimen when compared to mortar specimen. For mortar specimen the change in diffusivity (i.e. $D_{control}$ / $D_{40\%}$) was 33.33 where as for the paste specimen the change in diffusivity (i.e. $D_{control}$ / $D_{20\%}$) was 100.

7.6. Results of Modified Size Paste Specimen

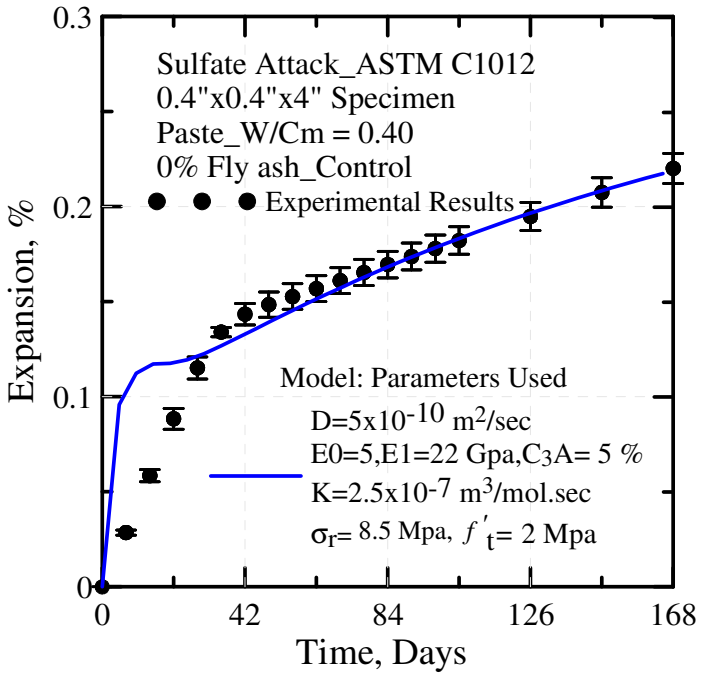

Figure. 7.6.1 Modeling for Control Paste Sample-B Specimen

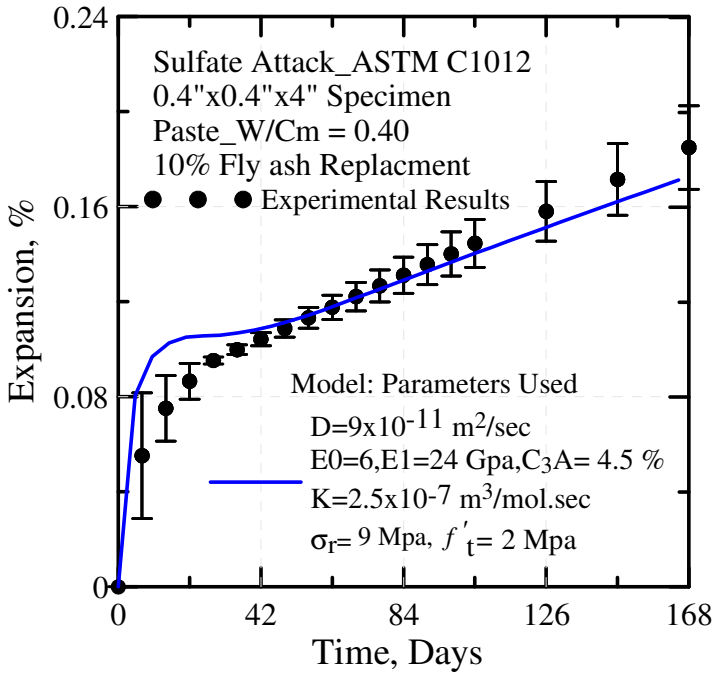

Figure. 7.6.2 Modeling for 10 % Fly Ash Replacement Paste Sample-B Specimen

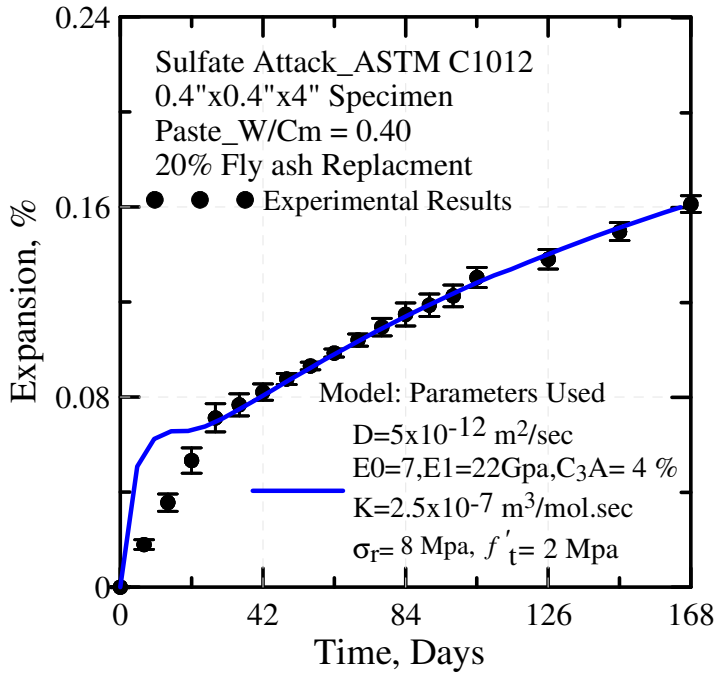

Figure. 7.6.3 Modeling for 20 % Fly Ash Replacement Paste Sample-B Specimen

Figures 7.6.1, 7.6.2 and 7.6.3 show the comparison between experimental and simulation data for the modified sized 0% (Control), 10 and 20% fly ash paste specimen respectively.

1) One of the most critical observations was with the modeling of modified sized specimen (0.4”x0.4”x4”) the Diffusion (i.e. D) and rate constant of reaction between sulfates and aluminates (i.e. K) changed by 10 and 2.5 times respectively when compared to standard sized specimen (1”x 1”x 11”).

   This was assumed to be because of the (Surface area to volume) ratio of modified size specimen was 2.5 times the standard size specimen as it can be observed in the table below.

Table 7.7.1

Surface area to Volume Ratio of Standard and Modified Sample.

Specimen Size	Volume V ($in.^3$)	Surface area Sa ($in.^2$)	Ratio Sa/V
1" x 1" x 11"	11	46	4.18
0.4"x0.4"x4"	0.64	6.72	10.5
		Ratio = 10.5/4.18	2.52

2) The change in Young's modulus of material at exposure time (t < 28 days) (i.e. E0) for the modified size specimen (0.4"x0.4"x4") had to be considered for the fitting of curves as 7 Mpa when compared to standard size specimen (1"x 1"x 11") of 14 Mpa, which could not be explained.

8. CONCLUDING REMARKS

Table 8.1

Concluding Remarks for Standard mortar samples.

Fly Ash Replacement in %	Sulfate Attack Nist limit in %	ESA - Results	ASR – ASTM limit in %	ASR - Results	SAI (28 Days)	SAI - Results	Check
Control							
0.00	< 0.1%	0.227	< 0.1%	0.2789	-	100 %	Failed
Class C							
10	< 0.1%	0.1772			> 75 %	1.0808	Failed
20	< 0.1%	0.0957	< 0.1%	0.2125	> 75 %	0.9463	Failed
25			< 0.1%	0.1678			Failed
30	< 0.1%	0.0778	< 0.1%	0.1196	> 75 %	1.1339	Failed
40	< 0.1%	0.0495	< 0.1%	0.0752	> 75 %	1.11	Passed
Class F							
10	< 0.1%	0.0682			> 75 %	0.4969	Failed
20	< 0.1%	0.0954	< 0.1%	0.0814	> 75 %	1.0701	Passed
25			< 0.1%	0.0439			Passed
30	< 0.1%	0.0698	< 0.1%	0.0329	> 75 %	0.8767	Passed
40	< 0.1%	0.0558	< 0.1%	0.0208	> 75 %	0.8225	Passed

1) As it can be observed in Table 8.1, the Control Specimen failed both to meet the specified limits for ASTM C1012 and ASTM C1260. Hence we can conclude that it is not safe to use plain Portland cement as a construction material where the structure can be exposed to sulfates or alkali salts.

2) Though the Class C fly ash replacement mitigates sulfate attack and gains enough strength for 28 days it fails to mitigate Alkali Silica Reaction expansions for lower

levels of replacements (i.e. 10 though 30 %), hence if class C fly ash needs to be used as a replacement higher levels such as replacement more than 30 % needs to be used.

3) All % replacements of Class F fly ash (i.e.10 through 40) mitigated expansions for both sulfate attack and Alkali silica Reaction, but it was noticed throughout the research that the development of strength in Class F fly ash replaced specimen was slow and low % replacements as 10 % replacement did not pass the minimum strength requirement as specified by ASTM C618.
4) Modified samples followed similar trend to that of the standard size specimen. It was also noticed that the Modified samples (0.4”x0.4”x4”) could produce the same expansion in 3 months when compared to 6 months taken by the Standard samples (1”x1”x11”), Hence by reducing the size of the specimen we can get faster and accurate results.

REFERENCES

1. ASTM C618-92a.*Standard Specification for Fly Ash and Raw or Calcined Natural Pozzolan for Use as Mineral Admixture in Portland Cement Concrete"* American Society for Testing and Materials, Annual Book of ASTM Standards, Volume 04.02,

2. ASTM C 1012. *Standard Test Method for Length Change of Hydraulic-Cement Mortars Exposed to a Sulfate Solution*, American Society for Testing and Materials, Annual Book of ASTM Standards, Volume 04.01,

3. ASTM C1260.*Standard Test Method for Potential Alkali Reactivity of Aggregates (Mortar-Bar Method)*, American Society for Testing and Materials, Annual Book of ASTM Standards, Volume 04.01,

4. ASTM C109. *Standard Test Method for Compressive Strength of Hydraulic Cement Mortars*, American Society for Testing and Materials, Annual Book of ASTM Standards, Volume 04.01,

5. American Coal Ash Association. *Fly Ash Facts for Highway Engineers.* Federal Highway Administration, Report No. FHWA-SA-94-081, Washington, DC, December 1995.

6. University of Pretoria etd - Landman, AA (2003). *Literature Review of Fly Ash in Aspects of Solid-State Chemistry of Fly Ash and Ultramarine Pigments.*

7. R.A.Kruger, South African Journal of science, 1986, 82,177.

8. U.S. Department of transportation, Federal highway administration. *Turner-Fairbank Highway Research Center Recycled waste Material.*

9. Halstead, Woodrow J. *Use of Fly Ash in Concrete. National Cooperative Highway Research Program Synthesis of Highway Practice No. 127*, Transportation Research Board, Washington, DC, 1986.

10. Javed I. Bhatty and Peter C. Taylor, *Sulfate Resistance of Concrete Using Blended Cements or Supplementary Cementitious Materials*. Portland Cement Association 2006. PCA R&D Serial No. 2916a

11. Fernandez-Jimenez, I. Garcıa-Lodeiro. *Durability of alkali-activated fly ash cementitious materials.* Springer Science Business Media, LLC 2006, J Mater Sci (2007) 42:3055–3065.

12. C. Richard Brundle, Charles A. Evans, Jr., Shaun Wilson. *Encyclopedia of material characterization. Surfaces*, Interfaces, Thin Films

13. M.Collepardi, S. Collepardi, J.J.Ogoumah Olagot, and R.Troli, *Delayed Ettringite Formation Due to Sulfate Attack Cement Content and Curing Temperature.*

14. M. Collepardi, *A state-of-the-art review on delayed ettringite attack on concrete*, Cem. Concr. Compos. 25(2003) 401-407.

15. Omar S.Baghabra Al-Amoudi, *Attack on plain and blended cements exposed to aggressive sulfate environments*, Cem. Concr. Compos. 24 (2002) 305–316.

16. K.Ramyar, G.Inan, *Sodium Sulfate Attack on Plain and Blended Cements*, Building and Environment 42 (2007) 1368-1372.

17. Manu Santhanam, Menashi D.Cohen, Jan Olek. *Mechanism of Sulfate Attack: Afresh Look Part1: Summary of Experimental Results*. Cement and Concrete Research 32 (2002) 915 – 921.

18. Manu Santhanam, Menashi D.Cohen, Jan Olek. Mechanism of Sulfate Attack: *Afresh Look Part 2: Proposed mechanisms.* Cement and Concrete Research 33 (2003) 341–346.

19. I. Sims and P. Nixon, RILEM Recommended Test Method AAR-I: *Detection of potential alkali-reactivity of aggregates-Petrographic method*, RILEM TC 191-ARP

20. L.J. Malvar, G.D.Cline, D.F.Burke, R.Rolling, T.W.Sherman, and J.L.Greene, *Alkali-Silica Reaction Mitigation State-Of-The-Art and Recommendations*, ACI Materials Journal, Technical Paper Title no. 99-M49

21. George J.Z. Xu, Daniel F. Watt, Peter P. Hudec, *Effectiveness of Mineral Admixture in Reducing ASR Expansion.* Cement ad Concrete Research, Vol. 25. No. 6. pp. 1225-1236.1995

22. Medhat H.Shehata, Michael D.A.Thomas, *The Effect of Fly Ash Composition on the Expansion of Concrete due to Alkali-Silica Reaction*. Cement ad Concrete Research, 30 (2000) 1063-1072.

23. Roland F. Bleszynski and Michael D.A. Thomas, *Microstructural Studies of Alkali-Silica Reaction in Fly Ash Concrete Immersed in Alkaline Solution*, Advanced Cement Based Materials 1998,7,66-78.

24. Richard Helmuth, David Stark, Sidney Diamond, Micheline Moranville-Regourd, *Alkali-Silica Reactivity an Overview of Research.* Strategic Highway Research Program, SHRP-C-342.

25. L. S. D Glasser, *Osmotic Pressure and the Swelling of Gels*. Cement at_ Concrete Research, Vol. 9, 1979, 515-517.

26. H.E. Vivian, Studies in cement aggregate reaction: XVI. *The effect of hydroxyl ions on the reaction of opal*, Australian Journal, Applied Science, 2 (1951) 108 - 113.

27. T.C. Powers, H.H. Steinour, *An interpretation of some published researches on the alkali – aggregate reaction. II. A hypothesis concerning safe and unsafe reactions with reactive silica in concrete*, American Concrete Institute journal, 26 (1955) 785–810.

28. T.C. Powers, H.H. Steinour, *An interpretation of some published researches on the alkali–aggregate reaction: I. The chemical reactions and mechanism of expansion*, American Concrete Institute journal, 26 (1955) 497– 516.

29. S.Chatterji, N.Thaulow, and A.D.Jensen. *Studies of Alkali-Silica Reaction.Part:5. Verification of A Newly Proposed Reaction Mechanism*, Cement and Concrete Research, Mar 1989, Vol. 19, No. 2, pp 177-183.

30. Della M. Roy, Paul J. Tikalsky, Barry E. Scheetz, James Rosenberger, Tara Cavalline, And Periaswamy Arjunan, *Influence of Portland Cement Characteristics on Alkali Silica Reactivity.* TRB 2003 Annual Meeting

31. F.B.Nelson and L.J.Struble, *Alkali Silica Reaction in Concrete, Center Of Excellence for Airport Technology.* Technical Note

32. Josee Duchesne, Marc-Andre Berube, *Long-term effectiveness of supplementary cementing materials against alkali–silica reaction*. Cement and Concrete Research 31 (2001)1057-1063.

33. Raphael Tixier and Barzin Mobasher, *Modeling of Damage in Cement-Based Material Subjected to External Sulfate Attack. 1: Formulation*, ASCE: DOI: 10.1061/ (ASCE) 0899 -1561(2003) 15:4(305).

34. Raphael Tixier and Barzin Mobasher, *Modeling of Damage in Cement-Based Material Subjected to External Sulfate Attack. 11: Comparison with Experiments*, ASCE: DOI: 10.1061/ (ASCE) 0899 -1561(2003) 15:4(314).

35. Mobasher, B. (2007), "*Modeling of Stiffness Degradation and Expansion in Cement Based Materials Subjected to External Sulfate Attack*." Materials Science of Concrete – Transport Properties and Concrete Quality, Special Volume, American Ceramic Society, pp. 3157-171.

36. Suzuki, T. and Sakai, M. (1994), *A Model for Crack-Face Bridging*, International Journal of Fracture, Vol. 65, pp. 329-344.

37. B. Mobasher, and C. Ferraris, *Simulation of Expansion in Cement Based Materials Subjected to External Sulfate Attack*. RILEM Technical Meeting on Durability of Cement Based Materials, March, 2004.

BIBLIOGRAPHY

A. B. S. Choo, John Brian Newman, *Advanced Concrete Technology*, from Google books.

B. Skalny, Marchand and Odler, *Sulfate Attack on Concrete.*

C. R.N.Swamy, *the Alkali-Silica Reaction in Concrete*, Department of Mechanical and Process Engineering University of Sheffield.

D. K. Wesche, *Fly Ash in Concrete,* from Google books.

E. (http://acept.asu.edu/PiN/rdg/elmicr/elmicr.shtml)

APPENDIX A

ABBREVIATIONS

HVFAC	High-Volume Fly Ash Concrete
ESA	External Sulfate-Attack
ISA	Internal Sulfate-Attack
AMBM	The Accelerated Mortar Bar Method
EEF	Early Ettringite Formation
DEF	Delayed Ettringite Formation
AAR	Alkali-Aggregate Reaction
AASHTO	American Association of State Highway and Transportation Officials
ACR	Alkali-Carbonate Reaction
AMBT	Accelerated Mortar bar Test
ASR	Alkali-Silica Reaction
ASTM	American Society for Testing and Materials
CPT	Concrete Prism Test
SAI	Strength Activity Index
DOT	Department of Transportation
FHWA	Federal Highway Administration
SCM	Supplementary Cementitous Material
SEM	Scanning Electron Microscopy
W/Cm	Water To Cementitous material Ratio
ASTM C 109	Standard Test Method for Compressive Strength of Hydraulic Cement Mortars (Using 2-in.x 4-in Cylinder Specimens)

ASTM C1012	Standard Test Method for Length Change of Hydraulic- Cement Mortars Exposed to a Sulfate Solution
ASTM C 1260	The Accelerated Mortar Bar Method (AMBM) or ASTM C 1260 Standard Test Method for Potential Alkali Reactivity of Aggregates (Mortar-Bar Method)

APPENDIX B

BATCHING OF SAMPLES

Table B.1

Sample Excel Sheet for Batching.

Sample A – dimensions		Compression Test cylinders	
Length, inches	11	Length, inches	4
Width, inches	1	Diameter , inches	2
Thickness, inches	1		
Volume, ft^3	0.006366	Volume, ft^3	0.007273
Number of samples	4	Number of samples	8
Total Volume =		0.08365	ft^3
Batch Size		Casting Date	3/7/2007
Volume Required+ 10% in ft3	0.092		
Volume Required in cm^3	2605.52		
Mix Proportions (Absolute)			
Cement	0.8	In %	
Fine Aggregate	2.25	Times (Cement + Fly ash)	
W/Cm	0.6	Times (Cement + Fly ash)	
Fly ash	0.2	In %	
Ingredient	Specific	abs vol., cm^3	weight
Cement	3.15	402.81	1.27
Water	1	951.65	0.95
Fly ash	3	105.74	0.32
Fine Aggregates	2.5	1427.47	3.57
Total =		2887.67	5.18
Volume Required in cm^3 + 10 % (Wastage)			2866.07
Volume of the material obtained based on the weight			2887.67

APPENDIX C

CLEANING OF GRAPHS FROM RAW DATA

Table C.1

Excel Sheet for Raw Data.

Weeks	Date Cast	Batch ID : C60-CF40-W/Cm47 where CF- Class F				Change in length of samples in mm			
	11/10/06	Sample Measurement							
		1	2	3	4	1	2	3	4
0	11/12/06	-0.31	-0.03	-0.17	-0.26	0.00	0.00	0.00	0.00
0.4	11/15/06	-0.30	-0.02	-0.17	-0.24	0.01	0.01	0.01	0.02
1	11/19/06	-0.29	-0.01	-0.16	-0.23	0.01	0.02	0.02	0.02
2	11/26/06	-0.27	0.00	-0.15	-0.23	0.04	0.02	0.02	0.03
3	12/3/06	-0.27	0.00	-0.15	-0.22	0.04	0.03	0.03	0.03
4	12/10/06	-0.25	0.02	-0.13	-0.20	0.05	0.05	0.04	0.05
6	12/24/06	-0.24	0.02	-0.13	-0.20	0.06	0.05	0.05	0.06
8	1/7/07	-0.24	0.02	-0.12	-0.19	0.07	0.05	0.05	0.07
10	1/21/07	-0.23	0.02	-0.12	-0.18	0.07	0.05	0.06	0.08
12	2/4/07	-0.22	0.04	-0.10	-0.16	0.09	0.06	0.07	0.10
14	2/18/07	-0.19	0.07	-0.08	-0.12	0.12	0.10	0.09	0.13
18	3/18/07	-0.16	0.09		-0.09	0.15	0.12	0.12	0.16
22	4/15/07	-0.10	0.14	-0.02	-0.04	0.21	0.17	0.16	0.22

Samples	Original length in mm	% of expansion = change in length (Δ) / Original length *100				Average
		1	2	3	4	
		0.000	0.000	0.000	0.000	0
1	279.09	0.003	0.003	0.002	0.005	0.003
2	279.37	0.005	0.007	0.006	0.009	0.007
3	279.23	0.013	0.008	0.007	0.010	0.009
4	279.15	0.015	0.010	0.009	0.012	0.011
		0.019	0.018	0.015	0.018	0.017
		0.022	0.017	0.016	0.020	0.019
		0.024	0.017	0.018	0.024	0.021
		0.026	0.018	0.020	0.027	0.023
		0.032	0.023	0.026	0.035	0.029
		0.043	0.034	0.034	0.048	0.04
		0.054	0.043	0.043	0.059	0.05
		0.074	0.061	0.056	0.079	0.067

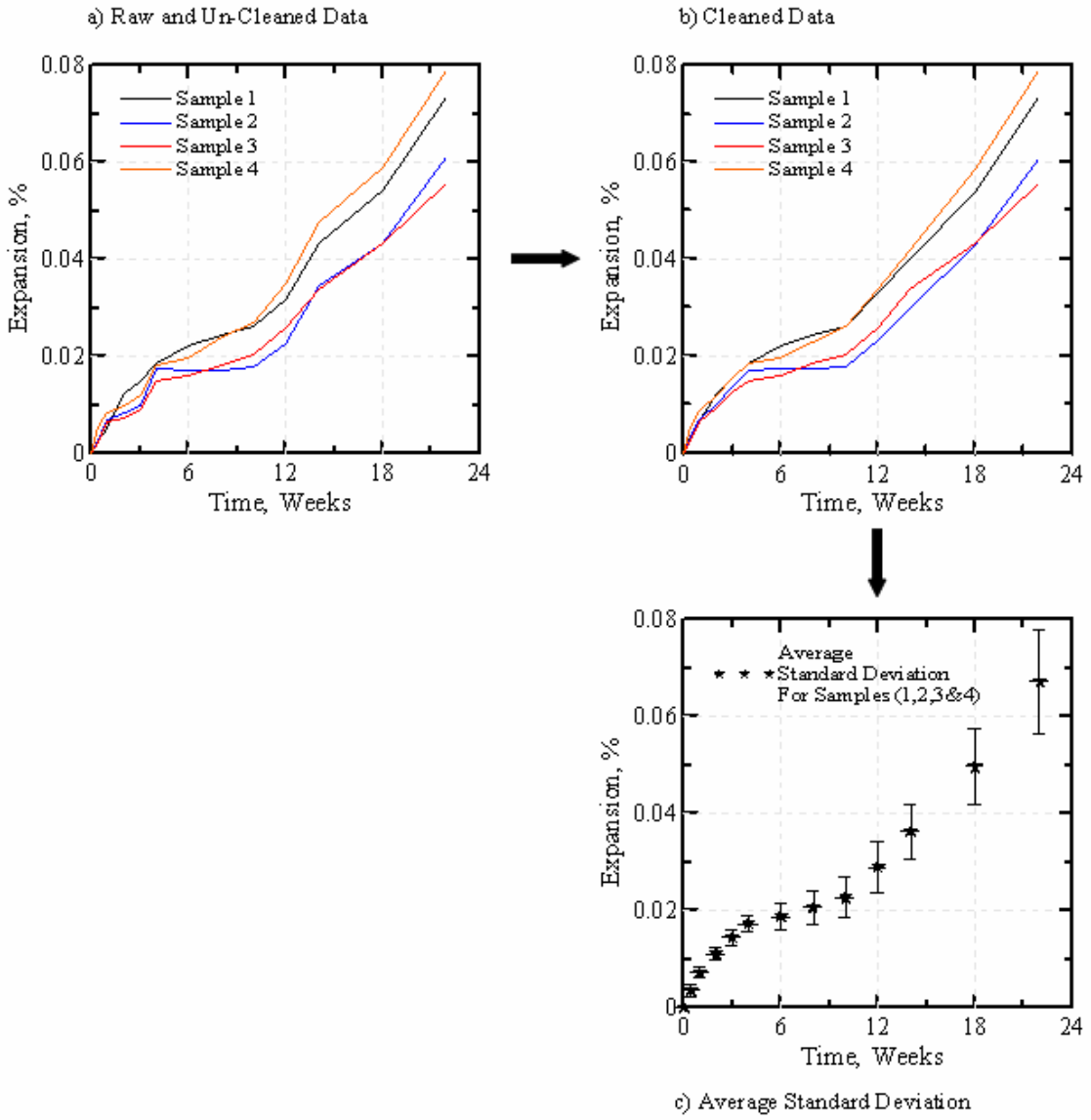

Figure. C.1 Schematic Diagram for Cleaning up of Raw Data